PNNL-13583

Pacific Northwest
National Laboratory
Operated by Battelle for the
U.S. Department of Energy

Evaluation of Effect of Fuel Assembly Loading Patterns on Thermal and Shielding Performance of a Spent Fuel Storage/Transportation Cast

J. M. Cuta
U. P. Jenquin
M. A. McKinnon

November 2001

Prepared for the U.S. Department of Energy
under Contract DE-AC06-76RL01830

DISCLAIMER

This report was prepared as an account of work sponsored by an agency of the United States Government. Neither the United States Government nor any agency thereof, nor Battelle Memorial Institute, nor any of their employees, makes **any warranty, express or implied, or assumes any legal liability or responsibility for the accuracy, completeness, or usefulness of any information, apparatus, product, or process disclosed, or represents that its use would not infringe privately owned rights**. Reference herein to any specific commercial product, process, or service by trade name, trademark, manufacturer, or otherwise does not necessarily constitute or imply its endorsement, recommendation, or favoring by the United States Government or any agency thereof, or Battelle Memorial Institute. The views and opinions of authors expressed herein do not necessarily state or reflect those of the United States Government or any agency thereof.

PACIFIC NORTHWEST NATIONAL LABORATORY
operated by
BATTELLE
for the
UNITED STATES DEPARTMENT OF ENERGY
under Contract DE-AC06-76RL01830

Printed in the United States of America

Available to DOE and DOE contractors from the
Office of Scientific and Technical Information,
P.O. Box 62, Oak Ridge, TN 37831-0062;
ph: (865) 576-8401
fax: (865) 576-5728
email: reports@adonis.osti.gov

Available to the public from the National Technical Information Service,
U.S. Department of Commerce, 5285 Port Royal Rd., Springfield, VA 22161
ph: (800) 553-6847
fax: (703) 605-6900
email: orders@ntis.fedworld.gov
online ordering: http://www.ntis.gov/ordering.htm


This document was printed on recycled paper.
(8/00)

PNNL-13583

Evaluation of Effect of Fuel Assembly Loading Patterns on Thermal and Shielding Performance of a Spent Fuel Storage/Transportation Cask

Contributors:

J. M. Cuta
U. P. Jenquin
M. A. McKinnon

November 2001

Prepared for
the U.S. Department of Energy
under Contract DE-AC6-76RLO 1830

Pacific Northwest National Laboratory
Richland, Washington 99352

Executive Summary

The licensing of spent fuel storage casks is generally based on conservative analyses that assume a storage system uniformly loaded with design basis fuel. The design basis fuel typically assumes a maximum assembly enrichment, maximum burnup, and minimum cooling time. These conditions set the maximum decay heat loads and radioactive source terms for the design. Recognizing that reactor spent fuel pools hold spent fuel with an array of initial enrichments, burnups, and cooling times, this study was performed to evaluate the effect of load pattern on peak cladding temperature and cask surface dose rate.

In 1991, DOE pursued a cooperative program with the Sacramento Municipal Utility District (SMUD). Part of the cooperative program was to demonstrate the effect of cask loading on the thermal and shielding performance of a cask containing spent nuclear fuel. At the time the cooperative agreement was established between DOE and SMUD, SMUD had fuel with cooling times ranging from 5 to 17 years, burnups of 8 to 38 GWd/MTU, and enrichments of 2.01 to 3.43% at its Rancho Seco nuclear power plant. It was thought that there was enough variability in the fuel to determine the effect of load pattern on dose rates. The effect of load pattern on the thermal performance of the casks was to be determined analytically using a computer code that had been validated extensively. With the termination of the DOE/SMUD cooperative agreement prior to cask loading, an analytical method was chosen to determine the effect of load pattern on dose rates. The codes were validated using data generated in other DOE cooperative efforts.

The cask used in the analysis was similar to the TN-24P spent fuel storage cask. The TN-24P spent fuel storage cask is designed to hold 24 spent fuel assemblies with a total heat load of 24 kW. The cask body is forged steel surrounded by a resin layer for neutron shielding and a steel outer shell. The overall cask length is 16 ft (5.0 m), and the outer diameter is 7.5 ft (2.3 m). The spent fuel basket consists of stacked interlocking plates of borated aluminum. In a performance demonstration conducted at the Idaho National Engineering and Environmental Laboratory (INEEL) under the direction of Pacific Northwest National Laboratory (PNNL), the cask was loaded with spent fuel (Westinghouse 15 x 15 pressurized water reactor [PWR] fuel) from the Surry nuclear power plant. The fuel loaded in the cask had a nominal rod diameter of 0.420 in. (1.067 cm) in a square array with a 0.563 in. (1.430 cm) pitch. Nominal fuel column length was 144 in. (365.8 cm). The measured cask temperatures and dose rates obtained from the performance test were used in baselining the analysis results.

The influence of load pattern on the thermal performance of the cask was determined through analysis with the COBRA-SFS code. The same COBRA-SFS model previously developed for analyzing the TN-24P cask was used in this parametric study. Three radial power distributions were considered. Each load pattern had an average decay heat output of 1 kW per fuel assembly for a total output of 24 kW from the fully loaded cask. Seventeen different load patterns were selected, and three backfill conditions were considered for each load pattern. The backfill media selected were helium, nitrogen, and vacuum. Except for the backfill medium and the radial power distribution, nothing was changed in the COBRA-SFS input between cases. This combination of load patterns and backfill gases provided a total of 51 runs in the test matrix.

The load pattern types are as follows:

- Uniform—all assemblies with the same decay heat output (1 kW/fuel assembly)
- Hot assemblies loaded in the center of the cask and colder assemblies closest to the cask wall
- Cold assemblies loaded in the center of the cask and hotter assemblies closest to the cask wall.

Selected analytical results are given in Table ES.1 and are shown graphically in Figure ES.1. A more thorough listing of the results is included in the main body of the report. These results show the effects of backfill and radial peaking. Radial peaking is defined as the decay heat from the hot assembly divided by the average decay heat from the cask. As expected, the helium backfill results in the lowest peak cladding temperatures.

Table ES.1. Peak Clad Temperature for Selected Cases in the Test Matrix

Load Pattern	Radial Peaking[(a)]	Peak Clad Temperature with Listed Backfill, °C (°F)		
		Vacuum	Nitrogen	Helium
Uniform Load Case 1	1.0 (uniform)	279.0 (534.2)	252.1 (485.7)	239.9 (463.9)
Hot Inside Case 9	1.5 (inside)[(b)]	307.4 (585.4)	280.4 (536.7)	263.9 (507.0)
Case 7	1.5 (inside)	311.1 (592.0)	283.6 (542.5)	268.1 (514.5)
Case 2	1.7 (inside)	323.0 (613.4)	295.5 (563.9)	278.8 (533.8)
Hot Outside Case 13	1.2 (outside)	265.0 (509.0)	243.7 (470.6)	228.2 (442.7)
Case 14	1.3 (outside)	266.1 (511.0)	247.6 (477.6)	222.2 (431.9)
Case 10	1.5 (outside)[(b)]	272.6 (522.7)	255.4 (491.7)	224.9 (436.9)
Case 16	1.5 (outside)	272.7 (522.9)	255.4 (491.7)	225.1 (437.1)
Case 11	1.7 (outside)	279.3 (534.70	263.2 (505.7)	228.9 (444.0)

(a) A load pattern uses two decay heat values, 12 assemblies with the value listed and 12 assemblies with a complementary value (2.0 minus the value listed), unless otherwise noted. Each load pattern averages 1.0 kW/assembly. Thus radial peaking is the decay heat value of the hot assembly in the cask.
(b) Load pattern includes three decay heat values. The maximum value is listed.

Over the range of radial peaking considered, those with the hotter assemblies to the inside show an essentially linear increase in peak clad temperature with increasing radial peaking. For the cases with the hotter assemblies to the outside (Cases 10, 11, 12, 13, 14, 15, 16, and 17), something much more interesting happens. Up to radial peaking values of 1.2 to 1.3, the peak clad temperature shows a *decreasing* trend with increasing radial peaking. Above about 1.3, the peak clad temperature tends to increase with increasing radial peaking, but the rate of increase is slightly less than that seen in the cases with hotter fuel to the inside. The lowest peak cladding temperature corresponds to the crossover point, where the peak cladding temperature of the inner assembly is equal to the peak cladding temperature of the outer assembly.

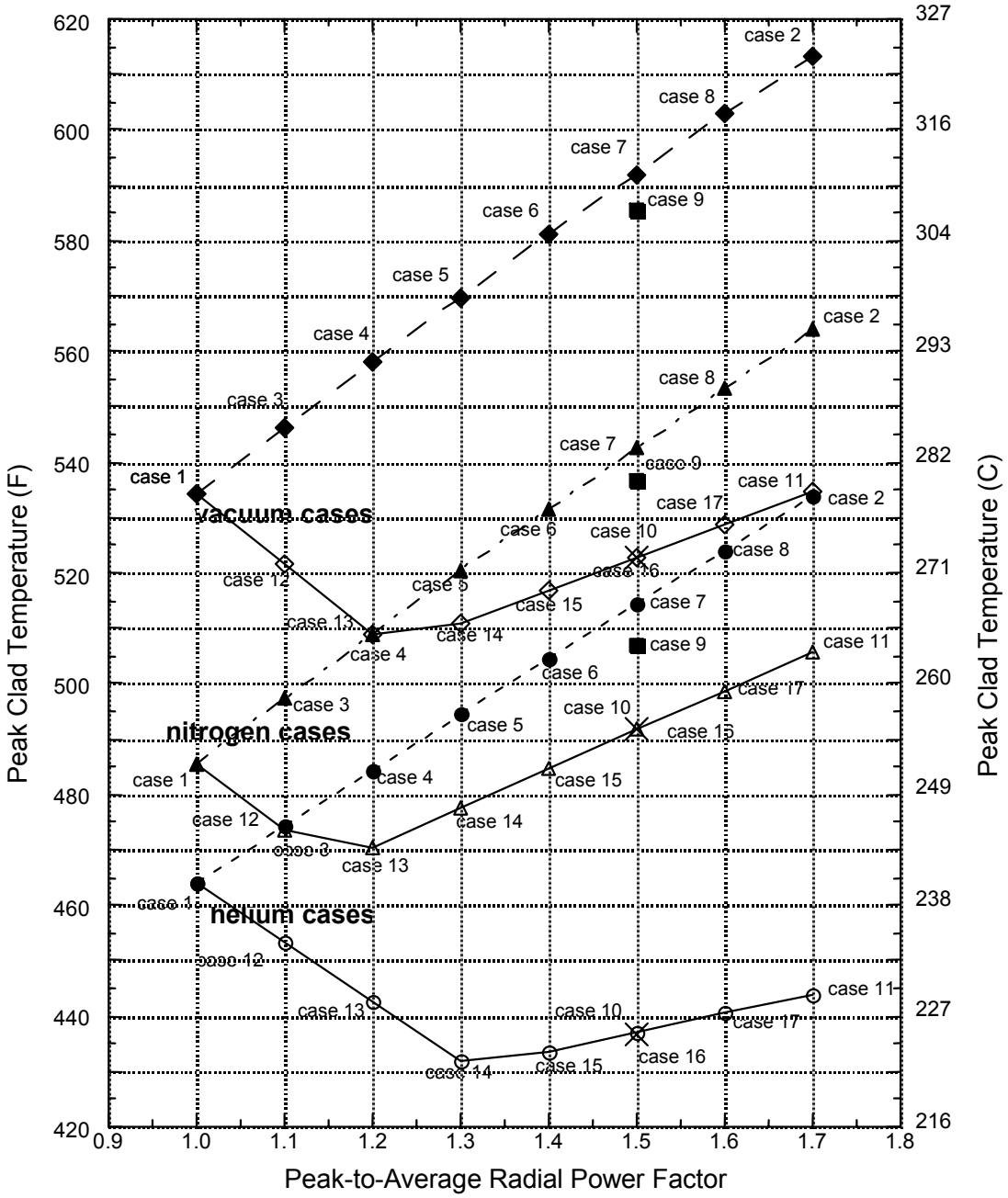

Figure ES.1. COBRA-SFS Results for the Full Matrix of Cases Investigated

Source terms and decay heat values were calculated for PWR fuel of various enrichments and cooling times. Enrichments ranged from 2.4 to 4.8% ^{235}U, and fuel burnups ranged from 15 GWd/MTU for 2.4% enriched fuel to 70 GWd/MTU for 4.8% enriched fuel. Cooling times ranged from three to 30 years. These ranges bound the majority of the fuel discharged or to be discharged from boiling water reactors (BWRs) and PWRs from the mid-1970s through the year 2020. Even with these bounds, there is a large array of initial fuel enrichments, burnups, and cooling times corresponding to each decay heat value. To perform the shielding analysis, seven source terms were selected corresponding to five of the decay heat values used in the thermal

analysis. Table ES.2 lists the seven source terms used in the shielding analysis. Neutron and photon source terms and decay heat values for the fuel used for the load-pattern analyses were calculated with the ORIGEN-ARP code.

Table ES.2. Source Terms Used in Shielding Calculations

Source Number	**1**	**2**	**3**	**4**	**5**	**6**	**7**
Decay Heat, kW/Assembly	1.0	1.0	1.7	0.3	1.3	0.7	1.7
Enrichment, % ^{235}U	3.0	4.8	4.2	2.4	4.8	3.0	4.8
Burnup, GWd/MTU	30	60	50	20	60	30	60
Cooling Time, yr	3.65	9.42	3.47	8.92	5.81	4.91	4.15
Load Pattern Case No. (see Table ES.1)	1	1	2 & 11	2 & 11	14	14	2 & 11

The dose-rate calculations were made with the MCNP code, which is a general-purpose, continuous-energy, generalized-geometry Monte Carlo transport code. Neutron and photon fluxes were calculated at numerous locations of interest and converted to dose rates. Dose rates were calculated on the surface of the cask and at 1 m and 2 m from the cask.

The dose rates obtained from the parametric analysis at three locations on the side of the cask are provided in Table ES-3. The higher values of photon and neutron dose rates at locations (1) and (3) of the graphical insert in the table reflect the absence of a neutron shield in these

Table ES.3. Peak Surface Dose Rates on the Side of the Cask for Various Loading Patterns

Source	Surface Dose Rates, mrem/hr		
	Neutron	Photon	Total
(3) Top Peak @ Elevation of 4.25 m			
1/1[a]	36	146	182
2/2	180	119	299
4/7	118	194	312
6/5	126	178	304
(1) Bottom Peak @ Elevation of 31 cm			
1/1	69	162	231
2/2	344	107	452
4/7	241	220	461
6/5	253	164	417
(2) Side Mid-Plane Dose @ 2.25-m Elevation			
1/1	2	60	62
2/2	11	18	29
4/7	9	65	74
6/5	9	38	47

(a) The notation "X/Y" is used to describe source arrangement. Source X was loaded in the center of the cask's basket, and source Y was loaded in the cask's outer basket. Source numbers match those given in Table ES.2.

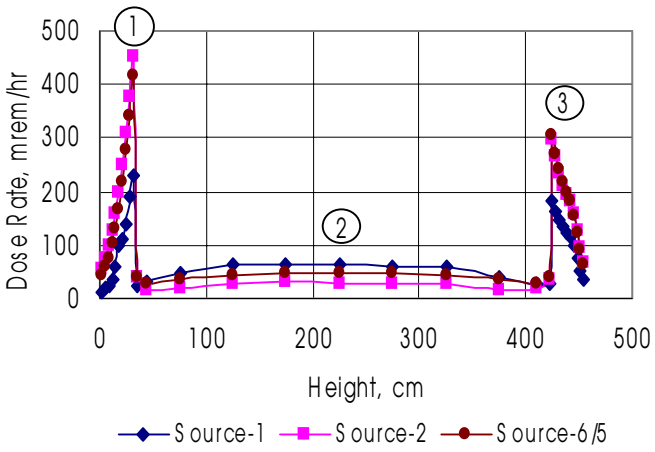

locations. They are just below and above the neutron shield, respectively. Fuel burnup dominates neutron dose rates and cooling time dominates photon dose rates.

Based on these analyses, load patterns can be used to reduce peak cladding temperatures in a cask without adversely affecting the surface dose rates. It is interesting that the uniform loadings of 30 and 60 GWd/MTU fuel bound the neutron dose rates for the other loadings. If cooling times were limited to five years or greater, the uniform loadings of 30 GWd/MTU and 60 GWd/MTU fuel would probably bound the photon dose rates as well.

Contents

Figures

Tables

1.0 Introduction

Through demonstration programs and cooperative agreements, the U.S. Department of Energy (DOE) has gained considerable experience in contributing to the development of systems for dry storage and transport of spent nuclear fuel. One of the earliest demonstrations of a storage-only system was for the REA 2023 cask (McKinnon et al. 1986) that contained boiling water reactor (BWR) spent fuel. It was demonstrated at General Electric Company's Morris Storage facility during the winter of 1984–85. The demonstrations were accompanied by predictions (Wiles et al. 1986) and measurements of temperatures and shielding performance of the cask. Through various cooperative agreements, DOE and the Electric Power Research Institute (EPRI) participated in performance tests of the Castor V/21, TN-24P, MC-10, NUHOMS, and VSC-17 dry storage systems (McKinnon and DeLoach 1993) using intact and consolidated pressurized water reactor (PWR) fuel. Most of the performance tests were conducted at the Idaho National Engineering and Environmental Laboratory (INEEL).[(a)] Participants in the tests included Virginia Power, Carolina Power and Light, and Sierra Nuclear Company. DOE's transportation demonstrations have included Nuclear Fuel Services (NFS) transportable storage cask and the Cask System Development Program (CSDP). At the time the program was initiated, there were no licensed dual-purpose casks.

In 1991, DOE pursued a cooperative program with the Sacramento Municipal Utility District (SMUD) to demonstrate a dry transfer system and a transportable storage system at SMUD's Rancho Seco reactor site. Congress allocated funding for the cooperative program in 1992 and 1993, and the cooperative agreement between DOE and SMUD followed in September 1994.

Part of the cooperative program was to demonstrate the effect of cask loading on the thermal and shielding performance of a cask containing spent nuclear fuel. The licensing for spent fuel storage casks is generally based on conservative analyses that assume a uniform loading of design basis fuel in a storage system. Storage systems are then approved for this design basis fuel with its maximum assembly enrichment, maximum burnup, and minimum cooling times. Based on the results of prior cask demonstrations, the thermal performance of the casks was expected to be adequately predicted for various heat loads by analytical methods. The effect of load pattern on dose rates was to be determined experimentally.

When a cooperative agreement was established between DOE and SMUD, the fuel at Rancho Seco nuclear power plant had been cooled (time out of the reactor core) for 5 to 17 years. Burnups ranged from 8 to 38 GWd/MTU and enrichments from 2.01 to 3.43%. It was thought that there was enough variability in the fuel to give meaningful dose rate differences on the surface of the cask based on load pattern in the cask; however, licensing difficulties delayed fabrication of the MP-187 cask until the variation in fuel source terms was too small to be able to provide meaningful dose rate differences on the outside of the cask based on load pattern. Additionally, experimental measurement of surface dose rates was not carried out due to the termination of the DOE/SMUD cooperative agreement.

With the termination of the DOE/SMUD cooperative agreement, an alternative method of determining the effect of load pattern on dose rate was pursued. It consisted of an analytical

(a) INEEL is operated for DOE by EG&G, Inc.

approach using the TN-24P cask tested (Creer et al. 1987) by DOE in a prior cooperative effort. The post-loading surface and surrounding dose rate measurements were used to benchmark the code, and then various load patterns were analyzed to determine the effect of cask loading on dose rate.

The influence of load pattern on the thermal performance of the cask was also determined through analysis using the COBRA-SFS code (Michener et al. 1995). The extensive program of cask heat transfer carried out under the Commercial Spent Fuel Management (CSFM) Program demonstrated the reliability of the COBRA-SFS code in predicting the heat transfer capabilities of spent fuel storage casks. In the CSFM Program, analytical results derived from using the COBRA-SFS code to model the casks were compared with measured temperatures within the cavities of commercial storage casks for several different cask designs from different vendors. The analytical results of the code were obtained in advance of cask loading and performance measurements. The excellent agreement of code output with measured values justified using the analytical results for the current effort without going to the expense of providing thermal instrumentation in the cask.

The influence of load pattern on cask dose rates was determined through analyses using the ORIGEN-ARP (Bowman and Leal 1998) and MCNP codes. ORIGEN-ARP was used to determine the source terms corresponding to the decay heat values used in the thermal analyses. Cask dose rates were determined using the MCNP code.

This report documents the results of an analytical study that examines the effect of load pattern on the thermal and shielding performance of a cask. The total heat load in the cask has been held constant; however, the distribution of the heat load in the cask has been varied. Section 2 contains a description of the cask and the analytical models used in the analysis. Section 3 describes the test matrix. A discussion of the analytical results is given in Section 4, and the conclusions are presented in Section 5. Section 6 comprises the cited references and bibliography.

2.0 Cask Modeling

The TN-24P spent fuel storage cask was constructed by Transnuclear, Inc. under a cooperative program between Virginia Power and DOE. Performance testing was conducted jointly by Virginia Power, Pacific Northwest National Laboratory,[(b)] and INEEL. EPRI also participated in the program through a separate agreement with Virginia Power. The latter program is fully documented (Creer et al. 1987; Transnuclear 1985a, 1985b). This section presents a summary description of the cask, the COBRA-SFS model, and the MCNP model.

2.1 Description of TN-24P Cask

The TN-24P spent fuel storage cask holds up to 24 spent fuel assemblies and can dissipate a total heat load of up to 24 kW. A cutaway diagram of the cask is shown in Figure 2.1. The cask body is forged steel, surrounded by a resin layer for neutron shielding and a steel outer shell. The overall cask length is 16 ft (5.0 m), and the outer diameter is 7.5 ft (2.3 m). When loaded with unconsolidated spent fuel, it weighs approximately 100 tons.

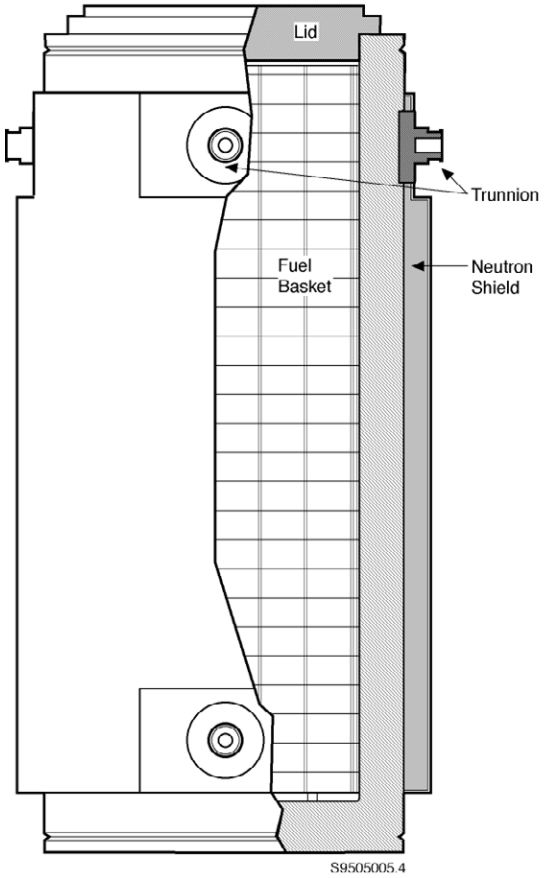

Figure 2.1. TN-24P PWR Spent Fuel Storage Cask

(a) Pacific Northwest National Laboratory is operated by Battelle for DOE under Contract DE-AC06-76RL01830.

Figure 2.2 shows a cross-section through the center of the upper trunnions of the cask. The spent fuel basket consists of stacked interlocking plates of borated aluminum. In the experimental program, the cask was loaded with spent fuel from the Surry nuclear plant. This fuel was Westinghouse 15 x 15 PWR fuel with nominal rod diameter of 0.420 in. (1.067 cm) in a square array with a 0.563 in. (1.430 cm) pitch. Nominal fuel column length was 144 in. (365.8 cm), and burnup was approximately 30 GWd/MTU for each assembly. Decay heat rates in the fuel rods for the duration of the tests were calculated using ORIGEN2 (Croff 1980). The predicted power was 20.6 kW at the start of testing and 20.3 kW at the end. The average power per assembly was approximately 850 W.

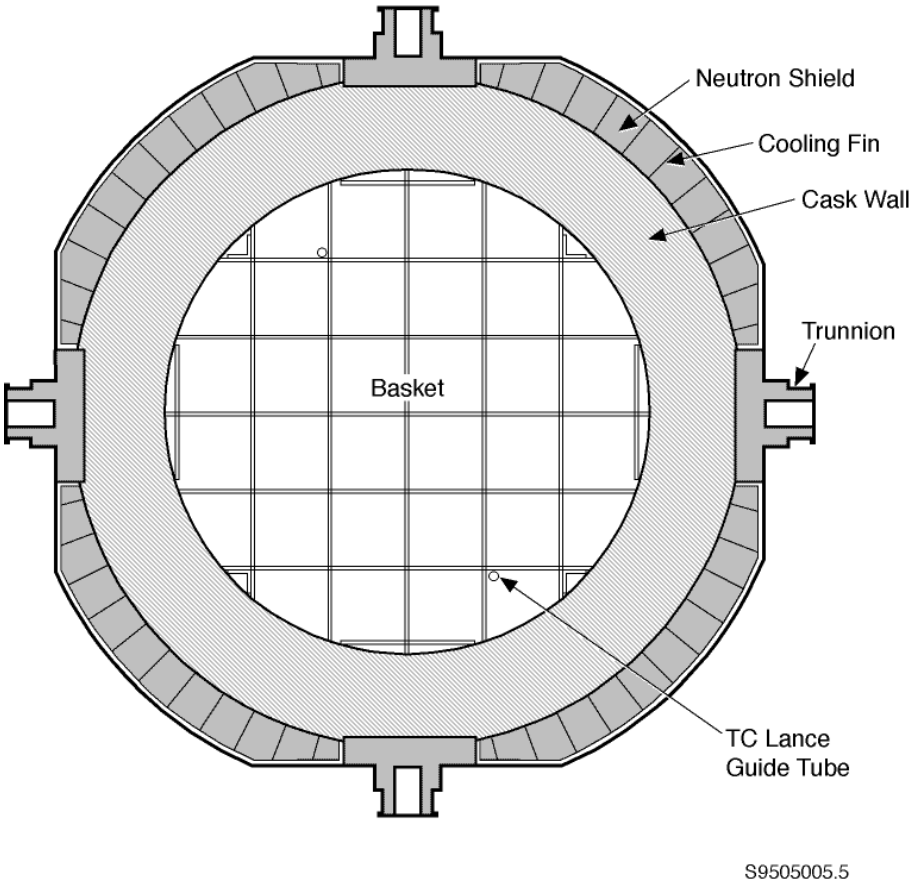

Figure 2.2. Cross-Section of TN-24P Spent Fuel Storage Cask

2.2 Cask Model Used for Thermal Analysis

A cross-section of the thermal model of a one-eighth section of symmetry of the cask is shown in Figure 2.3. For simplicity, this diagram does not include the subchannel modeling of the individual fuel assemblies within the basket. The cask is represented with 51 slab nodes: 27 for modeling the spent fuel basket, 12 for the cask body, 4 for the neutron shield, and 8 for the cask outer shell. The outermost nodes of the cask shell are zero-thickness boundary nodes to represent the cask surface temperature. They are used to calculate the appropriate contribution of radiative and convective heat transfer to the environment.

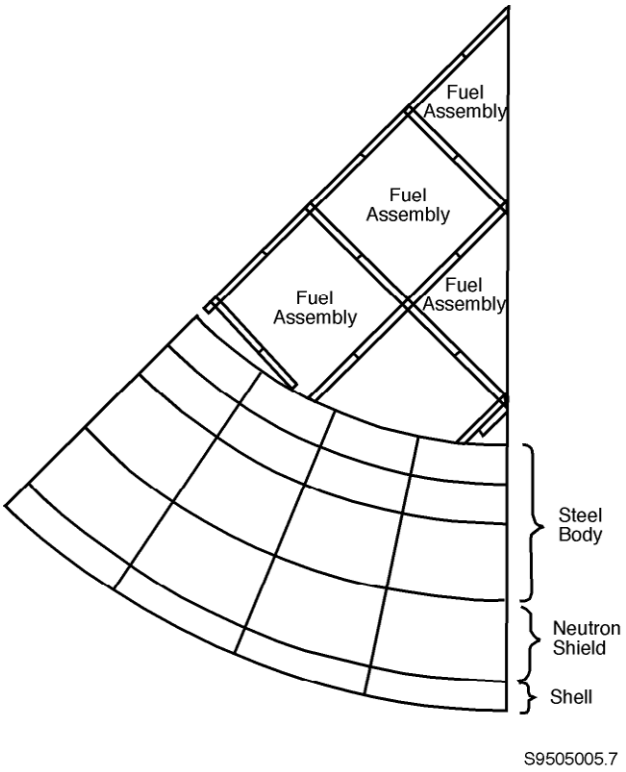

Figure 2.3. COBRA-SFS Model of 1/8th Section of Symmetry of TN-24P Cask

Within the spent fuel basket, the fuel assemblies were modeled using subchannel analysis. In the one-eighth section of symmetry, there are two types of fuel assemblies: half-symmetry assemblies and whole assemblies. The half-symmetry assemblies were modeled with a subchannel array. In the assemblies of this type, the model includes 136 subchannels and 120 rods. A lumped rod-and-channel arrangement was used to model the whole assemblies. Modeling studies (Rector et al. 1986) have shown that this type of modeling gives adequate resolution of temperature gradients within an unconsolidated spent fuel assembly. This model requires only 57 channels and 105 rods to represent the assembly.

The COBRA-SFS model developed for analyzing the TN-24P cask experimental program was used in this parametric study. Table 2.1 provides a comparison of code predictions and experimental results taken from the TN-24P cask experimental program (Creer et al. 1987). No changes were made in the geometry descriptions or thermal connections except for required

Table 2.1. Peak Cladding Temperatures for the TN-24P Cask with a Total Decay Heat Load of 20.6 kW

Backfill Gas	Predicted Temperature °C	Measured Temperature °C
Helium	220	211
Nitrogen	247	232
Vacuum	273	275

changes to the input for the different backfill media of helium, nitrogen, and vacuum. In all cases considered, the same axial power distribution was used, and the total power was specified at 24 kW.

2.3 Cask Models Used in the Shielding Analysis

The dose rate calculations were made with the MCNP4B code (Briesmeister 1997), which is a general-purpose, continuous-energy, generalized Monte Carlo transport code. Neutron and photon fluxes were calculated at numerous locations of interest and converted to dose rates using the ANSI/ANS-6.1.1-1977 (ANS 1977) flux-to-dose-rate conversion factors. The primary locations of interest are the surfaces of the cask.

The major features of the shielding model are shown in Figure 2.4. Air was assumed to be the medium surrounding the cask on all sides. The basket is modeled discretely as aluminum plates that are 1 in. thick. The fuel compartment spacing is 23.1 cm (9.1 in.). The fuel assemblies are modeled as homogeneous regions that completely fill the fuel compartments. Likewise, the plenum region and end fitting regions are modeled as homogeneous regions. Grid spacers are not modeled explicitly; they are homogenized with the fuel and the cladding.

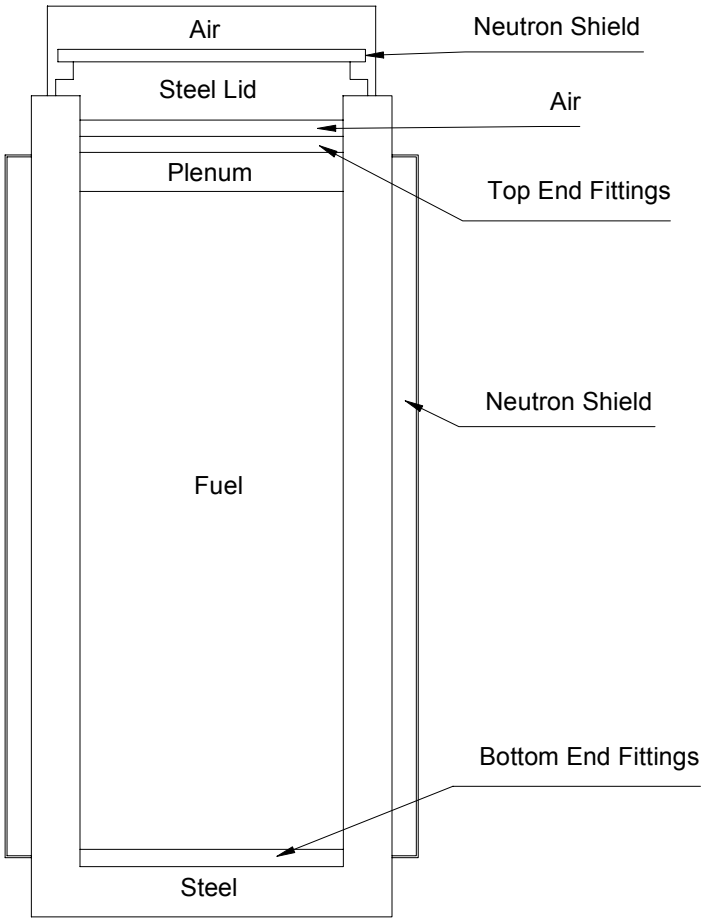

Figure 2.4. Cask Model Used for Shielding Calculations

Material densities used in the model for the TN-24P analyses are given in Table 2.2. The fuel density in Table 2.2 is a combination of the mass of UO_2, Zircaloy cladding, and Zircaloy grid spacers for a 17 x 17 array of fuel rods, which is similar to the densities for a 15 x 15 array of fuel rods averaged over the compartment volume of the active length of the assembly.

Table 2.2. Material Densities Used in the MCNP Model for the TN-24P Cask

Description	**Density, g/cm^3**
Steel	7.92
Al	2.7
Radial Neutron Shield	1.7
Top Neutron Shield	0.9
Copper	8.92
Fuel	3.53
Plenum	0.327
Top End Fitting	2.715
Bottom End Fitting	1.44

The steel sidewall of the TN-24P cask is thicker than that of several other dry storage casks; hence, the dose rates are unusually low. For the purposes of the load-pattern shielding analyses, the sidewall steel density was arbitrarily reduced by 10% to calculate dose rates that represent a typical storage cask.

3.0 Test Matrix

The objective of this study was to determine the effect of a spent fuel load pattern in a cask on the peak fuel temperature in the cask and the dose rates on and near the surface of the cask. This required the coupling of neutronic and thermal analyses. The thermal analysis assumed decay heat values ranging from 0.3 kW to 1.7 kW per assembly. The neutronic calculations determined the combination of fuel enrichments, burnups, and cooling times that would produce the decay heat values assumed for the thermal analysis. These values were then used for determining the radioactive source terms that were used for shielding analysis. Analysts took advantage of an existing thermal model for the TN-24P cask that was developed in conjunction with the cask performance tests.

Parameters given consideration in the study include backfill gases, fuel enrichment, burnup, and cooling time. The backfill gases have a big effect on the thermal behavior of the cask but negligible influence on shielding performance. The burnups and enrichments were selected to provide an envelope for old, cold spent fuel and future discharges from reactors. Wall materials, thickness, and gaps also can affect cask performance. Varying these parameters, however, was not within the scope of this study.

Three radial power distributions were considered. Each load pattern had an average decay heat output of 1 kW per fuel assembly for a total output of 24 kW from the fully loaded cask. Seventeen different load patterns were selected. The load pattern types are as follows:

- Uniform—all assemblies with the same decay heat output (1 kW/fuel assembly)
- Hot assemblies (1.0 kW < decay heat ∗ 1.7 kW) loaded in the center of the cask and colder assemblies loaded closest to the cask wall
- Cold assemblies loaded in the center of the cask and hotter assemblies loaded closest to the cask wall.

The thermal analysis included three backfill mediums for each of the load patterns for a total of 51 runs in the test matrix. The backfill media selected were helium, nitrogen, and vacuum. In all cases, the total power was specified at 24 kW, which is the design heat load for the TN-24P cask. The loading patterns provided $1/8^{th}$ symmetry in the cask. Except for the backfill medium and the radial power distribution, nothing was changed in the COBRA-SFS input between cases. Table 3.1 lists the 17 radial power distribution patterns selected for this study.

For all but two of the radial power distributions selected, 12 hot assemblies at one power and 12 complementary cold assemblies at another power were chosen to produce the load pattern. Two patterns (Cases 9 and 10) were devised using three different assembly powers (hot, intermediate, and cold) to evaluate the effect of smoothing the bundle-to-bundle gradient as much as possible. The diagrams in Table 3.2 show the radial power distribution for each case.

Table 3.1. Selected Cases for Parametric Study of Radial Power Distribution Patterns

Case	Loading Pattern	Hot Assemblies (watts)	Cooler Assemblies (watts)	Total Load Power (kW)	Peak-To-Average Ratio
1	uniform power	1000	1000	24	1.0
2	hotter inside	1700	300	24	1.7
3	hotter inside	1100	900	24	1.1
4	hotter inside	1200	800	24	1.2
5	hotter inside	1300	700	24	1.3
6	hotter inside	1400	600	24	1.4
7	hotter inside	1500	500	24	1.5
8	hotter inside	1600	400	24	1.6
9	3 levels of power; hottest inside	1500	1200, 700	24	1.5
10	3 levels of power; hottest outside	1500	600, 300	24	1.5
11	hotter outside	1700	300	24	1.7
12	hotter outside	1100	900	24	1.1
13	hotter outside	1200	800	24	1.2
14	hotter outside	1300	700	24	1.3
15	hotter outside	1400	600	24	1.4
16	hotter outside	1500	500	24	1.5
17	hotter outside	1600	400	24	1.6

Table 3.2. Radial Power Distributions (for 24 kW total power)

Case 1—Uniform Power Distribution												
					1.000	1.000						
				1.000	1.000	1.000	1.000					
			1.000	1.000	1.000	1.000	1.000	1.000				
			1.000	1.000	1.000	1.000	1.000	1.000				
				1.000	1.000	1.000	1.000					
					1.000	1.000						
"Hotter Inside" Power Distributions							**"Hotter Outside" Power Distributions**					
Case 2							**Case 11**					
		0.300	0.300						1.700	1.700		
	0.300	1.700	1.700	0.300				1.700	0.300	0.300	1.700	
0.300	1.700	1.700	1.700	1.700	0.300		1.700	0.300	0.300	0.300	0.300	1.700
0.300	1.700	1.700	1.700	1.700	0.300		1.700	0.300	0.300	0.300	0.300	1.700
	0.300	1.700	1.700	0.300				1.700	0.300	0.300	1.700	
		0.300	0.300						1.700	1.700		

Table 3.2 (contd)

"Hotter Inside" Power Distributions							"Hotter Outside" Power Distributions					
Case 3							**Case 12**					
		0.900	0.900						1.100	1.100		
	0.900	1.100	1.100	0.900				1.100	0.900	0.900	1.100	
0.900	1.100	1.100	1.100	1.100	0.900		1.100	0.900	0.900	0.900	0.900	1.100
0.900	1.100	1.100	1.100	1.100	0.900		1.100	0.900	0.900	0.900	0.900	1.100
	0.900	1.100	1.100	0.900				1.100	0.900	0.900	1.100	
		0.900	0.900						1.100	1.100		
Case 4							**Case 13**					
		0.800	0.800						1.200	1.200		
	0.800	1.200	1.200	0.800				1.200	0.800	0.800	1.200	
0.800	1.200	1.200	1.200	1.200	0.800		1.200	0.800	0.800	0.800	0.800	1.200
0.800	1.200	1.200	1.200	1.200	0.800		1.200	0.800	0.800	0.800	0.800	1.200
	0.800	1.200	1.200	0.800				1.200	0.800	0.800	1.200	
		0.800	0.800						1.200	1.200		
Case 5							**Case 14**					
		0.700	0.700						1.300	1.300		
	0.700	1.300	1.300	0.700				1.300	0.700	0.700	1.300	
0.700	1.300	1.300	1.300	1.300	0.700		1.300	0.700	0.700	0.700	0.700	1.300
0.700	1.300	1.300	1.300	1.300	0.700		1.300	0.700	0.700	0.700	0.700	1.300
	0.700	1.300	1.300	0.700				1.300	0.700	0.700	1.300	
		0.700	0.700						1.300	1.300		
Case 6							**Case 15**					
		0.600	0.600						1.400	1.400		
	0.600	1.400	1.400	0.600				1.400	0.600	0.600	1.400	
0.600	1.400	1.400	1.400	1.400	0.600		1.400	0.600	0.600	0.600	0.600	1.400
0.600	1.400	1.400	1.400	1.400	0.600		1.400	0.600	0.600	0.600	0.600	1.400
	0.600	1.400	1.400	0.600				1.400	0.600	0.600	1.400	
		0.600	0.600						1.400	1.400		
Case 7							**Case 16**					
		0.500	0.500						1.500	1.500		
	0.500	1.500	1.500	0.500				1.500	0.500	0.500	1.500	
0.500	1.500	1.500	1.500	1.500	0.500		1.500	0.500	0.500	0.500	0.500	1.500
0.500	1.500	1.500	1.500	1.500	0.500		1.500	0.500	0.500	0.500	0.500	1.500
	0.500	1.500	1.500	0.500				1.500	0.500	0.500	1.500	
		0.500	0.500						1.500	1.500		
Case 8							**Case 17**					
		0.400	0.400						1.600	1.600		
	0.400	1.600	1.600	0.400				1.600	0.400	0.400	1.600	
0.400	1.600	1.600	1.600	1.600	0.400		1.600	0.400	0.400	0.400	0.400	1.600
0.400	1.600	1.600	1.600	1.600	0.400		1.600	0.400	0.400	0.400	0.400	1.600
	0.400	1.600	1.600	0.400				1.600	0.400	0.400	1.600	
		0.400	0.400						1.600	1.600		
Case 9 (three power levels)							**Case 10 (three power levels)**					
		0.700	0.700						1.500	1.500		
	0.700	1.200	1.200	0.700				1.500	0.600	0.600	1.500	
0.700	1.200	1.500	1.500	1.200	0.700		1.500	0.600	0.300	0.300	0.600	1.500
0.700	1.200	1.500	1.500	1.200	0.700		1.500	0.600	0.300	0.300	0.600	1.500
	0.700	1.200	1.200	0.700				1.500	0.600	0.600	1.500	
		0.700	0.700						1.500	1.500		

4.0 Analytical Results

The analysis includes three efforts: thermal analysis, source term calculations, and shielding calculations. The thermal analysis was completed first and provided guidance to the shielding calculations. The source terms were calculated explicitly for the Surry fuel and parametrically for the load-pattern analyses as a function of fuel enrichment, burnup, and cooling time.

The results of the thermal analysis, which were obtained using the COBRA-SFS code (Rector 1986), are presented in Section 4.1. Source term calculations are presented in Section 4.2, followed by the shielding calculations in Section 4.3. The source terms were calculated with ORIGEN2 (Croff 1980) and ORIGEN-ARP (Bowman and Leal 1998), and the shielding results were obtained with MCNP (Briesmeister 1997).

4.1 Thermal Performance

The peak clad temperature values obtained with COBRA-SFS for all 51 cases in the test matrix are presented in Table 4.1. Figure 4.1 presents the same results graphically as a further

Table 4.1. Peak Clad Temperature for All Cases in Test Matrix

Load Pattern	Radial Peaking[(a)]	Peak Clad Temperature with Listed Backfill, °C (°F)		
		Vacuum	Nitrogen	Helium
Uniform Load Case 1	1.0 (uniform)	279.0 (534.2)	252.1 (485.7)	239.9 (463.9)
Hot Inside Case 3	1.1 (inside)	285.7 (546.3)	258.6 (497.5)	245.7 (474.3)
Case 4	1.2 (inside)	292.3 (558.1)	265.0 (509.0)	251.4 (484.5)
Case 5	1.3 (inside)	298.7 (569.7)	271.3 (520.3)	257.0 (494.6)
Case 6	1.4 (inside)	305.0 (581.0)	277.5 (531.5)	262.6 (504.6)
Case 9	1.5 (inside)[(b)]	307.4 (585.4)	280.4 (536.7)	263.9 (507.0)
Case 7	1.5 (inside)	311.1 (592.0)	283.6 (542.5)	268.1 (514.5)
Case 8	1.6 (inside)	317.1 (602.8)	289.6 (553.3)	273.4 (524.2)
Case 2	1.7 (inside)	323.0 (613.4)	295.5 (563.9)	278.8 (533.8)
Hot Outside Case 12	1.1 (outside)	272.1 (521.8)	245.4 (473.8)	234.1 (453.4)
Case 13	1.2 (outside)	265.0 (509.0)	243.7 (470.6)	228.2 (442.7)
Case 14	1.3 (outside)	266.1 (511.0)	247.6 (477.6)	222.2 (431.9)
Case 15	1.4 (outside)	269.4 (517.0)	251.5 (484.7)	223.1 (433.6)
Case 10	1.5 (outside)[(b)]	272.6 (522.7)	255.4 (491.7)	224.9 (436.9)
Case 16	1.5 (outside)	272.7 (522.9)	255.4 (491.7)	225.1 (437.1)
Case 17	1.6 (outside)	276.0 (528.8)	259.3 (498.8)	226.9 (440.5)
Case 11	1.7 (outside)	279.3 (534.7)	263.2 (505.7)	228.9 (444.0)

(a) A load pattern uses two decay heat levels, 12 assemblies with the value listed and 12 assemblies with a complementary value (2.0 minus the value listed), unless otherwise noted. Each load pattern averages 1.0 kW/assembly. Thus the radial peaking is the decay heat value of the hot assembly in the cask.
(b) Load pattern includes three decay heat levels.

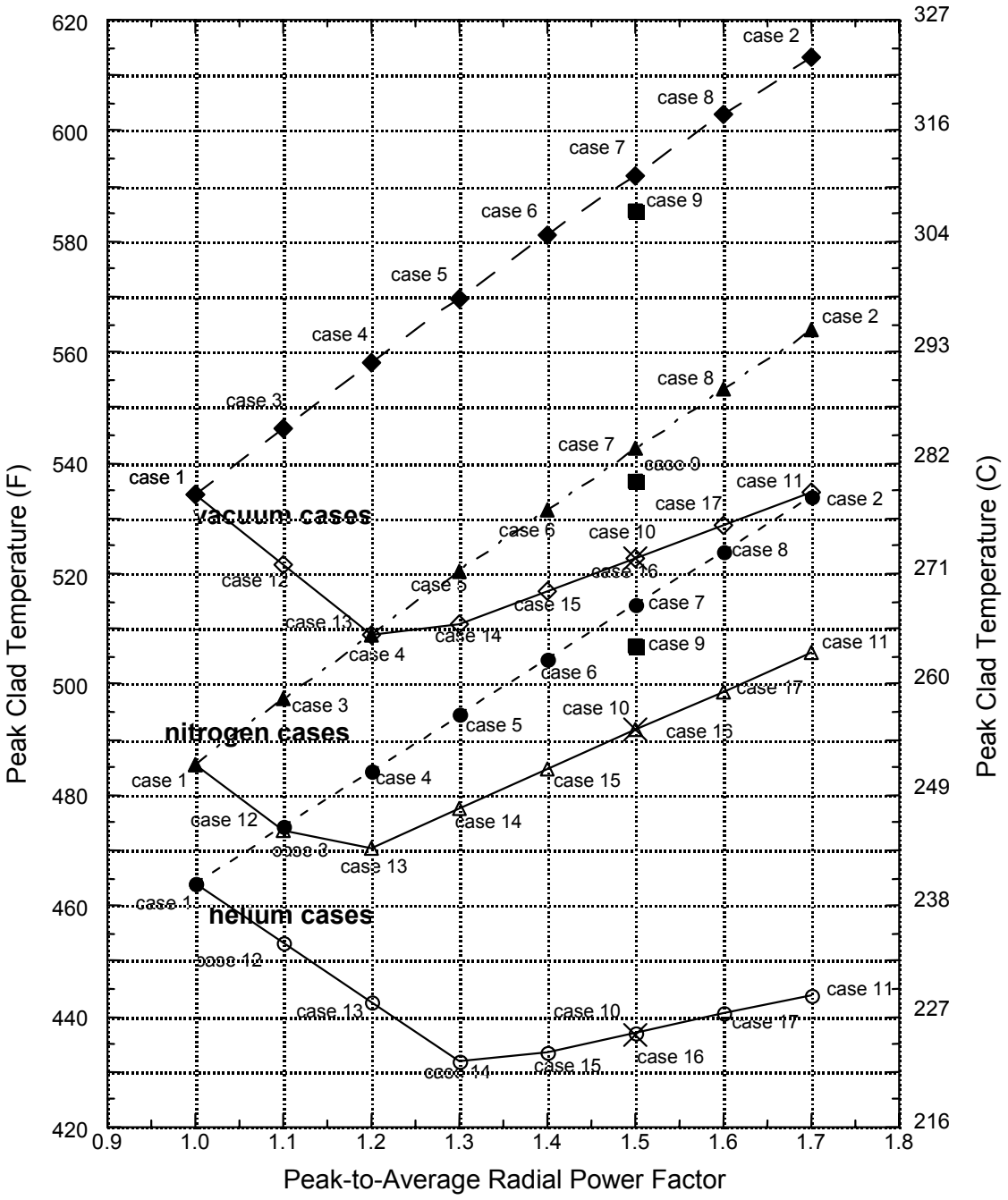

Figure 4.1. COBRA-SFS Results for the Full Matrix of Cases Investigated

aid to comparison between cases. These results show that the peak clad temperature is highest for vacuum backfill over the full range of variation of the radial power distribution. The peak clad temperature is lowest for helium backfill in any given case. The peak clad temperature for nitrogen backfill is above that of the corresponding cases with helium backfill but below that of the same cases with vacuum backfill.

Over the range of radial peaking considered in this study, the cases with the hotter assemblies to the inside show an essentially linear increase in peak clad temperature with increasing radial peaking. For the cases with the hotter assemblies to the outside, however (Cases 10, 11, 12, 13, 14, 15, 16, and 17), something much more interesting happens. Up to radial peaking values of 1.2 to 1.3, the peak clad temperature shows a *decreasing* trend with increasing radial peaking when the hotter bundles are closer to the cask wall. Above about 1.3, the trend becomes one of increasing peak clad temperature with increasing radial peaking, but the rate of increase is slightly less than that seen in the cases with hotter fuel to the inside. The lowest peak cladding temperature corresponds to the crossover point, where the peak cladding temperature of the inner assembly is equal to the peak cladding temperature of the outer assembly. This is seen from a comparison of the radial temperature profiles, as shown in Figure 4.2.

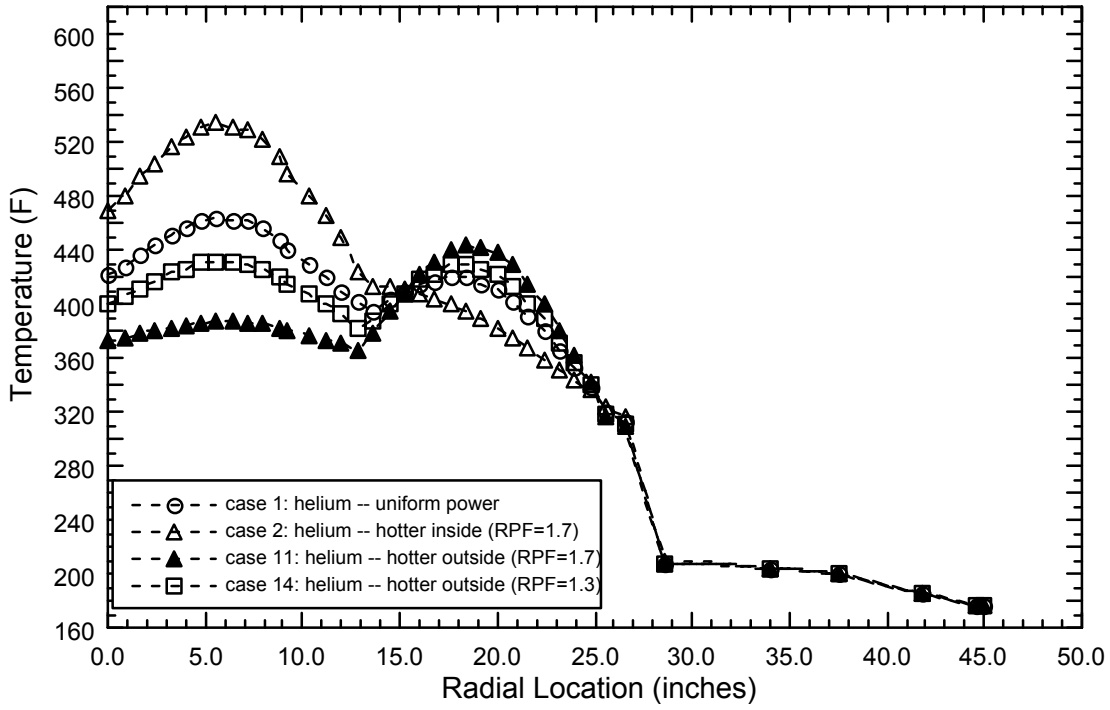

Figure 4.2. Radial Temperature Profiles Through the Hot Rod with Helium Backfill

The effect of load pattern selection is most noticeable with helium backfill, in which all cases with the hotter fuel to the outside yield a lower peak clad temperature than the reference case with uniform power (Case 1). The lowest peak clad temperature (obtained for Case 14 with radial peaking of 1.3) is more than 30°F below that of the uniform power case. For the largest radial power factor considered (1.7, in Case 11), the peak clad temperature is nearly 20°F below that of the uniform power case (Case 1) and almost 90°F below the peak clad temperature of the corresponding case with hotter fuel to the inside (Case 2).

The vacuum backfill calculations show similar behavior, and the "hotter outside" cases yield peak clad temperatures well below those of the uniform power case, even at the highest radial peaking. The trend line turns around somewhere between the radial peaking values of 1.2 and 1.3, with the peak clad temperature about 25°F cooler than that of the uniform power case. For

the largest radial peaking factor (1.7), the peak clad temperature for the "hotter inside" pattern is nearly 80°F above that for the corresponding "hotter outside" pattern.

The trends are less dramatic with nitrogen backfill but follow essentially the same pattern. The lowest peak clad temperature for the "hotter outside" patterns with nitrogen backfill was obtained with a radial peaking of 1.2 (Case 13). The peak clad temperature for this case is approximately 15°F lower than the uniform power case. The peak clad temperatures for the "hotter outside" patterns are higher than that of the optimum power case for radial peaking above 1.3, but the values are still significantly lower than those of the corresponding "hotter inside" cases. For radial peaking of 1.7, the peak clad temperature for the "hotter outside" case (Case 11) is about 55°F lower than that for the "hotter inside" case (Case 2).

For the radial peaking patterns with hotter assemblies to the inside (Cases 3, 4, 5, 6, 7, 8, and 9), the peak clad temperature for vacuum backfill is approximately 50°F above that of the corresponding cases with nitrogen backfill. The cases with nitrogen backfill are about 30°F cooler with helium backfill (consequently, the results with helium backfill are about 80°F cooler than the temperatures in the corresponding cases with vacuum backfill.) Table 4.2 summarizes the differences in peak clad temperature obtained with the different radial power configurations for each backfill medium. In all cases, the peak clad temperature is lower with the "hotter outside" radial power distribution than the temperature for the corresponding radial peaking with the "hotter inside" distribution.

These results show that the lowest temperatures should be obtained in a cask with helium backfill and a loading pattern that puts the hotter fuel closest to the cask wall and the cooler fuel in the center. If other considerations make helium an impractical choice for the backfill medium, the next best choice is nitrogen, also with a "hotter outside" loading pattern. These results suggest further that the loading pattern can have significant effects on determining peak clad temperature. In this study, cases with nitrogen backfill yielded lower temperatures than those with helium backfill when the nitrogen cases had "hotter outside" radial power distributions and the helium cases had "hotter inside" radial power distributions. The same pattern was observed for the vacuum cases with "hotter outside" distributions when compared with the peak clad temperature results for the "hotter inside" nitrogen cases.

Appendix A provides more detail on the thermal analysis and additional discussion of the results. It also presents axial and radial temperature profiles for the cases considered in the study.

Table 4.2. Summary of Effect of Radial Power Distribution on Peak Clad Temperature

Backfill Medium	Difference Between Hotter Inside and Hotter Outside at Maximum Radial Peaking Factor of 1.7	Difference Between Hotter Inside and Hotter Outside for Case with Lowest Peak Clad Temperature	Difference Between Uniform Power Case and Case with Lowest Peak Clad Temperature
Helium	50°C (90°F)	35°C (63°F)	18°C (32°F)
Nitrogen	32°C (58°F)	21°C (38°F)	8°C (15°F)
Vacuum	44°C (79°F)	27°C (49°F)	14°C (25°F)

4.2 Source Term Analysis

To perform the shielding analysis, it is necessary to determine source terms that correspond to the decay heat values used in the thermal analysis. For each decay heat value used in the thermal analysis, there is an array of initial fuel enrichment, burnup, and cooling times. To limit the extent of the analysis, bounding conditions were selected. Cooling times were selected to span 3.5 to 10 years. This is consistent with current spent fuel storage cask technology. Burnups were selected to span from 20 to 60 GWd/MTU with corresponding enrichments of 2.4% and 4.8% ^{235}U, respectively. These values bound the majority of the fuel discharged from BWR and PWR reactors from the mid-1970s through expected discharges in the year 2020.

4.2.1 Surry Fuel

Neutron and photon source terms for the Surry Fuel used in the TN-24P Cask Performance Test were calculated with ORIGEN2 (Croff 1980) using the PWRU library. The Surry fuel is assembled using Inconel grid spacers, which contain a large amount of cobalt. Therefore, the photon source term from decay of ^{60}Co was treated separately from the other photon source in the fuel. Estimation of the ^{60}Co photon source terms in the top and bottom end fittings and the plenum is detailed in Appendix B. The axial shape of the photon and neutron source terms is discussed in Appendix B as well.

4.2.2 Generic PWR Fuel

Neutron and photon source terms and decay heat values for the fuel used for the load pattern analyses were calculated with the ORIGEN-ARP code (Bowman and Leal 1998) for the enrichments and burnups listed in Table 4.3. Calculations were made for four burnup values at each fuel enrichment. The burnup values selected were slightly less than nominal (low), nominal, slightly more than nominal (high), and very high burnup. A constant power density of 32 MW/MTU was used for all irradiation calculations. Source terms and decay heat values were obtained for cooling times of 3, 4, 5, 6, 8, 10, 12, 15, 20, and 30 years. The source terms and decay heat values resulting from these calculations are listed in Appendix B.

Decay heat values as a function of time are shown in Figure 4.3 for nominally burned fuel. The values shown include decay heat from the actinides and activation products in the fuel. Activation products in the plenum and end fittings were neglected because they add very little to the decay heat values shown. The decay heat values for 3-, 5-, 10-, and 20-year cooled fuel are shown as a function of burnup in Figure 4.4. For a given cooling time, the decay heat is nearly proportional to burnup.

The dominant contributor to the neutron source term is ^{244}Cm, which has a half-life of 18 years. The effect of burnup on the neutron source term is shown in Figure 4.5 for a cooling time of five years. For a given enrichment, the neutron source term increases very quickly with burnup. As an example, the neutron source term for very high burnup 3% enriched fuel is a factor of 3.5 times the value for nominal burnup 3% enriched fuel. The neutron source term for very high burnup 4.8% enriched fuel is a factor of two times the value for nominal burnup 4.8% enriched fuel. Figure 4.6 shows the neutron source term for each enrichment with nominal burnups with cooling times of 3 to 10 years.

Table 4.3. Fuel Enrichment and Fuel Burnup Used for Source Term Evaluation

Burnup,	Enrichment, wt% U-235				
GWd/MTU	2.4	3.0	3.6	4.2	4.8
15	Low				
20	Nominal				
25	High	Low			
30	Very high	Nominal			
35		High	Low		
40		Very high	Nominal		
45			High	Low	
50			Very high	Nominal	
55				High	Low
60				Very high	Nominal
65					High
70					Very high

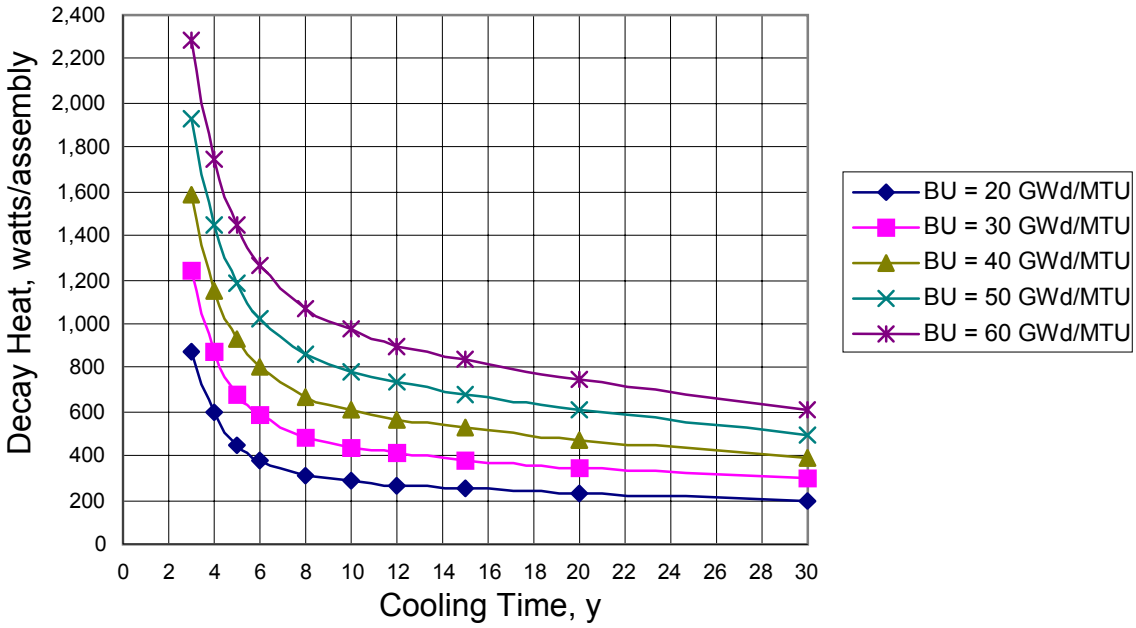

Figure 4.3. Decay Heat for Nominal-Burnup PWR Fuel as a Function of Cooling Time

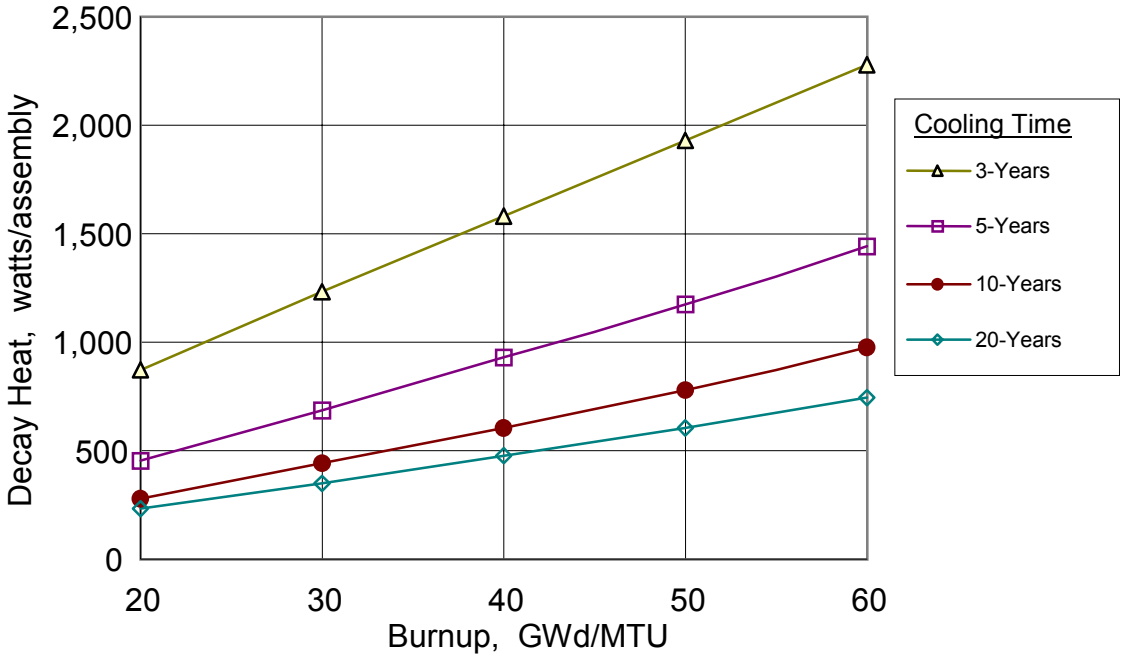

Figure 4.4. Decay Heat for PWR Fuel as a Function of Burnup for Various Cooling Times

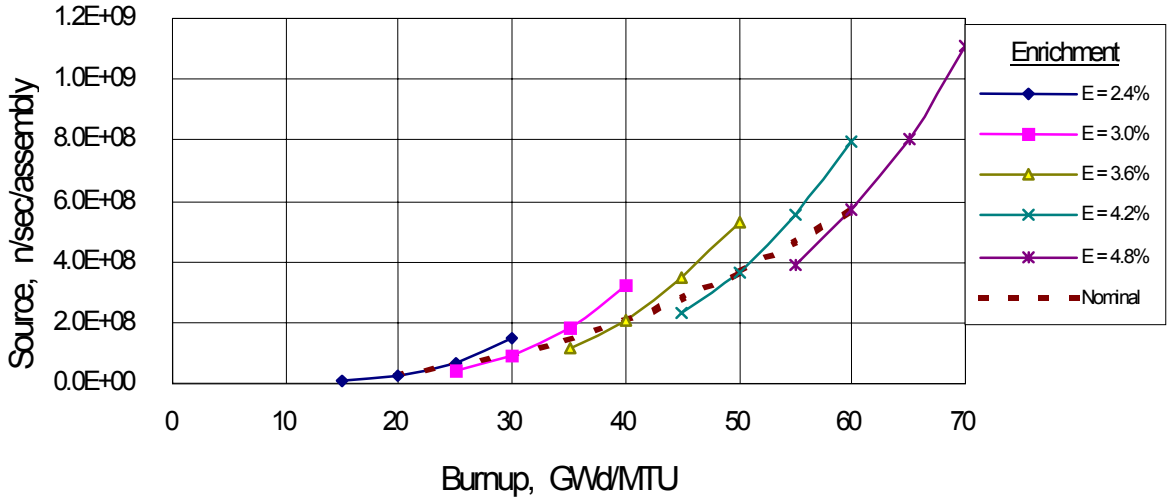

Figure 4.5. Neutron Source Term for PWR Fuel with Five Years of Cooling Time

Photon source terms were calculated for a group structure tailored for cask shielding. Between 0.0 and 2.5 MeV, the energy widths are 0.1 MeV. This energy range contributes 95% of the fuel dose rate. The most important contributors to the photon source term from a shielding point of view are ^{137}Cs (^{137m}Ba), ^{154}Eu, ^{144}Pr (^{144}Ce), ^{134}Cs, and ^{106}Rh. For cooling times of 10 years and more, ^{137}Cs is the dominant photon source term. Because the grid spacers were assumed to be Zircaloy for the load-pattern analysis, the ^{60}Co photon source in the fuel is minimal.

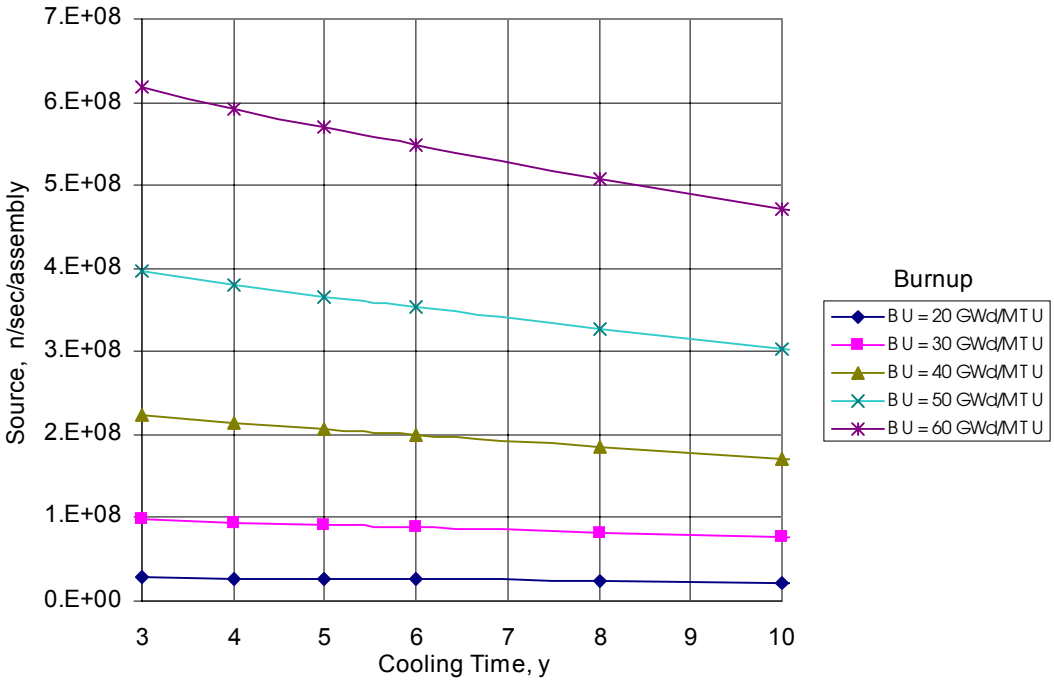

Figure 4.6. Influence of Cooling Time on Neutron Source Term Strength

Zero cooling ^{60}Co photon source terms for the plenum and bottom end fitting were approximated as 0.5 Ci ^{60}Co /GWd/MTU/gCo. For the top end fitting, the zero cooling ^{60}Co photon source term was approximated as 0.2 Ci ^{60}Co /GWd/MTU/gCo. The ^{60}Co source terms are decay-corrected for cooling time. It was assumed that the stainless steel contains 800 ppm cobalt.

4.2.3 Load Pattern Analyses

Corresponding to each decay heat value given in Table 3.1 is an array of fuel enrichments, fuel burnups, and cooling times that could produce the decay heat. Results of the thermal analyses assisted in the selection of seven source terms used for the shielding analyses. Characteristics of the source terms are given in Table 4.4.

Source-1 is for a decay heat value of 1.0 kW/assembly. The fuel is enriched to 3%, burned to 30 GWd/MTU, and decayed for 3.65 years. It serves as a base case because the enrichment and burnup is representative of fuel discharged from PWRs in the 1970s and 1980s. Source-2 is also for a decay heat value of 1.0 kW/assembly. The objective was to choose fuel with a high neutron source. The fuel is enriched to 4.8%, burned to 60 GWd/MTU, and decayed for 9.42 years. Source-1 and Source-2 represent opposite ends of the spectrum in terms of enrichment, burnup, and cooling time. Source-1 has a high photon dose rate component and a low neutron dose rate component. The dose rate components are reversed for Source-2.

Sources-3, -4, and -7 were selected to maximize and minimize the decay heat value. Sources-3 and -7 represent fuel with decay heat of 1.7 kW/assembly. Source-4, which represents fuel with decay heat of 0.3 kW/assembly, complements Sources-3 and -7.

Table 4.4. Source Terms Used in Shielding Calculations

	Source-1	**Source-2**	**Source-3**	**Source-4**	**Source-5**	**Source-6**	**Source-7**
Decay Heat, kW/Assembly	1.0	1.0	1.7	0.3	1.3	0.7	1.7
Enrichment, %	3.0	4.8	4.2	2.4	4.8	3.0	4.8
Burnup, GWd/MTU	30	60	50	20	60	30	60
Cooling Time, yr	3.6	9.4	3.5	8.9	5.8	4.9	4.1
^{60}Co Source (photons/sec/assembly)							
Bottom End Fittings	3.13E+12	2.93E+12	5.34E+12	1.04E+12	4.71E+12	2.65E+12	5.86E+12
Plenums	1.09E+12	1.02E+12	1.85E+12	3.62E+11	1.63E+12	9.19E+11	2.03E+12
Top End Fittings	3.27E+12	3.06E+12	5.58E+12	1.09E+12	4.92E+12	2.77E+12	6.12E+12
Fuel Region							
Neutrons (neutrons/ sec/assembly)	9.63E+07	4.81E+08	3.90E+08	2.33E+07	5.52E+08	9.15E+07	5.73E+08
Photons (photons/ sec/assembly)	5.64E+15	4.47E+15	9.45E+15	1.53E+15	6.50E+15	3.87E+15	9.08E+15
E, MeV	**Energy Dependent Photon Source in Fuel (photons/sec/assembly)**						
0.05	1.93E+15	1.31E+15	2.85E+15	4.81E+14	1.72E+15	1.18E+15	2.46E+15
0.15	4.42E+14	2.40E+14	6.42E+14	8.45E+13	3.35E+14	2.44E+14	5.19E+14
0.25	1.21E+14	7.02E+13	1.77E+14	2.52E+13	9.63E+13	6.91E+13	1.46E+14
0.35	9.05E+13	4.56E+13	1.30E+14	1.71E+13	6.45E+13	4.95E+13	1.03E+14
0.45	7.32E+13	3.16E+13	1.12E+14	1.26E+13	5.96E+13	4.41E+13	9.69E+13
0.55	3.18E+14	8.08E+13	5.68E+14	2.43E+13	2.56E+14	1.72E+14	4.95E+14
0.65	1.89E+15	2.32E+15	3.36E+15	7.94E+14	3.00E+15	1.60E+15	3.66E+15
0.75	5.91E+14	2.47E+14	1.27E+15	6.13E+13	7.45E+14	3.86E+14	1.28E+15
0.85	4.64E+13	2.63E+13	9.03E+13	6.78E+12	5.49E+13	2.97E+13	8.76E+13
0.95	1.43E+13	1.37E+13	2.51E+13	3.49E+12	1.90E+13	9.99E+12	2.47E+13
1.05	3.18E+13	2.04E+13	5.60E+13	5.14E+12	3.50E+13	2.00E+13	5.27E+13
1.15	2.40E+13	1.02E+13	4.21E+13	4.08E+12	2.39E+13	1.55E+13	3.95E+13
1.25	2.59E+13	3.67E+13	5.05E+13	8.47E+12	4.93E+13	2.23E+13	5.74E+13
1.35	2.63E+13	1.15E+13	5.09E+13	4.24E+12	3.02E+13	1.77E+13	5.00E+13
1.45	4.35E+12	1.02E+12	6.06E+12	3.10E+11	1.95E+12	1.82E+12	4.10E+12
1.55	3.40E+12	1.94E+12	5.69E+12	4.95E+11	3.11E+12	1.94E+12	4.90E+12
1.65	7.29E+11	1.07E+11	1.02E+12	4.59E+10	2.78E+11	3.09E+11	6.86E+11
1.75	8.81E+11	7.12E+10	1.25E+12	3.60E+10	2.97E+11	3.63E+11	8.27E+11
1.85	3.48E+11	3.21E+10	4.88E+11	1.53E+10	1.16E+11	1.41E+11	3.17E+11
1.95	6.52E+11	3.13E+10	9.26E+11	1.92E+10	2.00E+11	2.62E+11	6.00E+11
2.05	2.75E+11	1.33E+10	3.86E+11	8.02E+09	8.18E+10	1.09E+11	2.47E+11
2.15	6.17E+12	5.79E+10	7.68E+12	6.88E+10	9.77E+11	1.94E+12	4.02E+12
2.25	2.44E+10	8.76E+08	3.55E+10	6.06E+08	7.78E+09	1.00E+10	2.35E+10
2.35	4.48E+11	1.36E+10	6.43E+11	1.06E+10	1.36E+11	1.80E+11	4.19E+11
2.45	2.80E+11	8.24E+09	3.99E+11	6.47E+09	8.29E+10	1.12E+11	2.58E+11
2.75	1.60E+11	5.33E+09	2.32E+11	3.91E+09	4.98E+10	6.53E+10	1.52E+11
3.25	2.18E+10	7.30E+08	3.17E+10	5.39E+08	6.89E+09	8.94E+09	2.09E+10
3.75	1.33E+07	1.87E+07	2.88E+07	1.10E+06	2.41E+07	7.42E+06	3.17E+07
4.5	3.30E+06	1.66E+07	1.34E+07	7.83E+05	1.90E+07	3.14E+06	2.03E+07
5.5	1.11E+06	5.58E+06	4.52E+06	2.64E+05	6.40E+06	1.06E+06	6.83E+06
7.0	4.83E+05	2.42E+06	1.96E+06	1.14E+05	2.78E+06	4.59E+05	2.97E+06
9.0	5.52E+04	2.77E+05	2.24E+05	1.31E+04	3.18E+05	5.24E+04	3.39E+05

Source-5 and Source-6 correspond to intermediate decay heat values (1.3 and 0.7 kW/ assembly, respectively) and complement each other. This combination of decay heat values results in a minimal peak clad temperature (see Figure 4.1). Additional information on the source term calculations and results is provided in Appendix B.

4.3 Dose Rates

The derived source terms were used as input to the dose rate calculations, which were made with MCNP. Calculations are reported in the following subsections.

4.3.1 Surry Fuel

Dose rates on the side of the TN-24P cask, calculated with MCNP, are compared with measured dose rates in Figures 4.7 and 4.8. The calculated photon dose rates perpendicular to the active fuel are somewhat higher than the measured values. This is probably because the cobalt content of the grid spacers was assumed to be higher than actually existed. Photon dose rate peaks near the top and bottom of the cask are due to ^{60}Co photons in the plenum and end fittings. The calculated photon dose rates near the bottom of the cask are in excellent agreement with measured dose rates. The calculated photon dose rates near the top of the cask are a factor of 2 higher than the measured dose rates. This is attributable to the conservative method of estimating the ^{60}Co photon source in the plenum and top end fitting (see Appendix B).

The calculated neutron dose rates on the side of the cask are in good agreement with measured dose rates. Neutron dose rate peaks near the top and bottom of the cask occur because the radial neutron shield terminates at these elevations. The tabulated neutron and photon dose rates are given in Appendix C. Calculated neutron and photon dose rates for the top of the TN-24P cask are compared with measured values in Appendix C.

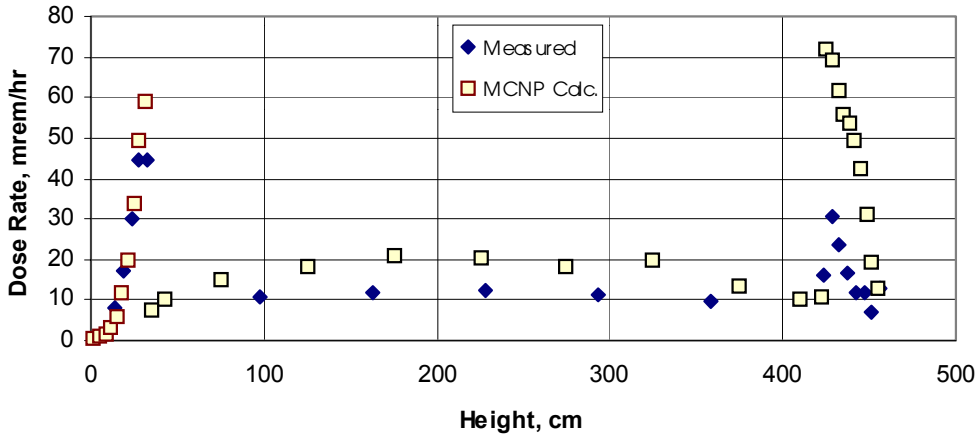

Figure 4.7. Comparison of the Measured and Predicted Photon Dose Rates on the Side of the TN-24P Cask

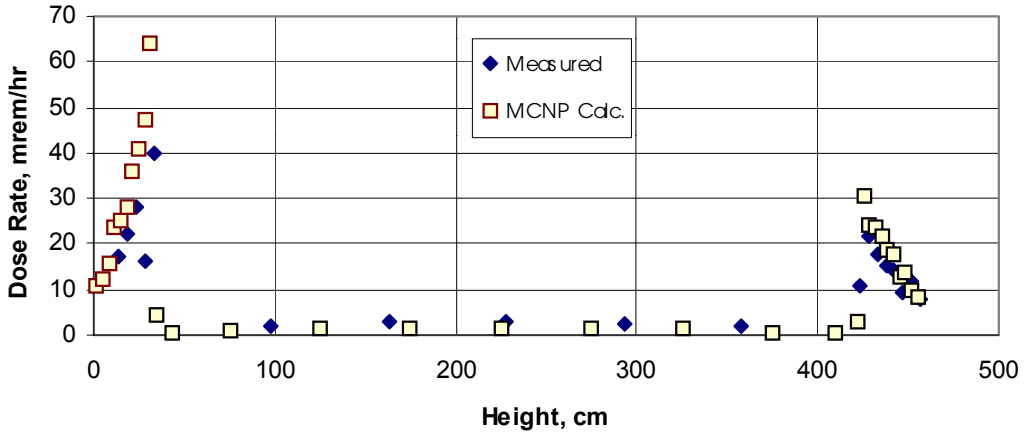

Figure 4.8. Comparison of the Measured and Predicted Neutron Dose Rates on the Side of the TN-24P Cask

4.3.2 Load Pattern Effects

The second part of the shielding analysis was to use the source terms thus derived, corresponding to various decay heat values, to determine the dose rates on the outside of the cask. The decay heats selected included those associated with a uniform heat load in the cask (Case 1 of Table 4.1), the decay heat combination required for the lowest peak clad temperature in the cask for nitrogen and vacuum backfills (Case 14), and the extremes of the thermal analysis (Case 2 and Case 11). The dose rates were calculated with the MCNP code.

Dose rate profiles for the top and bottom of the cask are shown in Figures 4.9 and 4.10. A typical dose profile for the side of the cask is shown in Figure 4.11. Numerical values for the top and bottom peak values and the mid-plane value on the side of the cask are given in Table 4.5.

The photon dose rate on the top of the cask is dominated by the ^{60}Co in the plenum and top end fittings. The photon dose rate on the top of the cask has two peaks (see Figure 4.9a), one at a radius of 85 cm and one at a radius of 135 cm. These locations reflect the geometry of stepped thickness of the lid, where the minimum thickness of steel corresponds to the photon dose rate peaks. The bottom of the cask has a uniform thickness and does not have the peaks in photon dose rates that are apparent on the lid (see Figure 4.10a). Examination of the photon dose rate at the center of the lid and center of the bottom of the cask shows the predominant influence of the fuel loaded in the center of the cask with some contribution of hotter fuel loaded around the periphery of the cask.

The neutron source is associated with the fuel and is farther from the lid and bottom of the cask than the photon source. Comparison of the dose rates from parts (a) and (b) of Figures 4.9 and 4.10 show that neutron dose rate is generally greater than the photon dose rate. This is caused by the relative thickness of the steel lid and the neutron shield. The effectiveness of the neutron shield can be seen by comparing the neutron dose rates for the top of the cask, which

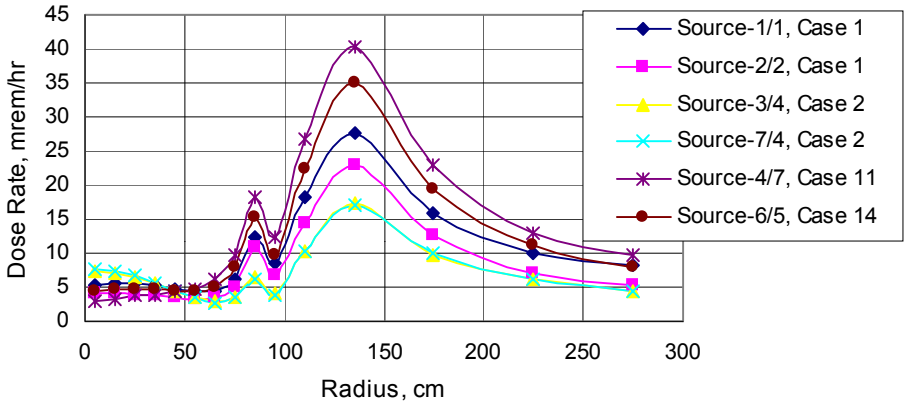

(a) Gamma dose rate profile

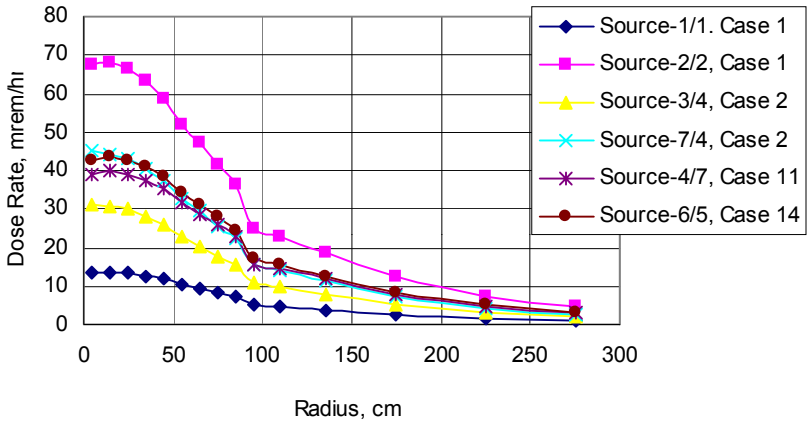

(b) Neutron dose rate profile

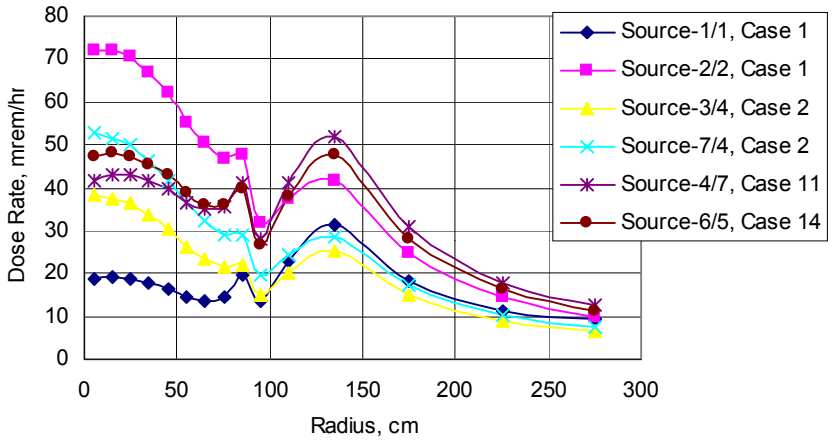

(c) Total dose rate profile

Figure 4.9. Dose Rate Profiles on the Top Surface of the Cask for Various Load Patterns

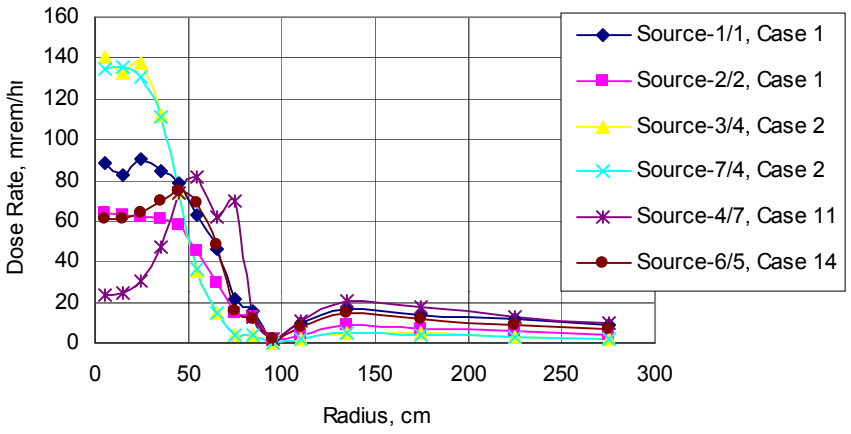

(a) Gamma dose rate profile

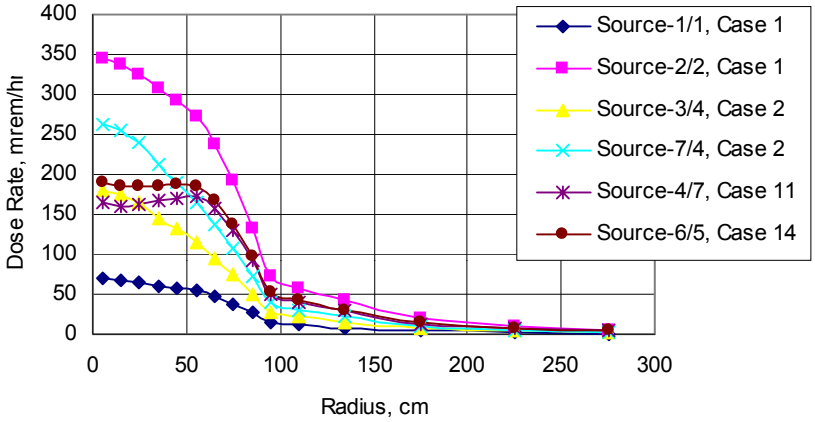

(b) Neutron dose rate profile

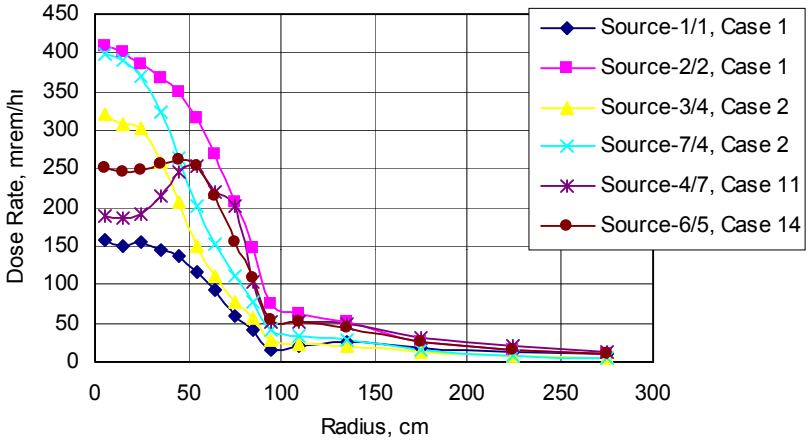

(c) Total dose rate profile

Figure 4.10. Dose Rate Profiles on the Bottom Surface of the Cask for Various Load Patterns

has a neutron shield, with the neutron dose rate for the bottom of the cask, which does not have a neutron shield. As expected, the uniform loading of 30 and 60 GWd/MTU fuel bound the neutron dose rates for the other loadings.

The total dose rates on the side of the cask are shown in Figure 4.11 for the uniform loadings and one of the mixed loadings. Dose rate peaks at locations 1 and 3 are caused by a combination of the neutron dose rate increasing above and below the radial neutron shield and the ^{60}Co source in the plenum and end fittings. Numerical values for the peak photon and neutron dose rates are provided in Table 4.5. Table 4.5 also compares the peak dose rates on the side of the cask with uniform fuel loadings of 30 and 60 GWd/MTU fuel, Source 1/1 and Source 2/2, respectively. In general, the various load patterns result in dose rates less than that of a uniform loading of high-burnup fuel. The exceptions are cases on the side of the cask, but in these instances, the total dose rates are much less than the peak dose rates and are too low to be of significance.

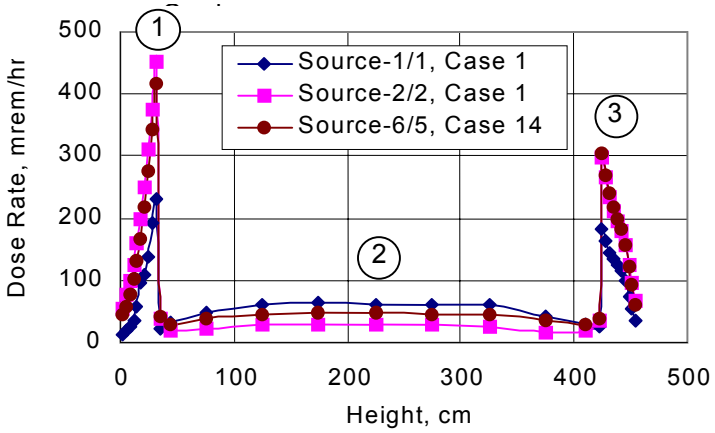

Figure 4.11. Total Dose Rates on the Side of the Cask for Three Loadings

A more limited prior analytical study addressed the effect of mixed loadings on the surface dose rate of a transportation cask. That study was performed with a two-dimensional transport theory code. Those calculations encompassed three cask designs and five burnup/cooling time sets of fuel characteristics. The results of that study showed that the external radiation surface dose rates at a location corresponding to location 2 on Figure 4.11 were determined primarily by the characteristics of the fuel assemblies immediately adjacent to the cask cavity wall. That study has been attached as Appendix D.

Table 4.5. Peak Dose Rates on the Side of the Cask for Various Loading Patterns

Source	Inside Fuel Loading			Outside Fuel Loading			Surface Dose Rates, mrem/hr			Dose relative to Source 1/1			Dose relative to Source 2/2		
	Assembly Decay Heat, kW	Burnup, GWd/MTU	Cooling time, y	Assembly Decay Heat, kW	Burnup, GWd/MTU	Cooling time, y	Neutron	Gamma	Total	Neutron	Gamma	Total	Neutron	Gamma	Total
Top Peak at an elevation of 4.25 m				Position 3 on Figure 4.11											
1/1	1.0	30	3.65	1.0	30	3.65	36	146	182	1.0	1.0	1.0	0.2	1.2	0.6
2/2	1.0	60	9.42	1.0	60	9.42	180	119	299	5.0	0.8	1.6	1.0	1.0	1.0
3/4	1.7	50	3.47	0.3	20	8.92	73	106	178	2.0	0.7	1.0	0.4	0.9	0.6
7/4	1.7	60	4.15	0.3	20	8.92	105	109	214	2.9	0.7	1.2	0.6	0.9	0.7
4/7	0.3	20	8.92	1.7	60	4.15	118	194	312	3.3	1.3	1.7	0.7	1.6	1.0
6/5	0.7	30	4.91	1.3	60	5.81	126	178	304	3.5	1.2	1.7	0.7	1.5	1.0
Bottom Peak at an elevation of 31 cm				Position 1 on Figure 4.11											
1/1	1.0	30	3.65	1.0	30	3.65	69	162	231	1.0	1.0	1.0	0.2	1.5	0.5
2/2	1.0	60	9.42	1.0	60	9.42	344	107	452	5.0	0.7	2.0	1.0	1.0	1.0
3/4	1.7	50	3.47	0.3	20	8.92	130	70	199	1.9	0.4	0.9	0.4	0.7	0.4
7/4	1.7	60	4.15	0.3	20	8.92	186	67	253	2.7	0.4	1.1	0.5	0.6	0.6
4/7	0.3	20	8.92	1.7	60	4.15	241	220	461	3.5	1.4	2.0	0.7	2.0	1.0
6/5	0.7	30	4.91	1.3	60	5.81	253	164	417	3.7	1.0	1.8	0.7	1.5	0.9
Mid-plane dose at an elevation of 2.25 m				Position 2 on Figure 4.11											
1/1	1.0	30	3.65	1.0	30	3.65	2	60	62	1.0	1.0	1.0	0.2	3.3	2.1
2/2	1.0	60	9.42	1.0	60	9.42	11	18	29	5.0	0.3	0.5	1.0	1.0	1.0
3/4	1.7	50	3.47	0.3	20	8.92	4	11	14	1.5	0.2	0.2	0.3	0.6	0.5
7/4	1.7	60	4.15	0.3	20	8.92	5	12	17	2.2	0.2	0.3	0.4	0.7	0.6
4/7	0.3	20	8.92	1.7	60	4.15	9	65	74	4.0	1.1	1.2	0.8	3.6	2.5
6/5	0.7	30	4.91	1.3	60	5.81	9	38	47	4.1	0.6	0.8	0.8	2.1	1.6

5.0 Conclusions

The conclusions are presented in two sections. The first deals with the thermal performance and the second with shielding performance.

5.1 Thermal Performance

The thermal performance was assessed for 17 different cases that varied from a uniform load pattern, where each of the 24 fuel assemblies was assumed to generate 1 kW, to load patterns where the hot assemblies generated 1.7 kW while their complimentary assemblies generated 0.3 kW. Each load pattern examined resulted in a total decay heat load for the cask of 24 kW. Because of the ease of changing backfill gas properties in the model, the analysis was duplicated for three backfill gases, helium, nitrogen, and vacuum.

- All other things being equal, the most significant parameter in determining cask thermal performance is the backfill medium, with helium providing the lowest temperatures, nitrogen or air giving temperatures 5–10% higher, and vacuum giving temperatures about 15% higher than those obtained with helium.

- The results of this study show that fuel loading patterns with cooler fuel assemblies in the middle and hotter fuel assemblies to the periphery of the cask will give better thermal performance regardless of the backfill medium.

- For a given decay heat load in the cask, loading assemblies with higher decay heat output around the outside of the cask will result in lower peak fuel cladding temperatures than loading hotter assemblies in the center of the cask.

- For all practical loadings using helium or vacuum backfills, loading the hot assemblies around the outside of the cask basket will result in lower peak clad fuel temperatures than a uniformly loaded cask with the same total decay heat output.

- With optimum loading in the cask, the peak fuel clad temperature can be reduced 17°, 8°, and 13°C for helium, nitrogen, and vacuum backfills, respectively.

- Reversing the load pattern so the hot assemblies are moved to the inside of the cask increases peak fuel clad temperatures by 35°, 22°, and 55°C for helium, nitrogen, and vacuum backfills, respectively.

5.2 Shielding Performance

Based on the outcome of the thermal analysis, seven source terms were generated that correspond to selected decay heat values used in the load-pattern thermal analysis. Source terms were calculated using fuel burnups of 20 to 60 GWd/MTU and enrichments of 2.4 to 4.8%. Cooling times were selected to provide decay heat terms that correlate with the thermal analysis.

5.2.1 Photon Dose Rates

- Calculated photon dose rates for the TN-24P cask are in good agreement with measured values.
- Photon dose rates are dominated by the ^{60}Co in the bottom end fittings, top end fittings, and plenum.
- Photon dose rates are maximal in directions perpendicular to the surfaces and at angles where the effective steel thickness is reduced.
- Photon dose rates are proportional to fuel burnup and decrease with increasing cooling time reflecting the half-life of ^{60}Co.
- For short cooling times, photon dose rates on the side of the cask are somewhat higher due to short-lived fission products. For longer cooling times, ^{137}Cs is the dominant photon dose-rate contributor.
- Cask loadings with high decay heat assemblies near the periphery exhibit increased photon dose rates on the side surface and top and bottom surfaces away from the centerline. Near the centerline, the dose rates are reduced substantially.
- Load patterns result in dose rates less than a uniform loading of the highest burnup fuel.

5.2.2 Neutron Dose Rates

- Calculated neutron dose rates for the TN-24P cask are in good agreement with measured values
- Neutron dose rates increase exponentially with fuel burnup and are nearly independent of cooling time.
- Neutron dose rates peak in directions where there is no neutron shield such as oblique angles near the top and bottom of the cask as well as directly through the bottom of the cask.
- Cask loadings with high decay heat assemblies minimally impact the neutron dose rates.

.

6.0 References

American Nuclear Society (ANS). 1977. *American National Standard Neutron and Gamma-Ray Flux-to-Dose-Rate Factors.* ANSI/ANS-6.1.1-1977, American Nuclear Society, LaGrange Park, Illinois.

Bowman SM and LC Leal. 1998. *ORIGEN-ARP: Automatic Rapid Process for Spent Fuel Depletion, Decay, and Source Term Analysis*. NUREG/CR-0200 Rev. 6, Oak Ridge National Laboratory, Oak, Ridge, Tennessee.

Briesmeister JF. 1997. *MCNP—A General Monte Carlo N-Particle Transport Code.* LA-2625-M Ver. 4B, Los Alamos National Laboratory, Los Alamos, New Mexico.

Creer JM, TE Michener, MA McKinnon, JE Tanner, ER Gilbert, RL Goodman, DH Schoonen, M Jensen, C Mullen, D Dziadosz, EV Moore, HS McKay, and DP Batalo. 1987. *The TN-24P PWR Spent Fuel Storage: Testing and Analyses*. EPRI NP-5128 (PNL-6054), Electric Power Research Institute, Palo Alto, California.

Croff AG. 1980. *ORIGEN2—A Revised and Updated Version of the Oak Ridge Isotope Generation and Depletion Code*. ORNL-5621, Oak Ridge National Laboratory, Oak Ridge, Tennessee.

McKinnon MA, JW Doman, JE Tanner, RJ Guenther, JM Creer, and CE King. 1986. *BWR Spent Fuel Storage Cask Performance Test, Volume I, Cask Handling Experience and Decay Heat, Heat Transfer, and Shielding Data*. PNL-5777 Vol. 1, Pacific Northwest Laboratory, Richland, Washington.

McKinnon MA and VA Deloach. 1993. *Spent Nuclear Fuel Storage - Performance Tests and Demonstrations*. PNL-8451, Pacific Northwest Laboratory, Richland, Washington.

Michener TE, DR Rector, JM Cuta, RE Dodge, and CW Enderlin. 1995. *COBRA-SFS: A Thermal-Hydraulic Analysis Code for Spent Fuel Storage and Transportation Casks*. PNL-10782, Pacific Northwest National Laboratory, Richland, Washington.

Rector DR, RA McCann, UP Jenquin, CM Heeb, JM Creer, and CL Wheeler. 1986. *CASTOR-1C Spent Fuel Storage Cask Decay Heat, Heat Transfer, and Shielding Analysis.* PNL-5974, Pacific Northwest Laboratory, Richland, Washington.

Transnuclear Inc. 1985a. *TN-24 Dry Storage Cask Topical Report.* E-7107, Transnuclear Inc., White Plains, New York.

Transnuclear Inc. 1985b. *TN-24P Cask Operations Manual*. E-7455 Rev. 0, Transnuclear Inc., White Plains, New York

Wiles LE, NJ Lombardo, CM Heeb, UP Jenquin, TE Michener, CL Wheeler, JM Creer, and RA McCann. 1986. *BWR Spent Fuel Storage Cask Performance Test, Volume II, Pre- and Post-Test Decay Heat, Heat Transfer, and Shielding Analyses*. PNL-5777 Vol. II, Pacific Northwest Laboratory, Richland, Washington.

Appendix A

Additional Detail Resulting from the Thermal Analysis

Appendix A:
Additional Detail Resulting from the Thermal Analysis

The cask performance tests performed by DOE at INEEL have shown the effect of backfill medium on the thermal performance of casks. This study investigates the effect of the fuel loading pattern on thermal performance

A.1 Backfill Medium

The first and most obvious choice for the backfill of any cask is air, which is readily available at an extremely low cost and comes installed in the cask. Despite these advantages, air is not the ideal choice. It has relatively poor thermal properties because it is a poor conductor and has only a very modest convective capacity. Its only real advantage is that it is essentially transparent to radiative heat exchange, but this is true of most ideal gases at low temperatures. One major disadvantage of air in this application is that it contains oxygen and often a significant amount of water vapor, either or both of which can cause serious corrosion problems for the spent fuel and the cask internals. This can be obviated by using nitrogen, a relatively nonreactive gas that is the major constituent of air and readily and cheaply available. The thermal properties of nitrogen are essentially those of air (or, rather, the thermal properties of *air* are essentially those of nitrogen), so using nitrogen rather than air does not enhance the heat transfer effectiveness of the backfill medium.

An inert gas such as helium has the advantage of being chemically nonreactive and, as a backfill medium displaces the air in the cask, removing oxygen and water vapor, the main sources of potential corrosion problems. In addition, helium has far better thermal properties than air. Helium has a thermal conductivity that is an order of magnitude higher and has a specific heat nearly six times greater than that of air or nitrogen. As a backfill medium, helium does not tend to promote natural convection, but it allows much more heat transfer by conduction and is transparent to radiative heat transfer. This makes it an excellent choice as a backfill medium. Its only real disadvantage is the tendency of this extremely light gas to escape from whatever container it happens to be in.

A third option is to have no backfill medium at all; that is, to remove all internal gas by pumping the sealed cask down to a modest vacuum. This essentially eliminates any heat transfer by means of natural convection within the cask and cuts conduction through the fluid down to a very low level (but not exactly zero because the vacuum within the cask is unlikely to be *that* hard). The only effective means of heat transfer in this case is conduction in solid materials and radiative exchange between the fuel rods and the internal structures of the cask. These are the dominant modes of heat transfer in a cask, so the loss of natural convection and conduction in the fluid may not seriously compromise performance. For all cask configurations considered in this study, calculations were made with helium, nitrogen, and vacuum backfill.

A.2 Fuel Loading Pattern

A particular cask design will have a maximum permissible heat load per fuel assembly, which implies a uniformly loaded cask. The actual loading pattern in a given cask will depend on the characteristics of the fuel that is stored in it. If the real fuel has a significantly different power distribution bundle to bundle than the design basis fuel assembly, it can affect the peak clad temperature experienced in the cask substantially.

Basically only three radial power distributions are possible in a cask loaded with spent fuel: uniform (that is, with all assemblies at essentially the same power), hot assemblies in the center and colder assemblies closest to the cask wall, or colder assemblies in the center and hotter assemblies closest to the cask wall. It is not immediately obvious which pattern would be the most advantageous for heat transfer in a given cask design.

With the hottest fuel in the center, the radial temperature gradient is likely to be fairly steep, which would tend to promote radiative and conductive heat transfer. This arrangement results in the longest heat transfer path between the hottest fuel and the environment, however, which would tend to make the temperatures higher than with a uniform power distribution. With the hotter fuel near the cask wall and the colder fuel in the center, on the other hand, the heat transfer path between the hottest fuel and the environment would be much shorter, which would tend to reduce the peak temperature. But in this configuration, the hotter fuel would present a barrier to heat transfer from the colder fuel in the center, and this would tend to drive temperatures up.

For a given design power level for a cask, nonuniform loading patterns can be expected to enhance natural convection by creating larger radial temperature gradients within the cask. They also might be expected to enhance radiative heat transfer and possibly conduction heat transfer because of larger radial temperature differences between adjacent fuels. It is by no means clear, however, that this would outweigh the localized effects of higher power generation in individual rods within the hotter fuel bundles or the self-shielding effect that would be produced by placing colder fuel in the center of the cask and hotter fuel near the wall.

In this study, radial power distributions ranging from uniform to a peak-to-average bundle power ratio of 1.7 were considered. The value of 1.7 represents the upper limit of the range of powers likely to be encountered in spent fuel that is cool enough for dry storage. For each pattern with the hotter fuel in the center, the test matrix includes a complementary pattern with the hotter fuel on the outside and the colder fuel in the center.

The following subsections examine the temperatures in the cask for the various cases in somewhat greater detail, showing the sensitivity of the results to the parameters investigated. Table A.1 provides a listing of the various cases analyzed.

A.3 Axial Temperature Profiles

The axial distribution of power in a spent fuel bundle depends primarily on the burnup history of the assembly and can vary greatly from bundle to bundle and plant to plant, even for nominally identical fuel assemblies. However, for most light water reactor (LWR) fuel, the

Table A.1 Selected Cases for Parametric Study of Radial Power Distribution Patterns

Case	Loading Pattern	Hot Assemblies (kW)	Cooler Assemblies (kW)	Total Assembly Power (kW)	Radial Peaking (Peak-To-Average Ratio)
1	uniform power	1000	1000	24	1.0
2	hotter inside	1700	300	24	1.7
3	hotter inside	1100	900	24	1.1
4	hotter inside	1200	800	24	1.2
5	hotter inside	1300	700	24	1.3
6	hotter inside	1400	600	24	1.4
7	hotter inside	1500	500	24	1.5
8	hotter inside	1600	400	24	1.6
9	3 levels of power; hottest inside	1500	1200, 700	24	1.5
10	3 levels of power; hottest outside	1500	600, 300	24	1.5
11	hotter outside	1700	300	24	1.7
12	hotter outside	1100	900	24	1.1
13	hotter outside	1200	800	24	1.2
14	hotter outside	1300	700	24	1.3
15	hotter outside	1400	600	24	1.4
16	hotter outside	1500	500	24	1.5
17	hotter outside	1600	400	24	1.6

power shape at end of life tends to be very flat, with a relatively sharp rolloff at either end of the active length. An axial profile based on aged pressurized water reactor (PWR) fuel with a nominal peak-to-average ratio of 1.1 was selected for use in the COBRA-SFS calculations for this study. Figure A.1 shows a plot of the axial profile used.

With such a flat axial power profile, the general shape of the axial temperature distribution for the fuel in the storage cask depends primarily on the dominant mode of heat transfer to the environment outside the cask. For conditions where conduction and radiative heat exchange dominate, the temperature profile will have approximately the same shape as the axial power profile. If natural convection within the cask is a significant mode of heat transfer, the axial profile will be skewed, with the peak temperature somewhere in the upper third of the assembly axial length.

Figure A.2 shows axial temperature profiles for the hot rod obtained with helium backfill for uniform power (Case 1), the case highest peak clad temperature (Case 2), and the case with the lowest peak clad temperature (Case 14). The case with the highest radial peaking with the hotter fuel to the outside (Case 11) is also included, since it is the hottest case with this radial peaking pattern. The highest peak clad temperature occurs with the hotter fuel to the inside and maximum radial power factor of 1.7, the highest value in the range tested and the upper limit expected for spent fuel in dry storage. The lowest peak clad temperature occurs with the hotter fuel to the outside and a value of about 1.3 for the maximum radial power factor.

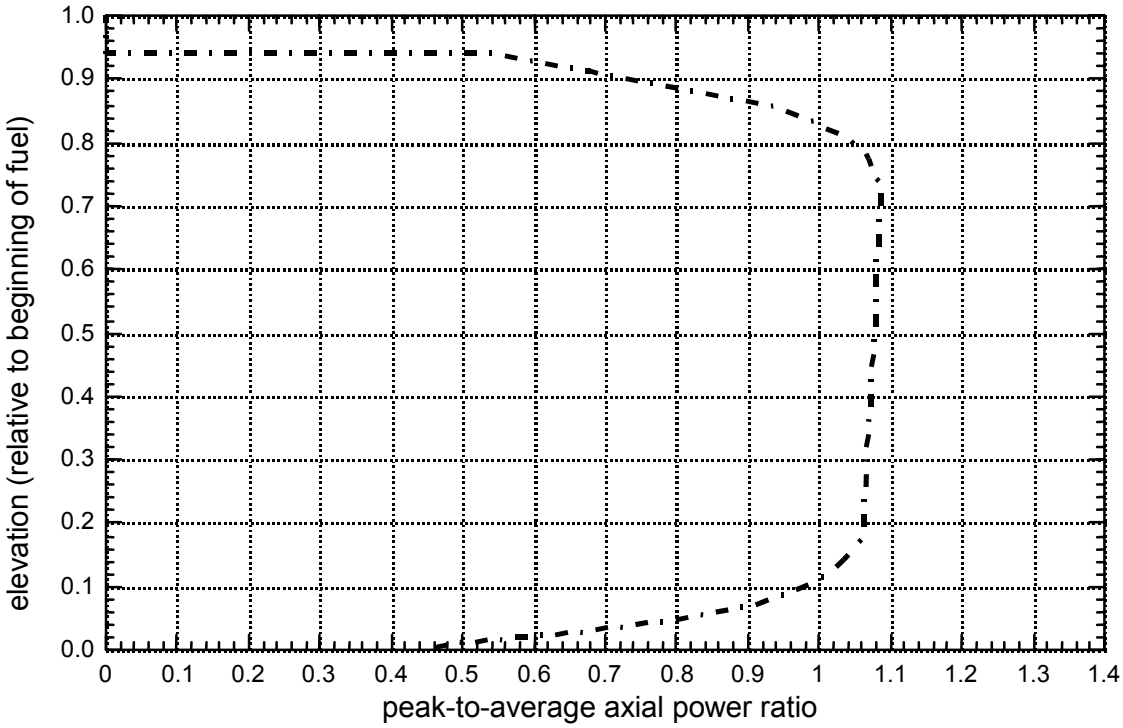

Figure A.1. Axial Power Profile Specified for COBRA-SFS Calculations in TN-24P Cask

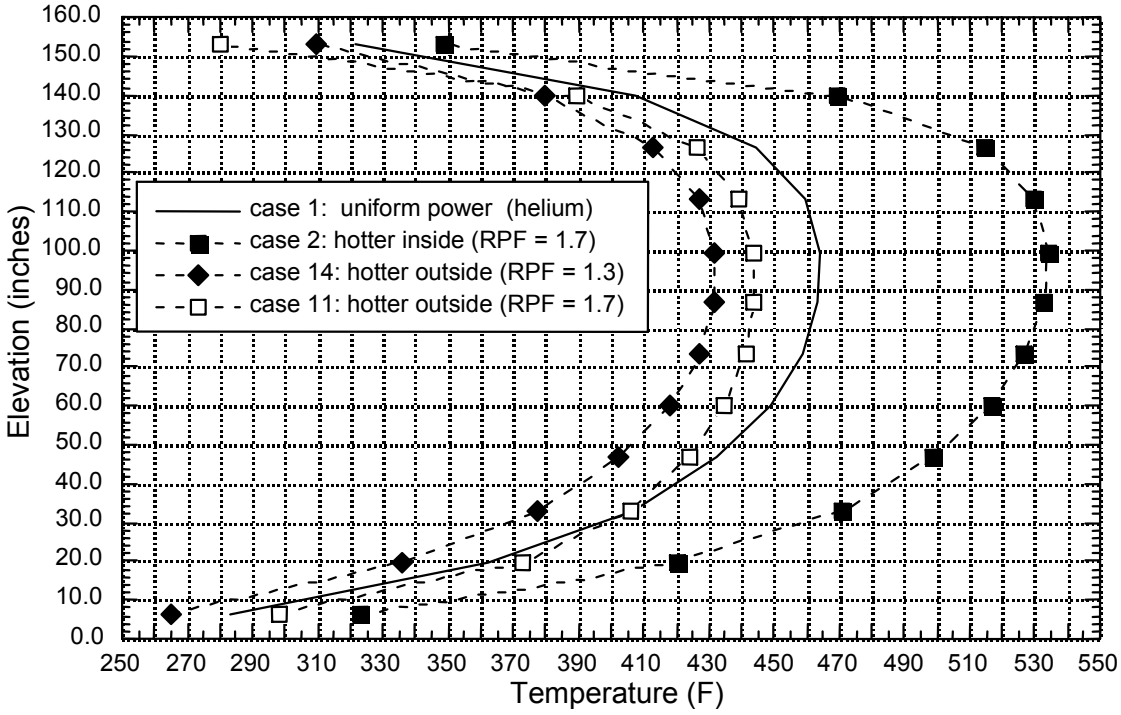

Figure A.2. Axial Temperature Profiles Predicted for the Hot Rod with Helium Backfill

The profiles in Figure A.2 show that, with helium backfill, nearly all the heat moves radially out of the cask by means of conduction and radiative heat transfer. Natural convection does not contribute significantly to the thermal behavior of the cask. This trend is further illustrated in Figure A.3, which shows axial temperature profiles for helium backfill for all cases with hotter fuel to the inside. As the peak radial power factor increases, the peak clad temperature increases in an essentially linear fashion over the range tested. The axial temperature profile of the hot rod retains the same conduction- and radiation-dominated shape as the uniform power case, only the peak value increases.

The axial temperature profiles for the cases with the hotter fuel to the outside also show the same behavior, as can be seen in Figure A.4. The profiles all have essentially the same shape, differing only by being stretched to slightly higher or lower peak clad temperatures, depending on the maximum radial peaking of a given case.

The axial temperature profiles for the hot rod with vacuum backfill show essentially the same shape as those with helium backfill, although at much higher peak temperature values, as shown in Figure A.5. The profiles are more symmetrical about the peak temperature than the profiles obtained for the same cases with helium backfill, which indicates that there is a small but not entirely negligible amount of natural convection heat transfer in the helium. This is not the case with vacuum backfill because natural convection is necessarily rather negligible when there is

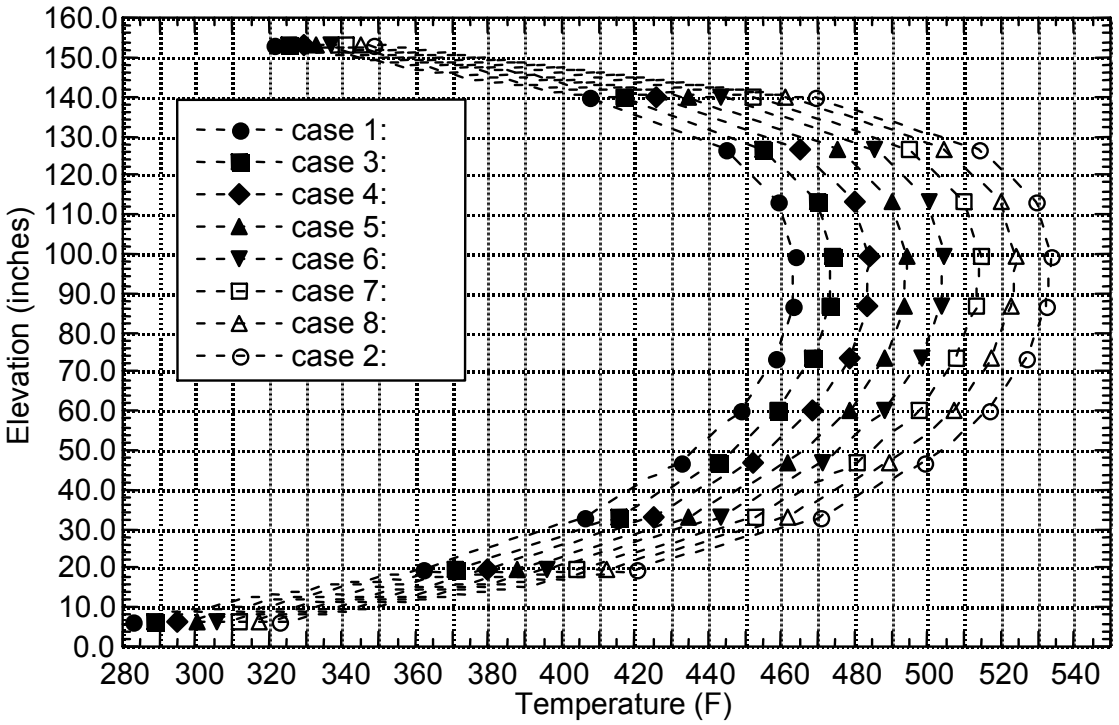

Figure A.3. Axial Temperature Profiles for the Hot Rod with Helium Backfill for all Cases with Hotter Fuel to the Inside

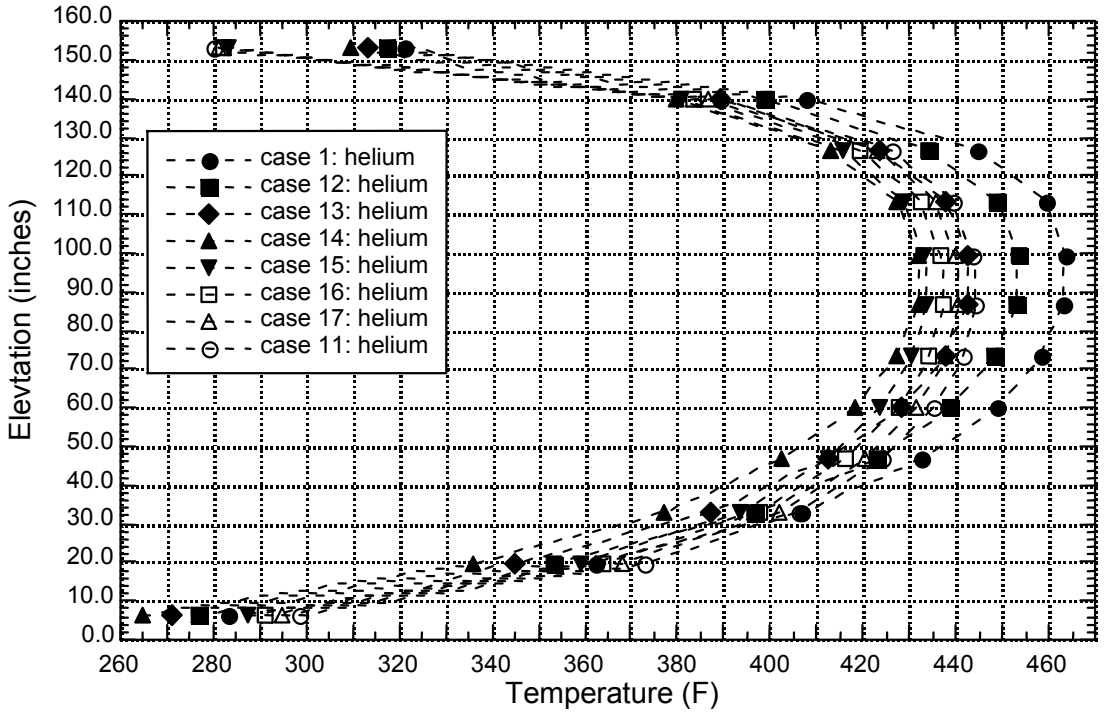

Figure A.4. Axial Temperature Profiles for the Hot Rod with Helium Backfill for all Cases with Hotter Fuel to the Outside

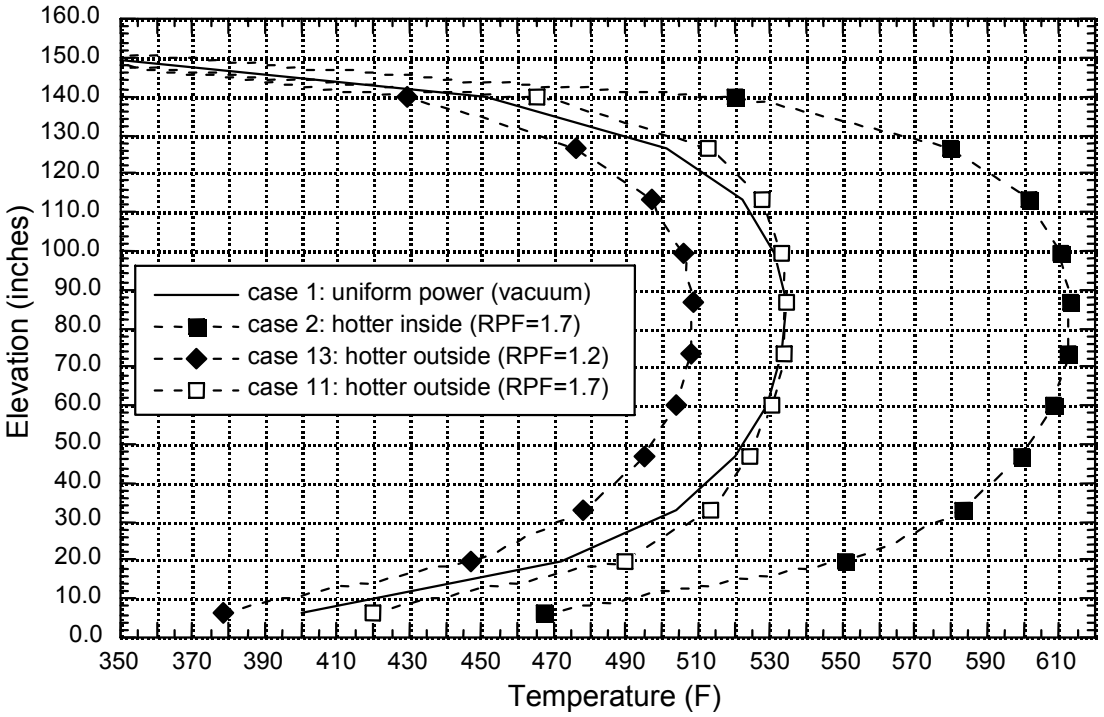

Figure A.5. Axial Temperature Profiles Predicted for the Hot Rod with Vacuum Backfill

essentially no gas available to serve as a convective heat transfer medium. Conduction through the solid material of the cask internals and radiative heat transfer are the dominant modes with vacuum backfill. This behavior was consistent over all radial power distributions tested.

With nitrogen backfill, the axial temperature profiles show clear evidence of natural convection heat transfer, as shown in Figure A.6. Other studies (Lombardo et al. 1986; Cuta and Creer 1986) have shown that conduction and radiative heat transfer are also important with nitrogen (or air) backfill, and none of the three modes can be neglected in the thermal analysis of the cask. This behavior was consistent over all radial power distributions tested.

The results of this study show that radial power distribution has essentially no effect on the shape of the axial temperature distribution in the cask. The axial power shape could have some effect on the temperature distribution, but in practice, spent fuel generally has a very flat axial power shape. As a result, the shape of the axial temperature distribution, and to some extent the peak temperatures value, is determined primarily by the backfill medium. All other things being equal, nitrogen backfill will produce a higher peak temperature than helium backfill, and vacuum backfill will yield an even higher peak temperature than nitrogen backfill. This behavior was consistent over the full range of radial power distributions tested and is consistent with previous experience in analyzing cask thermal performance with COBRA-SFS for many different cask designs.

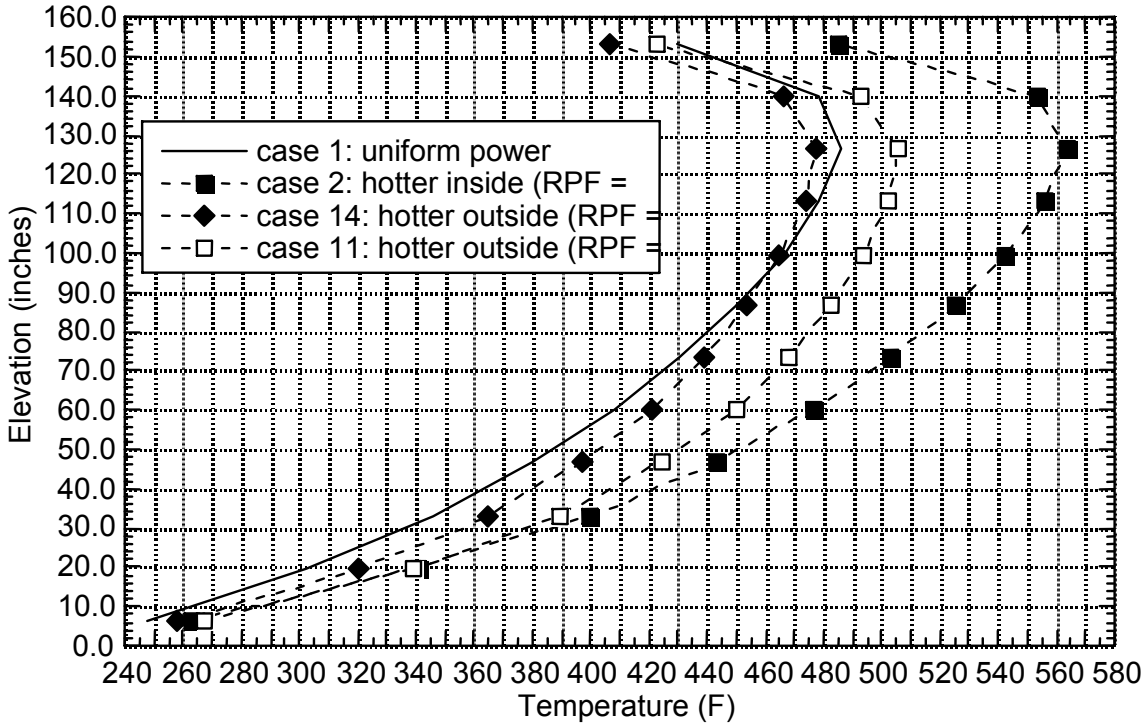

Figure A.6. Axial Temperature Profiles Predicted for the Hot Rod with Nitrogen Backfill

A.4 Radial Temperature Profiles

As with the axial distribution of power in a spent fuel bundle, the total power remaining in the spent fuel depends on the burnup history of the assembly. This will necessarily vary greatly from bundle to bundle and plant to plant, even for fuel assemblies that started life with identical power ratings. The eventual state of all spent fuel, however, is essentially the same because radioactive decay is gradually working the bundle toward a state of zero power generation. The approach is asymptotic and will take thousands of years, but the greatest part of the change occurs before the fuel is cool enough to be maintained in a dry storage environment. Consequently, the actual power difference between any two spent fuel assemblies has a fairly well-defined upper limit. For this study we have assumed that the radial peaking will probably be no more than about 1.7 and will more typically be in the range 1.1 to 1.3.

In this study, the full range of radial peaking from 1.0 up to 1.7 was investigated for all three backfill media. Not surprisingly, the results show that the more uniform the radial power distribution is, the more uniform the radial temperature distribution will be. This result is essentially independent of backfill media, as shown by the radial temperature profiles plotted in Figure A.7 for cases with uniform power, in Figure A.8 for cases with the maximum radial peaking with hotter fuel to the inside, and in Figure A.9 for cases with the maximum radial peaking with hotter fuel to the outside. The plots show the temperatures in the fuel rods and basket structure nodes at the axial location of the peak rod temperature along a radial line passing through the hot rod, extending from the center of the cask to the outer surface.

In all these cases, nearly all of the temperature drop occurs in the fuel assemblies and basket structure. The temperature drop through the cask wall is very nearly the same for all cases, regardless of backfill medium or radial power peaking pattern, and constitutes only a small fraction (about 10%) of the difference between the peak clad temperature and the temperature of the cask surface.

In each of these plots, neither the basic shape of the radial power profile nor the location of the peak clad temperature changes with backfill media. Only the magnitude of the peak temperature changes with changing backfill media. The location of the hot rod and the peak clad temperature both change with changing radial power distribution, even when the backfill medium remains the same.

Figures A.10, A.11, and A.12 illustrate this for the different backfill media by comparing plots of the radial temperature profile for the uniform power case with the profiles for the cases with the highest and lowest peak clad temperatures. With all three backfills, the lowest peak clad temperatures are obtained in radial power configurations with the hotter fuel to the outside (with radial peaking of 1.2 or 1.3). The radial temperatures through the hot rod for these configurations show that the hotter assemblies raise something of a barrier to heat transfer for the rods in the cooler assemblies in the center.

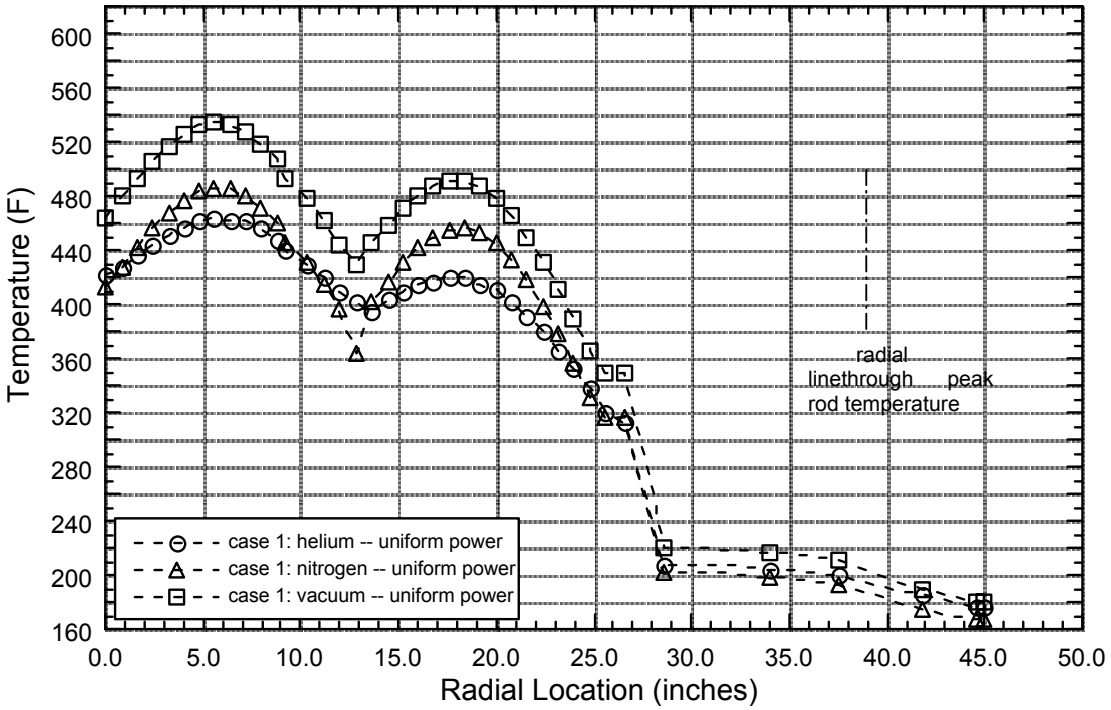

Figure A.7. Radial Temperature Profiles for Uniform Power Distribution

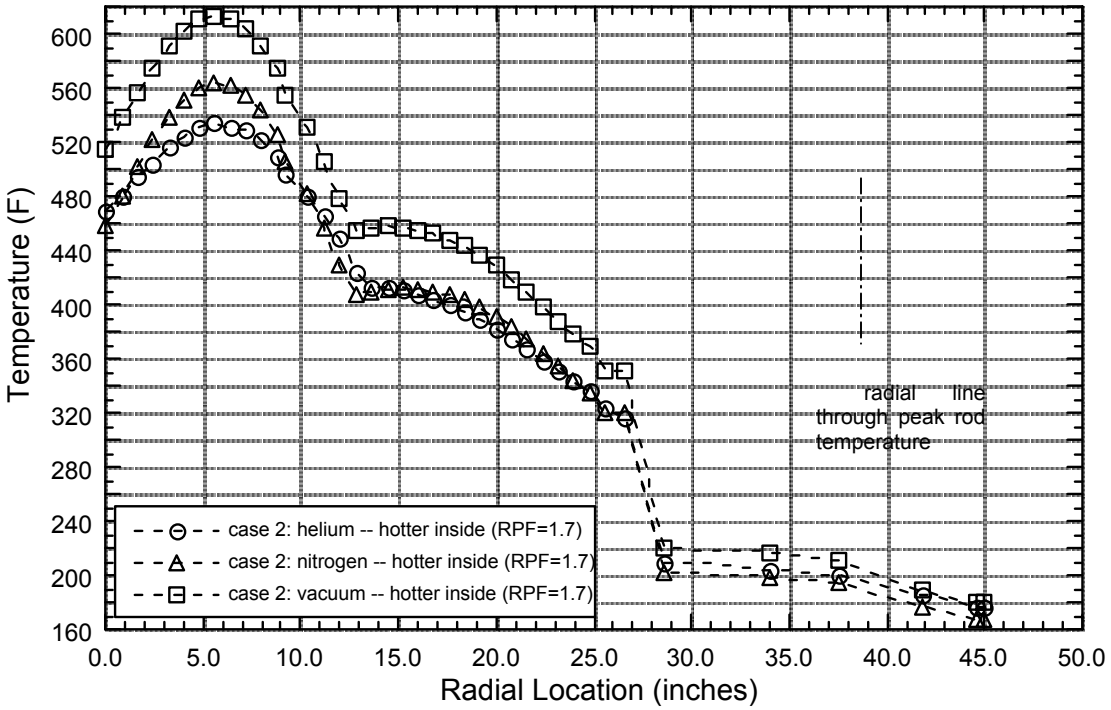

Figure A.8. Radial Temperature Profiles for Maximum Radial Peaking Hotter Fuel to Inside

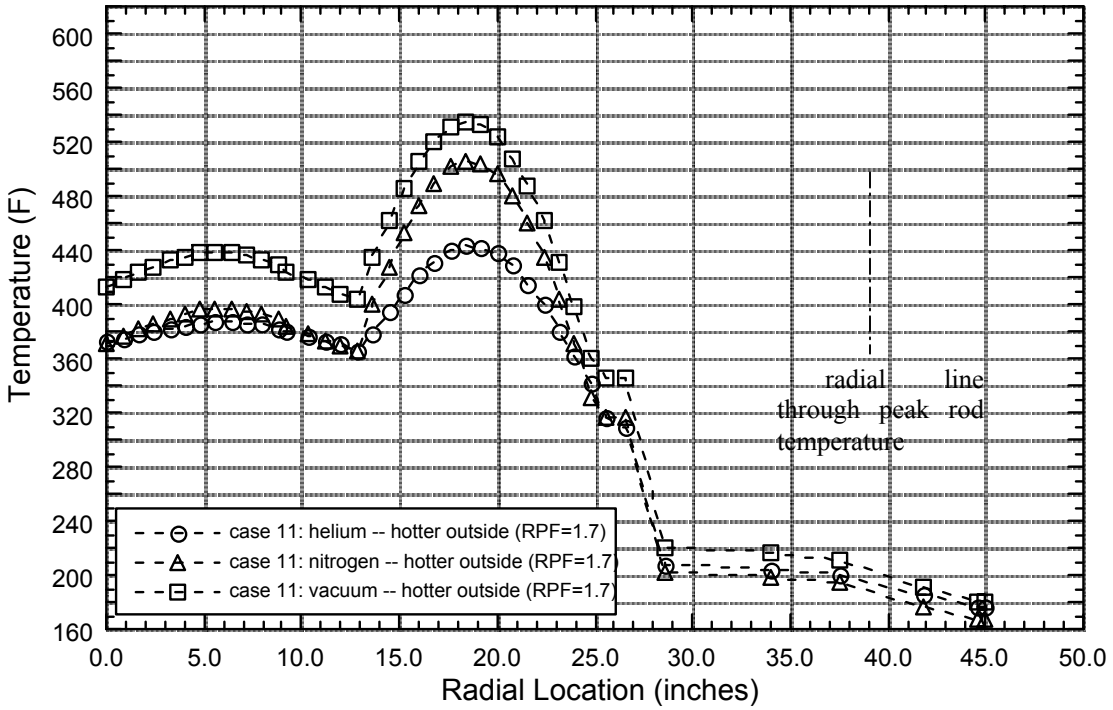

Figure A.9. Radial Temperature Profiles for Maximum Radial Peaking, Hotter Fuel to Outside

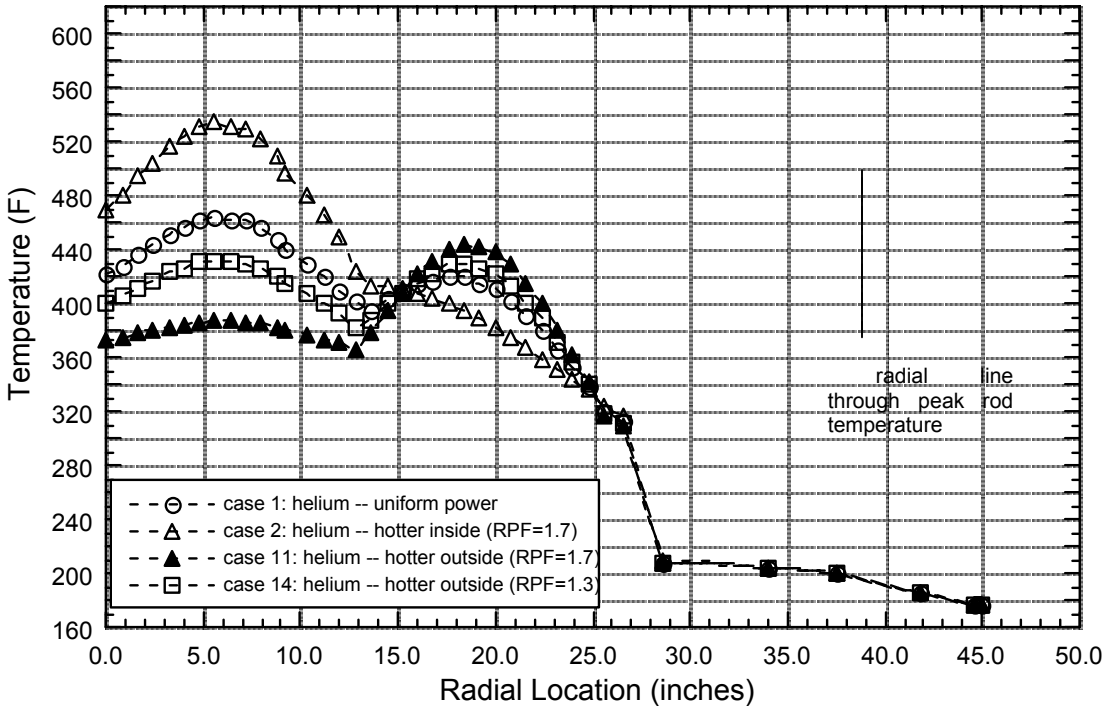

Figure A.10. Radial Temperature Profiles Through the Hot Rod with Helium Backfill

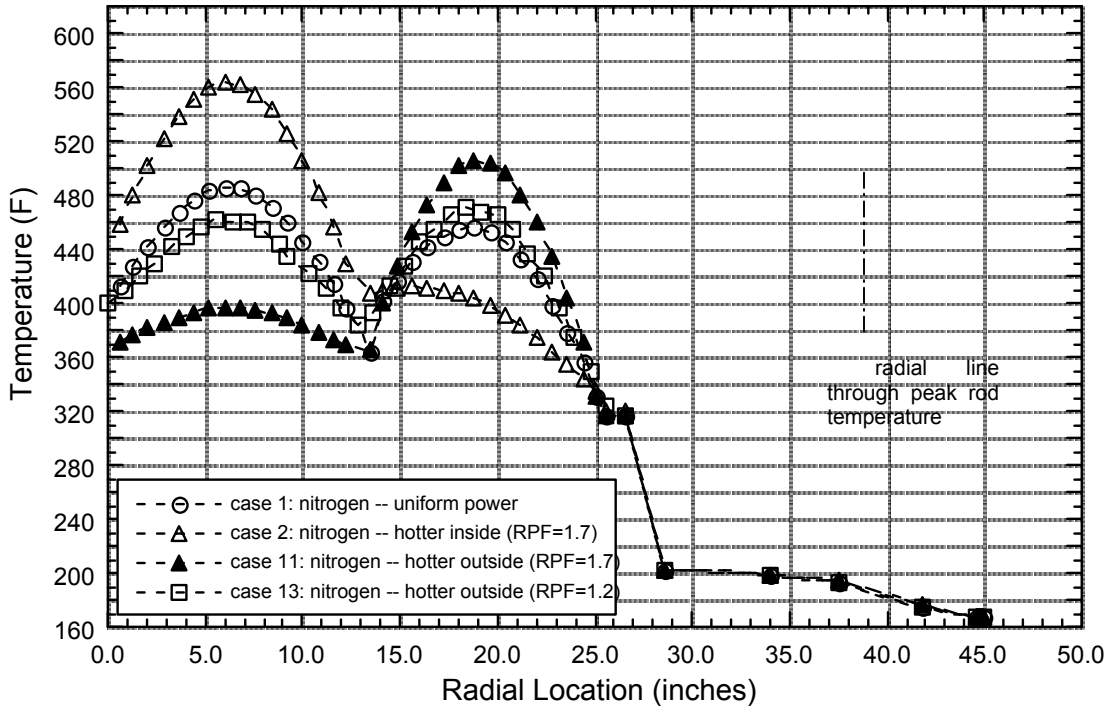

Figure A.11. Radial Temperature Profiles Through the Hot Rod with Nitrogen Backfill

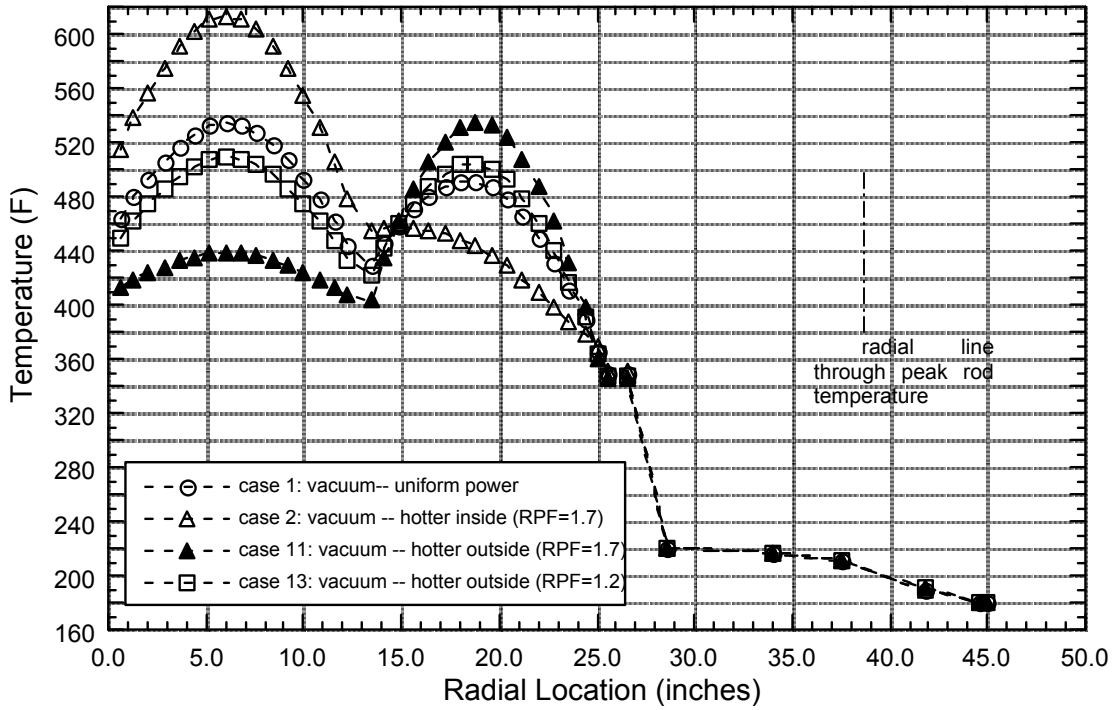

Figure A.12. Radial Temperature Profiles Through the Hot Rod with Vacuum Backfill

If there were no heat transfer paths other than through the rods in the outer assemblies, the temperature distributions shown for these cases would be physically impossible, and results of this form would call into serious question the accuracy of the COBRA-SFS thermal solution. However, the radial profiles shown in Figures A.10 through A.12 are for only a single line through the hot rod. A complete representation of the radial temperature distribution at the level of the peak clad temperature would show a temperature "surface" in three dimensions, with peaks of varying heights at the fuel bundle centers sloping down to long narrow “valleys” along the basket plates. Heat flows along these valleys exactly like water flows down a mountainside into a river valley. The basket structure is in effect a conduit for heat flow from the rods to the inner wall of the cask. Figure A.13 illustrates this path by showing the radial temperature profile along the basket structure at the axial location of the peak clad temperature. The case shown is the radial power configuration with the hottest fuel to the outside (Case 11) for all three backfill media.

These results show that the peak clad temperature in the cask depends on promoting the most effective heat transfer possible between the fuel rods and the basket structure and the inner surface of the cask wall. The backfill medium is an important factor in this endeavor because it will determine the effectiveness of heat transfer by natural convection and conduction through the fluid. The results of this study show that the radial power distribution can also be extremely important because it helps determine the steepness of the temperature gradients within the assemblies and the length of the heat transfer paths, either for conduction or radiative heat exchange.

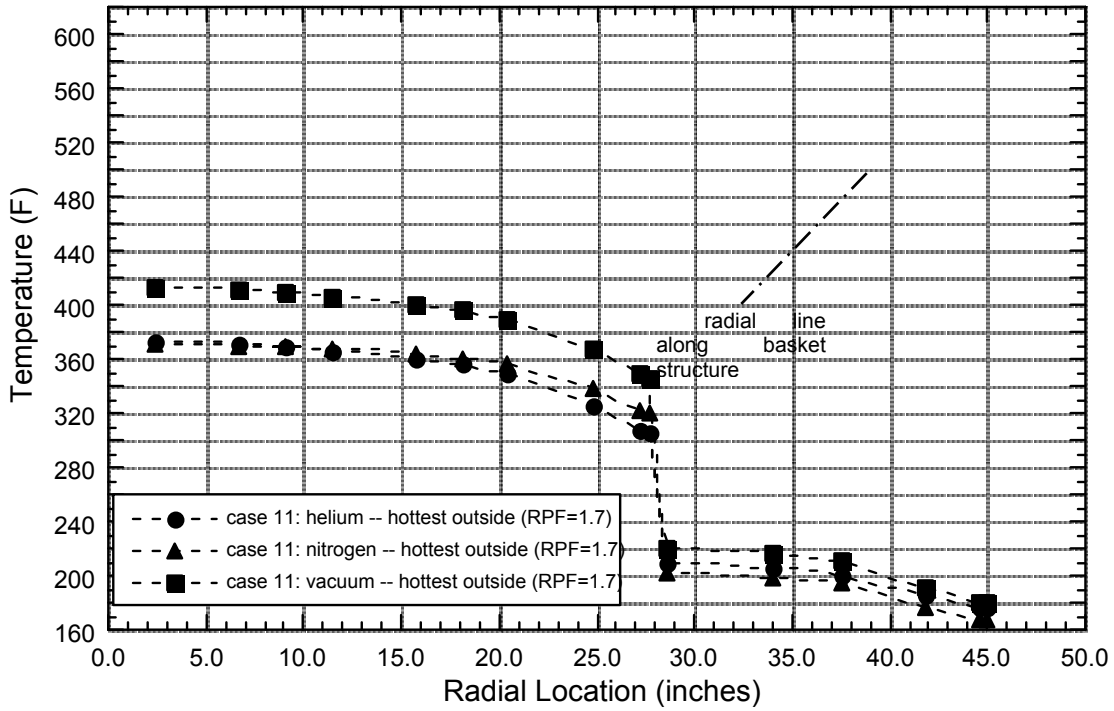

Figure A.13. Radial Temperature Profiles along the Basket Structure

References

Cuta JM and JM Creer. 1986. *Comparisons of COBRA-SFS Calculations to Data from Electrically Heated Test Sections Simulating Unconsolidated and Consolidated BWR Spent Fuel*. EPRI-NP-4593, Electric Power Research Institute, Palo Alto, California.

Lombardo NJ, JM Cuta, TE Michener, DR Rector, and CL Wheeler. 1986. *COBRA-SFS: A Thermal-Hydraulic Analysis Computer Code; Volume III: Validation Assessments*. PNL-6049 Vol. 3, Pacific Northwest Laboratory, Richland, Washington.

Appendix B

Additional Details of Source Term Calculations

Appendix B
Additional Details of Source Term Calculations

Neutron and Photon source terms for the Surry fuel were calculated with the ORIGEN2 code using the PWRU library. The Surry fuel enrichment ranges from 2.91% to 3.20%, and the cooling time is 1,530 days.

The cobalt content for the stainless steel hardware was assumed to be 800 ppm for the Surry fuel. The Surry fuel contains Inconel 718 grid spacers. Based on Luksic (1989), the cobalt content of the in-core grid spacers is assumed to be 1,160 ppm and the cobalt content of the top grid spacer 1,480 ppm.

The neutron flux in the plenum and the end fittings is lower than that in the active core; hence, the cobalt activation is less in the plenum and end fittings than it is in the active core. Neutron flux scaling factors were used for the Surry fuel. As recommended by Luksic (1989), the values were 0.2 for the bottom end fitting, 0.2 for the plenum, and 0.1 for the top end fitting. These scaling factors are intended to give conservatively high ^{60}Co activities (photon source terms).

The axial photon source shape for the Surry fuel is based on a ^{137}Cs scan of a 2.55% enriched PWR fuel rod burned to 28,000 MWd/MTU (Barner 1985). The axial photon source shape is shown in Figure B.1. The fuel rod is uniformly enriched the full length of the active fuel.

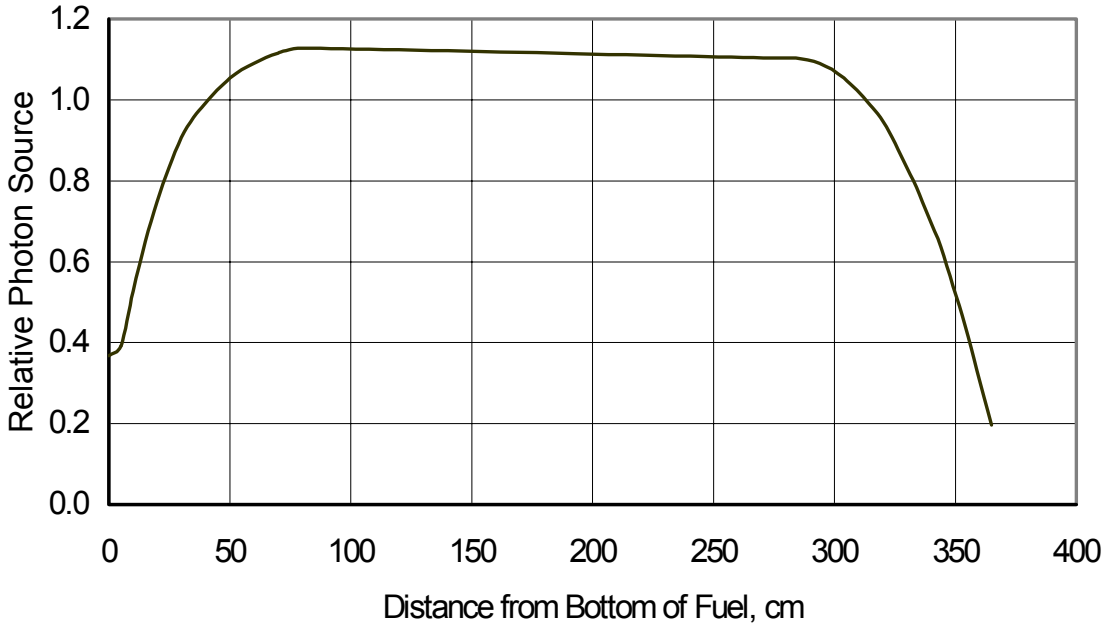

Figure B.1. Axial Photon Source Shape for Surry PWR Spent Fuel

The axial neutron source shape for Surry fuel was calculated with ORIGEN2 based on the axial photon source shape and is shown in Figure B.2. Because neutron source is proportional to the fourth power of burnup, the relative neutron source near the ends of the fuel is less than the relative photon source near the ends of the fuel. Between 50 cm and 300 cm, the relative neutron source is greater than the relative photon source. Additionally, the total neutron source is 28% greater than the neutron source calculated for the rod-average burnup.

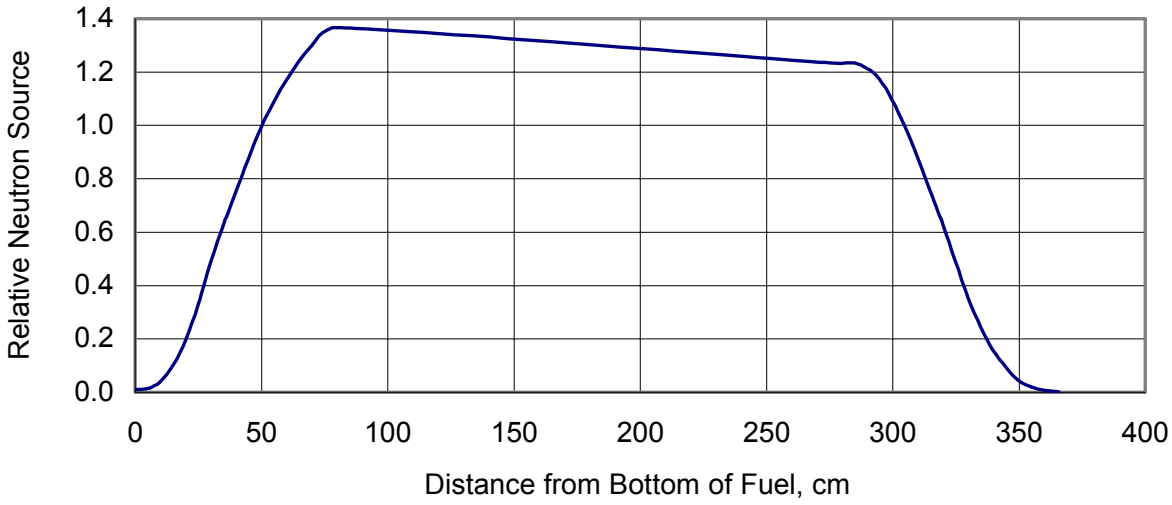

Figure B.2. Axial Neutron Source Shape for Surry PWR Spent Fuel

Neutron and photon source terms for the load-pattern fuel were calculated with the ORIGEN-ARP code using the 17 x 17 PWR cross-section libraries. Values were calculated for enrichments and burnups as shown in Table 4.3 of the main report. Cooling times are 3, 4, 5, 6, 8, 10, 12, 15, 20, and 30 years. Energy-dependent photon source terms for the fuel are given in Table B.1; neutron source terms are given in Table B.2, and decay heat values are given in Table B.3. The load-pattern fuel was assumed to have Zircaloy grid spacers.

The Luksic (1989) scaling factors for the plenum and end fittings are not appropriate for high-enriched fuel because the neutron flux in the fuel decreases with increasing enrichment, but the neutron flux in the plenum and end fittings is expected to remain unchanged with enrichment. Therefore, for the load-pattern fuel, ^{60}Co photon source terms for the plenum and bottom end fitting were approximated as 0.5 Ci ^{60}Co /GWd/MTU/gCo for zero cooling. For the top end fitting, the ^{60}Co photon source term was approximated as 0.2 Ci ^{60}Co /GWd/MTU/gCo for zero cooling. The ^{60}Co source terms are decay-corrected for the cooling time. The stainless steel was assumed to contain 800 ppm cobalt.

The axial photon source shape for the load-pattern fuel is based on a ^{137}Cs scan of a 2.72% enriched PWR fuel rod burned to 29,800 MWd/MTU (Guenther 1988). The axial photon source shape is shown in Figure B.3. It has more photons near the end of the active fuel than the source shape used for the Surry fuel. The fuel rod is uniformly enriched the full length of the active fuel.

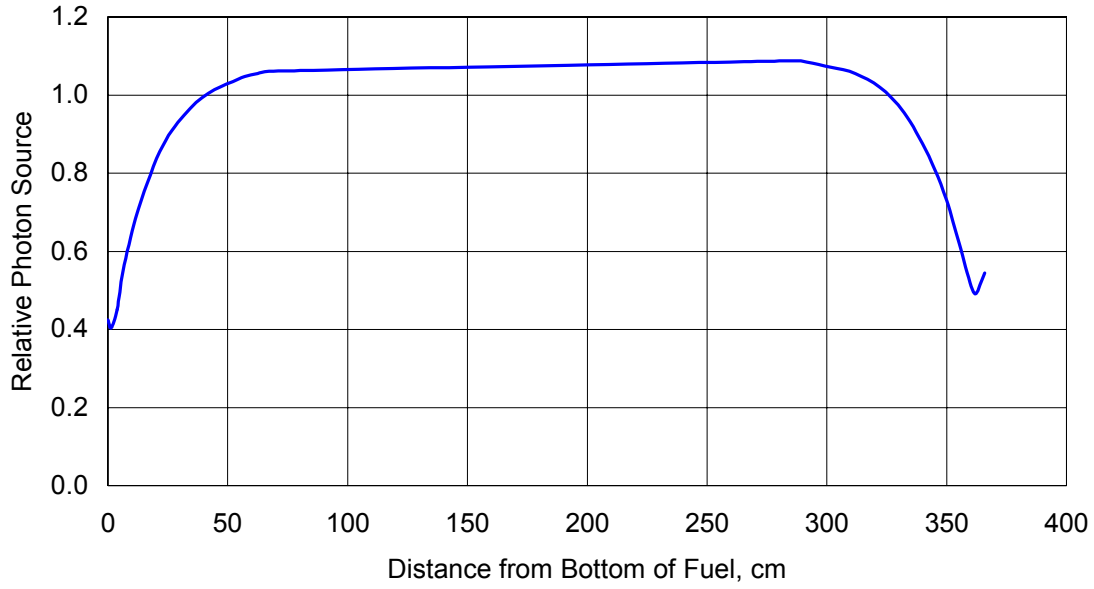

Figure B.3. Axial Photon Source Shape for PWR Spent Fuel Used in the Load-Pattern Analyses

The axial neutron source shape for load-pattern fuel is based on the axial photon source shape for the fuel and is shown in Figure B.4. The total neutron source is 17% greater than the neutron source calculated for the rod average burnup.

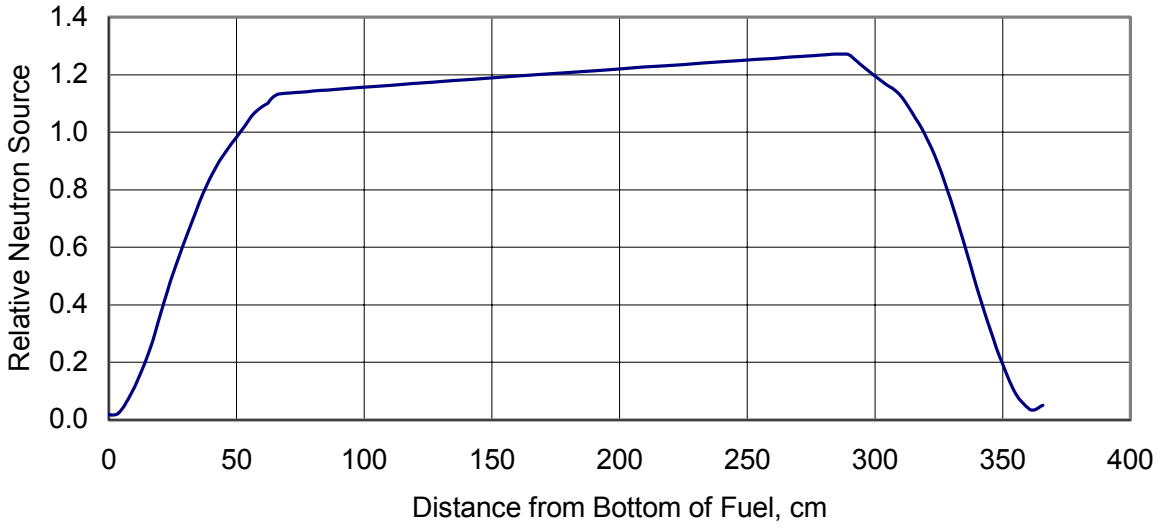

Figure B.4. Axial Neutron Source Shape for PWR Spent Fuel Used in Load-Pattern Analyses

Table B.1. Photon Source Terms

Energy, MeV		Photon Source with Enrichment = 4.8%, Burnup = 70 GWd/MTU, photons/sec/MTU									
Lower	Upper	3 years	4 years	5 years	6 years	8 years	10 years	12 years	15 years	20 years	30 years
0.0	0.1	9.55E+15	6.58E+15	5.12E+15	4.36E+15	3.66E+15	3.34E+15	3.12E+15	2.87E+15	2.53E+15	1.99E+15
0.1	0.2	2.15E+15	1.39E+15	1.02E+15	8.41E+14	6.79E+14	6.06E+14	5.58E+14	5.02E+14	4.27E+14	3.19E+14
0.2	0.3	6.00E+14	3.93E+14	2.92E+14	2.41E+14	1.96E+14	1.77E+14	1.65E+14	1.50E+14	1.30E+14	9.89E+13
0.3	0.4	4.40E+14	2.76E+14	1.98E+14	1.58E+14	1.26E+14	1.14E+14	1.06E+14	9.78E+13	8.60E+13	6.70E+13
0.4	0.5	3.99E+14	2.71E+14	1.97E+14	1.51E+14	1.01E+14	7.61E+13	6.18E+13	4.97E+13	3.95E+13	2.93E+13
0.5	0.6	2.32E+15	1.49E+15	9.92E+14	6.78E+14	3.42E+14	1.88E+14	1.13E+14	6.24E+13	3.46E+13	2.06E+13
0.6	0.7	1.23E+16	1.04E+16	9.08E+15	8.12E+15	6.87E+15	6.12E+15	5.62E+15	5.10E+15	4.47E+15	3.54E+15
0.7	0.8	5.53E+15	3.96E+15	2.85E+15	2.05E+15	1.08E+15	5.84E+14	3.25E+14	1.48E+14	5.56E+13	2.09E+13
0.8	0.9	3.71E+14	2.64E+14	1.95E+14	1.50E+14	9.56E+13	6.67E+13	4.99E+13	3.56E+13	2.34E+13	1.23E+13
0.9	1.0	9.20E+13	7.06E+13	5.89E+13	5.18E+13	4.28E+13	3.66E+13	3.16E+13	2.55E+13	1.81E+13	9.55E+12
1.0	1.1	2.15E+14	1.54E+14	1.18E+14	9.50E+13	6.85E+13	5.37E+13	4.39E+13	3.38E+13	2.28E+13	1.11E+13
1.1	1.2	1.67E+14	1.18E+14	8.57E+13	6.41E+13	3.83E+13	2.47E+13	1.70E+13	1.06E+13	5.89E+12	2.64E+12
1.2	1.3	1.84E+14	1.65E+14	1.50E+14	1.38E+14	1.17E+14	9.94E+13	8.47E+13	6.67E+13	4.48E+13	2.04E+13
1.3	1.4	2.12E+14	1.52E+14	1.11E+14	8.21E+13	4.65E+13	2.75E+13	1.71E+13	9.16E+12	4.07E+12	1.37E+12
1.4	1.5	2.06E+13	1.11E+13	6.82E+12	4.80E+12	3.22E+12	2.62E+12	2.25E+12	1.85E+12	1.36E+12	7.77E+11
1.5	1.6	2.19E+13	1.42E+13	1.04E+13	8.33E+12	6.26E+12	5.17E+12	4.38E+12	3.48E+12	2.40E+12	1.17E+12
1.6	1.7	3.66E+12	1.91E+12	1.06E+12	6.46E+11	3.36E+11	2.52E+11	2.22E+11	2.00E+11	1.75E+11	1.35E+11
1.7	1.8	4.62E+12	2.35E+12	1.24E+12	6.80E+11	2.63E+11	1.54E+11	1.22E+11	1.06E+11	9.26E+10	7.20E+10
1.8	1.9	1.76E+12	8.89E+11	4.68E+11	2.63E+11	1.11E+11	7.18E+10	5.96E+10	5.25E+10	4.56E+10	3.51E+10
1.9	2.0	3.43E+12	1.71E+12	8.70E+11	4.51E+11	1.39E+11	5.94E+10	3.82E+10	3.02E+10	2.60E+10	2.03E+10
2.0	2.1	1.41E+12	7.00E+11	3.53E+11	1.83E+11	5.73E+10	2.57E+10	1.73E+10	1.40E+10	1.21E+10	9.43E+09
2.1	2.2	2.42E+13	1.01E+13	4.24E+12	1.78E+12	3.21E+11	5.94E+10	1.14E+10	1.07E+09	5.22E+07	8.05E+06
2.2	2.3	1.35E+11	6.87E+10	3.50E+10	1.79E+10	4.92E+09	1.56E+09	6.78E+08	3.81E+08	2.86E+08	1.97E+08
2.3	2.4	2.42E+12	1.21E+12	6.09E+11	3.06E+11	7.77E+10	1.98E+10	5.07E+09	6.76E+08	4.48E+07	1.83E+07
2.4	2.5	1.49E+12	7.45E+11	3.72E+11	1.86E+11	4.71E+10	1.20E+10	3.06E+09	4.16E+08	3.53E+07	1.75E+07
2.5	3.0	8.78E+11	4.43E+11	2.24E+11	1.13E+11	2.98E+10	8.49E+09	3.08E+09	1.46E+09	1.19E+09	1.05E+09
3.0	3.5	1.21E+11	6.11E+10	3.10E+10	1.58E+10	4.14E+09	1.16E+09	3.91E+08	1.49E+08	9.68E+07	6.61E+07
3.5	4.0	1.61E+08	1.30E+08	1.12E+08	1.02E+08	8.93E+07	8.14E+07	7.51E+07	6.69E+07	5.55E+07	3.83E+07
4.0	5.0	9.71E+07	9.29E+07	8.91E+07	8.55E+07	7.90E+07	7.30E+07	6.76E+07	6.04E+07	5.00E+07	3.46E+07
5.0	6.0	3.27E+07	3.13E+07	3.00E+07	2.88E+07	2.66E+07	2.46E+07	2.28E+07	2.03E+07	1.69E+07	1.17E+07
6.0	8.0	1.42E+07	1.36E+07	1.30E+07	1.25E+07	1.16E+07	1.07E+07	9.90E+06	8.83E+06	7.32E+06	5.06E+06
8.0	10.0	1.62E+06	1.55E+06	1.49E+06	1.43E+06	1.32E+06	1.22E+06	1.13E+06	1.01E+06	8.36E+05	5.78E+05
Total		3.46E+16	2.57E+16	2.05E+16	1.72E+16	1.35E+16	1.15E+16	1.03E+16	9.16E+15	7.90E+15	6.14E+15
E, MeV/sec		1.62E+16	1.25E+16	1.01E+16	8.38E+15	6.35E+15	5.24E+15	4.58E+15	3.98E+15	3.38E+15	2.60E+15

Table B.1. Photon Source Terms

Energy, MeV		Photon Source with Enrichment = 4.8%, Burnup = 65 GWd/MTU, photons/sec/MTU									
Lower	Upper	3 years	4 years	5 years	6 years	8 years	10 years	12 years	15 years	20 years	30 years
0.0	0.1	9.17E+15	6.29E+15	4.87E+15	4.14E+15	3.48E+15	3.17E+15	2.97E+15	2.73E+15	2.40E+15	1.89E+15
0.1	0.2	2.08E+15	1.33E+15	9.77E+14	7.99E+14	6.45E+14	5.76E+14	5.31E+14	4.78E+14	4.07E+14	3.05E+14
0.2	0.3	5.77E+14	3.76E+14	2.79E+14	2.29E+14	1.87E+14	1.69E+14	1.57E+14	1.43E+14	1.24E+14	9.45E+13
0.3	0.4	4.24E+14	2.65E+14	1.89E+14	1.52E+14	1.21E+14	1.09E+14	1.02E+14	9.38E+13	8.25E+13	6.43E+13
0.4	0.5	3.76E+14	2.54E+14	1.85E+14	1.42E+14	9.55E+13	7.21E+13	5.88E+13	4.75E+13	3.79E+13	2.81E+13
0.5	0.6	2.12E+15	1.36E+15	9.01E+14	6.15E+14	3.10E+14	1.71E+14	1.03E+14	5.78E+13	3.26E+13	1.97E+13
0.6	0.7	1.13E+16	9.58E+15	8.38E+15	7.51E+15	6.38E+15	5.69E+15	5.24E+15	4.76E+15	4.18E+15	3.30E+15
0.7	0.8	4.96E+15	3.55E+15	2.55E+15	1.84E+15	9.72E+14	5.25E+14	2.93E+14	1.34E+14	5.10E+13	1.95E+13
0.8	0.9	3.37E+14	2.39E+14	1.77E+14	1.36E+14	8.71E+13	6.10E+13	4.58E+13	3.28E+13	2.17E+13	1.15E+13
0.9	1.0	8.53E+13	6.53E+13	5.44E+13	4.77E+13	3.94E+13	3.37E+13	2.91E+13	2.36E+13	1.68E+13	8.89E+12
1.0	1.1	1.98E+14	1.42E+14	1.08E+14	8.69E+13	6.27E+13	4.93E+13	4.03E+13	3.10E+13	2.10E+13	1.02E+13
1.1	1.2	1.52E+14	1.07E+14	7.82E+13	5.85E+13	3.51E+13	2.27E+13	1.57E+13	9.90E+12	5.53E+12	2.50E+12
1.2	1.3	1.69E+14	1.51E+14	1.38E+14	1.26E+14	1.07E+14	9.10E+13	7.75E+13	6.11E+13	4.11E+13	1.87E+13
1.3	1.4	1.91E+14	1.37E+14	1.00E+14	7.43E+13	4.22E+13	2.51E+13	1.57E+13	8.47E+12	3.80E+12	1.30E+12
1.4	1.5	2.01E+13	1.07E+13	6.48E+12	4.52E+12	3.00E+12	2.43E+12	2.09E+12	1.72E+12	1.27E+12	7.30E+11
1.5	1.6	2.02E+13	1.31E+13	9.59E+12	7.67E+12	5.76E+12	4.75E+12	4.03E+12	3.20E+12	2.21E+12	1.08E+12
1.6	1.7	3.50E+12	1.82E+12	1.01E+12	6.16E+11	3.21E+11	2.41E+11	2.13E+11	1.92E+11	1.68E+11	1.30E+11
1.7	1.8	4.38E+12	2.23E+12	1.17E+12	6.43E+11	2.50E+11	1.47E+11	1.17E+11	1.02E+11	8.88E+10	6.90E+10
1.8	1.9	1.68E+12	8.47E+11	4.46E+11	2.50E+11	1.06E+11	6.86E+10	5.71E+10	5.04E+10	4.37E+10	3.37E+10
1.9	2.0	3.24E+12	1.62E+12	8.22E+11	4.26E+11	1.31E+11	5.65E+10	3.66E+10	2.90E+10	2.50E+10	1.95E+10
2.0	2.1	1.34E+12	6.65E+11	3.35E+11	1.73E+11	5.43E+10	2.45E+10	1.66E+10	1.34E+10	1.16E+10	9.06E+09
2.1	2.2	2.45E+13	1.02E+13	4.28E+12	1.80E+12	3.23E+11	5.94E+10	1.13E+10	1.04E+09	4.94E+07	7.53E+06
2.2	2.3	1.27E+11	6.43E+10	3.27E+10	1.67E+10	4.52E+09	1.38E+09	5.57E+08	2.88E+08	2.11E+08	1.45E+08
2.3	2.4	2.28E+12	1.14E+12	5.73E+11	2.88E+11	7.29E+10	1.86E+10	4.75E+09	6.35E+08	4.26E+07	1.75E+07
2.4	2.5	1.41E+12	7.02E+11	3.51E+11	1.75E+11	4.42E+10	1.12E+10	2.87E+09	3.91E+08	3.36E+07	1.68E+07
2.5	3.0	8.24E+11	4.16E+11	2.10E+11	1.06E+11	2.78E+10	7.81E+09	2.74E+09	1.22E+09	9.75E+08	8.65E+08
3.0	3.5	1.13E+11	5.72E+10	2.90E+10	1.47E+10	3.85E+09	1.06E+09	3.40E+08	1.17E+08	7.14E+07	4.86E+07
3.5	4.0	1.28E+08	1.00E+08	8.49E+07	7.58E+07	6.58E+07	5.99E+07	5.52E+07	4.92E+07	4.08E+07	2.82E+07
4.0	5.0	7.07E+07	6.78E+07	6.51E+07	6.26E+07	5.79E+07	5.36E+07	4.97E+07	4.44E+07	3.68E+07	2.54E+07
5.0	6.0	2.38E+07	2.28E+07	2.19E+07	2.11E+07	1.95E+07	1.81E+07	1.68E+07	1.50E+07	1.24E+07	8.56E+06
6.0	8.0	1.04E+07	9.92E+06	9.53E+06	9.16E+06	8.48E+06	7.85E+06	7.27E+06	6.50E+06	5.39E+06	3.72E+06
8.0	10.0	1.18E+06	1.13E+06	1.09E+06	1.05E+06	9.68E+05	8.96E+05	8.31E+05	7.42E+05	6.15E+05	4.25E+05
Total		3.22E+16	2.39E+16	1.90E+16	1.60E+16	1.26E+16	1.08E+16	9.68E+15	8.61E+15	7.43E+15	5.78E+15
E, MeV/sec		1.48E+16	1.14E+16	9.22E+15	7.71E+15	5.87E+15	4.87E+15	4.26E+15	3.71E+15	3.15E+15	2.43E+15

Table B.1. Photon Source Terms

Energy, MeV		Photon Source with Enrichment = 4.8%, Burnup = 60 GWd/MTU, photons/sec/MTU									
Lower	Upper	3 years	4 years	5 years	6 years	8 years	10 years	12 years	15 years	20 years	30 years
0.0	0.1	8.76E+15	5.97E+15	4.61E+15	3.92E+15	3.29E+15	3.00E+15	2.81E+15	2.58E+15	2.28E+15	1.79E+15
0.1	0.2	2.00E+15	1.27E+15	9.26E+14	7.55E+14	6.08E+14	5.44E+14	5.02E+14	4.52E+14	3.86E+14	2.89E+14
0.2	0.3	5.51E+14	3.58E+14	2.64E+14	2.17E+14	1.77E+14	1.60E+14	1.49E+14	1.36E+14	1.18E+14	8.98E+13
0.3	0.4	4.06E+14	2.54E+14	1.81E+14	1.45E+14	1.15E+14	1.04E+14	9.72E+13	8.95E+13	7.88E+13	6.13E+13
0.4	0.5	3.52E+14	2.37E+14	1.72E+14	1.32E+14	8.94E+13	6.78E+13	5.56E+13	4.51E+13	3.61E+13	2.68E+13
0.5	0.6	1.91E+15	1.22E+15	8.09E+14	5.51E+14	2.77E+14	1.54E+14	9.36E+13	5.30E+13	3.04E+13	1.86E+13
0.6	0.7	1.03E+16	8.75E+15	7.67E+15	6.90E+15	5.88E+15	5.27E+15	4.85E+15	4.41E+15	3.88E+15	3.07E+15
0.7	0.8	4.38E+15	3.14E+15	2.26E+15	1.63E+15	8.61E+14	4.65E+14	2.60E+14	1.20E+14	4.62E+13	1.80E+13
0.8	0.9	3.02E+14	2.14E+14	1.59E+14	1.22E+14	7.83E+13	5.50E+13	4.15E+13	2.99E+13	1.99E+13	1.06E+13
0.9	1.0	7.83E+13	5.96E+13	4.96E+13	4.34E+13	3.59E+13	3.07E+13	2.65E+13	2.15E+13	1.53E+13	8.19E+12
1.0	1.1	1.80E+14	1.28E+14	9.76E+13	7.85E+13	5.66E+13	4.45E+13	3.65E+13	2.81E+13	1.90E+13	9.33E+12
1.1	1.2	1.37E+14	9.68E+13	7.05E+13	5.28E+13	3.18E+13	2.07E+13	1.44E+13	9.14E+12	5.15E+12	2.35E+12
1.2	1.3	1.53E+14	1.37E+14	1.24E+14	1.14E+14	9.64E+13	8.20E+13	6.99E+13	5.51E+13	3.71E+13	1.69E+13
1.3	1.4	1.70E+14	1.22E+14	8.96E+13	6.64E+13	3.79E+13	2.26E+13	1.42E+13	7.76E+12	3.53E+12	1.22E+12
1.4	1.5	1.95E+13	1.02E+13	6.12E+12	4.21E+12	2.76E+12	2.23E+12	1.92E+12	1.58E+12	1.17E+12	6.79E+11
1.5	1.6	1.85E+13	1.20E+13	8.73E+12	6.96E+12	5.22E+12	4.30E+12	3.65E+12	2.90E+12	2.00E+12	9.86E+11
1.6	1.7	3.33E+12	1.73E+12	9.56E+11	5.82E+11	3.05E+11	2.29E+11	2.03E+11	1.83E+11	1.60E+11	1.24E+11
1.7	1.8	4.12E+12	2.09E+12	1.10E+12	6.04E+11	2.35E+11	1.39E+11	1.11E+11	9.71E+10	8.47E+10	6.59E+10
1.8	1.9	1.59E+12	8.02E+11	4.21E+11	2.36E+11	1.00E+11	6.51E+10	5.43E+10	4.80E+10	4.17E+10	3.21E+10
1.9	2.0	3.05E+12	1.52E+12	7.70E+11	3.99E+11	1.23E+11	5.34E+10	3.48E+10	2.77E+10	2.39E+10	1.86E+10
2.0	2.1	1.27E+12	6.27E+11	3.15E+11	1.63E+11	5.11E+10	2.32E+10	1.58E+10	1.28E+10	1.11E+10	8.66E+09
2.1	2.2	2.48E+13	1.03E+13	4.33E+12	1.82E+12	3.24E+11	5.92E+10	1.12E+10	1.02E+09	4.64E+07	6.98E+06
2.2	2.3	1.18E+11	5.96E+10	3.03E+10	1.54E+10	4.12E+09	1.21E+09	4.55E+08	2.12E+08	1.50E+08	1.03E+08
2.3	2.4	2.13E+12	1.06E+12	5.34E+11	2.68E+11	6.79E+10	1.73E+10	4.42E+09	5.90E+08	4.01E+07	1.68E+07
2.4	2.5	1.32E+12	6.56E+11	3.27E+11	1.64E+11	4.12E+10	1.04E+10	2.67E+09	3.64E+08	3.18E+07	1.61E+07
2.5	3.0	7.67E+11	3.86E+11	1.95E+11	9.87E+10	2.57E+10	7.13E+09	2.41E+09	1.01E+09	7.84E+08	6.98E+08
3.0	3.5	1.05E+11	5.31E+10	2.69E+10	1.37E+10	3.55E+09	9.62E+08	2.95E+08	8.97E+07	5.09E+07	3.45E+07
3.5	4.0	1.02E+08	7.64E+07	6.28E+07	5.50E+07	4.70E+07	4.25E+07	3.92E+07	3.49E+07	2.89E+07	2.00E+07
4.0	5.0	4.99E+07	4.79E+07	4.60E+07	4.43E+07	4.10E+07	3.80E+07	3.52E+07	3.15E+07	2.61E+07	1.80E+07
5.0	6.0	1.68E+07	1.61E+07	1.55E+07	1.49E+07	1.38E+07	1.28E+07	1.19E+07	1.06E+07	8.80E+06	6.07E+06
6.0	8.0	7.31E+06	7.01E+06	6.73E+06	6.48E+06	6.00E+06	5.56E+06	5.16E+06	4.61E+06	3.82E+06	2.64E+06
8.0	10.0	8.34E+05	8.00E+05	7.69E+05	7.40E+05	6.85E+05	6.35E+05	5.89E+05	5.26E+05	4.36E+05	3.01E+05
Total		2.98E+16	2.20E+16	1.75E+16	1.47E+16	1.16E+16	1.00E+16	9.03E+15	8.05E+15	6.95E+15	5.41E+15
E, MeV/sec		1.34E+16	1.04E+16	8.38E+15	7.03E+15	5.38E+15	4.49E+15	3.94E+15	3.44E+15	2.93E+15	2.26E+15

Table B.1. Photon Source Terms

Energy, MeV		Photon Source with Enrichment = 4.8%, Burnup = 55 GWd/MTU, photons/sec/MTU									
Lower	Upper	3 years	4 years	5 years	6 years	8 years	10 years	12 years	15 years	20 years	30 years
0.0	0.1	8.33E+15	5.64E+15	4.34E+15	3.67E+15	3.09E+15	2.82E+15	2.64E+15	2.43E+15	2.14E+15	1.69E+15
0.1	0.2	1.91E+15	1.20E+15	8.71E+14	7.07E+14	5.69E+14	5.09E+14	4.70E+14	4.24E+14	3.63E+14	2.73E+14
0.2	0.3	5.24E+14	3.38E+14	2.49E+14	2.04E+14	1.66E+14	1.50E+14	1.40E+14	1.28E+14	1.11E+14	8.48E+13
0.3	0.4	3.88E+14	2.41E+14	1.71E+14	1.37E+14	1.09E+14	9.84E+13	9.21E+13	8.49E+13	7.47E+13	5.82E+13
0.4	0.5	3.27E+14	2.19E+14	1.59E+14	1.22E+14	8.29E+13	6.33E+13	5.21E+13	4.24E+13	3.41E+13	2.54E+13
0.5	0.6	1.71E+15	1.09E+15	7.16E+14	4.87E+14	2.45E+14	1.36E+14	8.37E+13	4.81E+13	2.82E+13	1.75E+13
0.6	0.7	9.27E+15	7.91E+15	6.96E+15	6.28E+15	5.38E+15	4.84E+15	4.46E+15	4.06E+15	3.57E+15	2.83E+15
0.7	0.8	3.81E+15	2.73E+15	1.96E+15	1.42E+15	7.49E+14	4.05E+14	2.27E+14	1.05E+14	4.12E+13	1.64E+13
0.8	0.9	2.67E+14	1.89E+14	1.40E+14	1.07E+14	6.92E+13	4.89E+13	3.70E+13	2.68E+13	1.80E+13	9.72E+12
0.9	1.0	7.09E+13	5.37E+13	4.45E+13	3.89E+13	3.21E+13	2.75E+13	2.38E+13	1.93E+13	1.38E+13	7.44E+12
1.0	1.1	1.62E+14	1.15E+14	8.69E+13	6.97E+13	5.03E+13	3.95E+13	3.24E+13	2.50E+13	1.70E+13	8.38E+12
1.1	1.2	1.23E+14	8.61E+13	6.27E+13	4.71E+13	2.85E+13	1.87E+13	1.30E+13	8.35E+12	4.74E+12	2.19E+12
1.2	1.3	1.36E+14	1.21E+14	1.10E+14	1.01E+14	8.53E+13	7.26E+13	6.19E+13	4.88E+13	3.29E+13	1.50E+13
1.3	1.4	1.49E+14	1.08E+14	7.88E+13	5.85E+13	3.36E+13	2.02E+13	1.27E+13	7.03E+12	3.24E+12	1.14E+12
1.4	1.5	1.88E+13	9.76E+12	5.74E+12	3.89E+12	2.51E+12	2.02E+12	1.74E+12	1.44E+12	1.07E+12	6.26E+11
1.5	1.6	1.67E+13	1.08E+13	7.82E+12	6.22E+12	4.65E+12	3.82E+12	3.25E+12	2.58E+12	1.79E+12	8.86E+11
1.6	1.7	3.14E+12	1.62E+12	8.98E+11	5.47E+11	2.87E+11	2.17E+11	1.92E+11	1.74E+11	1.52E+11	1.18E+11
1.7	1.8	3.84E+12	1.95E+12	1.02E+12	5.62E+11	2.20E+11	1.31E+11	1.05E+11	9.20E+10	8.03E+10	6.25E+10
1.8	1.9	1.50E+12	7.53E+11	3.95E+11	2.21E+11	9.41E+10	6.14E+10	5.13E+10	4.54E+10	3.95E+10	3.05E+10
1.9	2.0	2.84E+12	1.41E+12	7.15E+11	3.70E+11	1.15E+11	5.00E+10	3.29E+10	2.63E+10	2.26E+10	1.77E+10
2.0	2.1	1.19E+12	5.86E+11	2.94E+11	1.52E+11	4.77E+10	2.18E+10	1.49E+10	1.22E+10	1.05E+10	8.22E+09
2.1	2.2	2.51E+13	1.05E+13	4.37E+12	1.83E+12	3.25E+11	5.90E+10	1.11E+10	9.90E+08	4.33E+07	6.42E+06
2.2	2.3	1.08E+11	5.47E+10	2.78E+10	1.41E+10	3.73E+09	1.06E+09	3.70E+08	1.52E+08	1.02E+08	6.97E+07
2.3	2.4	1.97E+12	9.82E+11	4.92E+11	2.47E+11	6.25E+10	1.59E+10	4.06E+09	5.43E+08	3.75E+07	1.59E+07
2.4	2.5	1.22E+12	6.07E+11	3.03E+11	1.51E+11	3.80E+10	9.61E+09	2.46E+09	3.35E+08	2.98E+07	1.53E+07
2.5	3.0	7.06E+11	3.56E+11	1.79E+11	9.07E+10	2.35E+10	6.44E+09	2.10E+09	8.13E+08	6.12E+08	5.46E+08
3.0	3.5	9.63E+10	4.87E+10	2.47E+10	1.25E+10	3.24E+09	8.66E+08	2.55E+08	6.79E+07	3.48E+07	2.34E+07
3.5	4.0	7.99E+07	5.74E+07	4.54E+07	3.87E+07	3.22E+07	2.89E+07	2.66E+07	2.37E+07	1.97E+07	1.36E+07
4.0	5.0	3.38E+07	3.24E+07	3.12E+07	3.00E+07	2.78E+07	2.58E+07	2.39E+07	2.14E+07	1.77E+07	1.22E+07
5.0	6.0	1.14E+07	1.09E+07	1.05E+07	1.01E+07	9.37E+06	8.69E+06	8.06E+06	7.20E+06	5.98E+06	4.13E+06
6.0	8.0	4.95E+06	4.74E+06	4.56E+06	4.39E+06	4.07E+06	3.77E+06	3.50E+06	3.13E+06	2.59E+06	1.79E+06
8.0	10.0	5.65E+05	5.42E+05	5.21E+05	5.02E+05	4.65E+05	4.31E+05	4.00E+05	3.57E+05	2.96E+05	2.05E+05
Total		2.73E+16	2.01E+16	1.60E+16	1.35E+16	1.07E+16	9.25E+15	8.35E+15	7.47E+15	6.46E+15	5.04E+15
E, MeV/sec		1.21E+16	9.31E+15	7.54E+15	6.34E+15	4.89E+15	4.10E+15	3.62E+15	3.17E+15	2.70E+15	2.09E+15

Table B.1. Photon Source Terms

Energy, MeV		Photon Source with Enrichment = 4.2%, Burnup = 60 GWd/MTU, photons/sec/MTU									
Lower	Upper	3 years	4 years	5 years	6 years	8 years	10 years	12 years	15 years	20 years	30 years
0.0	0.1	8.82E+15	5.95E+15	4.55E+15	3.83E+15	3.19E+15	2.90E+15	2.71E+15	2.49E+15	2.19E+15	1.73E+15
0.1	0.2	2.01E+15	1.27E+15	9.17E+14	7.41E+14	5.90E+14	5.25E+14	4.83E+14	4.34E+14	3.70E+14	2.76E+14
0.2	0.3	5.58E+14	3.58E+14	2.61E+14	2.12E+14	1.71E+14	1.54E+14	1.43E+14	1.30E+14	1.12E+14	8.56E+13
0.3	0.4	4.12E+14	2.54E+14	1.78E+14	1.40E+14	1.10E+14	9.87E+13	9.22E+13	8.48E+13	7.46E+13	5.81E+13
0.4	0.5	3.63E+14	2.44E+14	1.76E+14	1.34E+14	8.92E+13	6.68E+13	5.41E+13	4.33E+13	3.43E+13	2.54E+13
0.5	0.6	2.03E+15	1.29E+15	8.50E+14	5.77E+14	2.88E+14	1.58E+14	9.54E+13	5.31E+13	2.98E+13	1.79E+13
0.6	0.7	1.05E+16	8.89E+15	7.77E+15	6.96E+15	5.91E+15	5.28E+15	4.86E+15	4.41E+15	3.87E+15	3.06E+15
0.7	0.8	4.58E+15	3.28E+15	2.36E+15	1.70E+15	8.98E+14	4.84E+14	2.70E+14	1.24E+14	4.72E+13	1.80E+13
0.8	0.9	3.16E+14	2.23E+14	1.65E+14	1.26E+14	8.09E+13	5.66E+13	4.25E+13	3.04E+13	2.01E+13	1.06E+13
0.9	1.0	8.16E+13	6.18E+13	5.12E+13	4.47E+13	3.68E+13	3.14E+13	2.71E+13	2.19E+13	1.56E+13	8.22E+12
1.0	1.1	1.90E+14	1.35E+14	1.02E+14	8.17E+13	5.87E+13	4.60E+13	3.76E+13	2.89E+13	1.95E+13	9.50E+12
1.1	1.2	1.45E+14	1.02E+14	7.41E+13	5.55E+13	3.34E+13	2.17E+13	1.50E+13	9.49E+12	5.27E+12	2.33E+12
1.2	1.3	1.59E+14	1.42E+14	1.29E+14	1.18E+14	1.00E+14	8.52E+13	7.26E+13	5.72E+13	3.84E+13	1.75E+13
1.3	1.4	1.79E+14	1.29E+14	9.41E+13	6.98E+13	3.98E+13	2.38E+13	1.50E+13	8.16E+12	3.68E+12	1.24E+12
1.4	1.5	1.98E+13	1.04E+13	6.25E+12	4.30E+12	2.81E+12	2.26E+12	1.94E+12	1.59E+12	1.17E+12	6.71E+11
1.5	1.6	1.97E+13	1.27E+13	9.16E+12	7.26E+12	5.40E+12	4.44E+12	3.76E+12	2.99E+12	2.06E+12	1.00E+12
1.6	1.7	3.49E+12	1.81E+12	9.92E+11	5.95E+11	3.00E+11	2.20E+11	1.93E+11	1.74E+11	1.52E+11	1.17E+11
1.7	1.8	4.40E+12	2.23E+12	1.16E+12	6.36E+11	2.39E+11	1.36E+11	1.07E+11	9.21E+10	8.02E+10	6.23E+10
1.8	1.9	1.68E+12	8.45E+11	4.42E+11	2.46E+11	1.01E+11	6.32E+10	5.19E+10	4.56E+10	3.95E+10	3.04E+10
1.9	2.0	3.27E+12	1.63E+12	8.25E+11	4.26E+11	1.29E+11	5.36E+10	3.37E+10	2.63E+10	2.25E+10	1.76E+10
2.0	2.1	1.35E+12	6.68E+11	3.36E+11	1.73E+11	5.31E+10	2.31E+10	1.52E+10	1.21E+10	1.05E+10	8.18E+09
2.1	2.2	2.43E+13	1.02E+13	4.26E+12	1.79E+12	3.21E+11	5.91E+10	1.13E+10	1.05E+09	4.95E+07	7.52E+06
2.2	2.3	1.28E+11	6.49E+10	3.30E+10	1.69E+10	4.56E+09	1.38E+09	5.56E+08	2.85E+08	2.08E+08	1.43E+08
2.3	2.4	2.30E+12	1.15E+12	5.78E+11	2.90E+11	7.36E+10	1.87E+10	4.80E+09	6.38E+08	4.06E+07	1.58E+07
2.4	2.5	1.42E+12	7.08E+11	3.54E+11	1.77E+11	4.46E+10	1.13E+10	2.90E+09	3.92E+08	3.17E+07	1.52E+07
2.5	3.0	8.32E+11	4.19E+11	2.12E+11	1.07E+11	2.79E+10	7.77E+09	2.64E+09	1.10E+09	8.55E+08	7.54E+08
3.0	3.5	1.14E+11	5.78E+10	2.93E+10	1.49E+10	3.89E+09	1.07E+09	3.41E+08	1.16E+08	7.05E+07	4.79E+07
3.5	4.0	1.28E+08	9.95E+07	8.40E+07	7.49E+07	6.50E+07	5.91E+07	5.45E+07	4.86E+07	4.03E+07	2.78E+07
4.0	5.0	6.97E+07	6.68E+07	6.42E+07	6.17E+07	5.71E+07	5.29E+07	4.91E+07	4.38E+07	3.63E+07	2.51E+07
5.0	6.0	2.35E+07	2.25E+07	2.16E+07	2.08E+07	1.93E+07	1.78E+07	1.65E+07	1.48E+07	1.22E+07	8.45E+06
6.0	8.0	1.02E+07	9.78E+06	9.40E+06	9.04E+06	8.36E+06	7.75E+06	7.18E+06	6.41E+06	5.32E+06	3.67E+06
8.0	10.0	1.17E+06	1.12E+06	1.07E+06	1.03E+06	9.55E+05	8.85E+05	8.20E+05	7.32E+05	6.07E+05	4.19E+05
Total		3.04E+16	2.24E+16	1.77E+16	1.48E+16	1.16E+16	9.94E+15	8.92E+15	7.93E+15	6.84E+15	5.32E+15
E, MeV/sec		1.39E+16	1.07E+16	8.57E+15	7.15E+15	5.44E+15	4.51E+15	3.95E+15	3.44E+15	2.92E+15	2.25E+15

Table B.1. Photon Source Terms

Energy, MeV		Photon Source with Enrichment = 4.2%, Burnup = 55 GWd/MTU, photons/sec/MTU									
Lower	Upper	3 years	4 years	5 years	6 years	8 years	10 years	12 years	15 years	20 years	30 years
0.0	0.1	8.40E+15	5.63E+15	4.28E+15	3.60E+15	2.99E+15	2.72E+15	2.55E+15	2.34E+15	2.06E+15	1.63E+15
0.1	0.2	1.93E+15	1.20E+15	8.65E+14	6.96E+14	5.53E+14	4.93E+14	4.54E+14	4.08E+14	3.48E+14	2.61E+14
0.2	0.3	5.32E+14	3.39E+14	2.46E+14	2.00E+14	1.61E+14	1.45E+14	1.34E+14	1.22E+14	1.06E+14	8.09E+13
0.3	0.4	3.94E+14	2.42E+14	1.69E+14	1.33E+14	1.04E+14	9.36E+13	8.75E+13	8.05E+13	7.08E+13	5.51E+13
0.4	0.5	3.39E+14	2.27E+14	1.63E+14	1.24E+14	8.30E+13	6.24E+13	5.08E+13	4.09E+13	3.25E+13	2.41E+13
0.5	0.6	1.82E+15	1.16E+15	7.58E+14	5.13E+14	2.56E+14	1.41E+14	8.57E+13	4.83E+13	2.76E+13	1.68E+13
0.6	0.7	9.49E+15	8.06E+15	7.07E+15	6.35E+15	5.41E+15	4.85E+15	4.47E+15	4.06E+15	3.57E+15	2.82E+15
0.7	0.8	4.01E+15	2.87E+15	2.07E+15	1.49E+15	7.88E+14	4.26E+14	2.38E+14	1.10E+14	4.24E+13	1.65E+13
0.8	0.9	2.82E+14	1.99E+14	1.47E+14	1.12E+14	7.20E+13	5.06E+13	3.82E+13	2.75E+13	1.82E+13	9.74E+12
0.9	1.0	7.44E+13	5.60E+13	4.62E+13	4.03E+13	3.32E+13	2.83E+13	2.45E+13	1.98E+13	1.41E+13	7.51E+12
1.0	1.1	1.72E+14	1.21E+14	9.15E+13	7.32E+13	5.25E+13	4.12E+13	3.37E+13	2.60E+13	1.76E+13	8.59E+12
1.1	1.2	1.30E+14	9.14E+13	6.65E+13	4.98E+13	3.01E+13	1.97E+13	1.37E+13	8.71E+12	4.88E+12	2.18E+12
1.2	1.3	1.42E+14	1.27E+14	1.15E+14	1.06E+14	8.94E+13	7.61E+13	6.48E+13	5.11E+13	3.44E+13	1.57E+13
1.3	1.4	1.58E+14	1.14E+14	8.34E+13	6.20E+13	3.56E+13	2.14E+13	1.35E+13	7.44E+12	3.40E+12	1.16E+12
1.4	1.5	1.91E+13	9.96E+12	5.88E+12	3.99E+12	2.57E+12	2.06E+12	1.77E+12	1.45E+12	1.07E+12	6.20E+11
1.5	1.6	1.80E+13	1.15E+13	8.28E+12	6.55E+12	4.85E+12	3.98E+12	3.38E+12	2.68E+12	1.85E+12	9.08E+11
1.6	1.7	3.31E+12	1.71E+12	9.36E+11	5.61E+11	2.83E+11	2.08E+11	1.83E+11	1.65E+11	1.44E+11	1.12E+11
1.7	1.8	4.13E+12	2.09E+12	1.09E+12	5.95E+11	2.25E+11	1.29E+11	1.01E+11	8.73E+10	7.61E+10	5.92E+10
1.8	1.9	1.59E+12	7.99E+11	4.17E+11	2.31E+11	9.48E+10	5.97E+10	4.91E+10	4.32E+10	3.75E+10	2.89E+10
1.9	2.0	3.06E+12	1.53E+12	7.72E+11	3.98E+11	1.21E+11	5.04E+10	3.19E+10	2.49E+10	2.14E+10	1.67E+10
2.0	2.1	1.27E+12	6.29E+11	3.15E+11	1.62E+11	4.99E+10	2.18E+10	1.44E+10	1.15E+10	9.95E+09	7.77E+09
2.1	2.2	2.46E+13	1.03E+13	4.29E+12	1.80E+12	3.22E+11	5.89E+10	1.11E+10	1.02E+09	4.63E+07	6.95E+06
2.2	2.3	1.19E+11	6.01E+10	3.05E+10	1.56E+10	4.15E+09	1.21E+09	4.52E+08	2.08E+08	1.46E+08	9.98E+07
2.3	2.4	2.14E+12	1.07E+12	5.38E+11	2.70E+11	6.84E+10	1.74E+10	4.45E+09	5.93E+08	3.81E+07	1.51E+07
2.4	2.5	1.33E+12	6.61E+11	3.30E+11	1.65E+11	4.15E+10	1.05E+10	2.69E+09	3.64E+08	2.98E+07	1.44E+07
2.5	3.0	7.73E+11	3.90E+11	1.97E+11	9.94E+10	2.58E+10	7.09E+09	2.32E+09	9.02E+08	6.77E+08	6.00E+08
3.0	3.5	1.06E+11	5.36E+10	2.71E+10	1.38E+10	3.58E+09	9.68E+08	2.95E+08	8.83E+07	4.96E+07	3.35E+07
3.5	4.0	1.00E+08	7.52E+07	6.15E+07	5.38E+07	4.58E+07	4.14E+07	3.81E+07	3.40E+07	2.82E+07	1.94E+07
4.0	5.0	4.85E+07	4.66E+07	4.48E+07	4.31E+07	3.99E+07	3.70E+07	3.43E+07	3.06E+07	2.54E+07	1.75E+07
5.0	6.0	1.64E+07	1.57E+07	1.51E+07	1.45E+07	1.34E+07	1.25E+07	1.16E+07	1.03E+07	8.56E+06	5.91E+06
6.0	8.0	7.10E+06	6.81E+06	6.55E+06	6.30E+06	5.84E+06	5.41E+06	5.02E+06	4.48E+06	3.72E+06	2.57E+06
8.0	10.0	8.11E+05	7.78E+05	7.48E+05	7.20E+05	6.67E+05	6.18E+05	5.73E+05	5.12E+05	4.25E+05	2.93E+05
Total		2.80E+16	2.05E+16	1.62E+16	1.36E+16	1.07E+16	9.18E+15	8.26E+15	7.36E+15	6.36E+15	4.95E+15
E, MeV/sec		1.25E+16	9.60E+15	7.73E+15	6.47E+15	4.95E+15	4.13E+15	3.63E+15	3.17E+15	2.70E+15	2.08E+15

Table B.1. Photon Source Terms

Energy, MeV		Photon Source with Enrichment = 4.2%, Burnup = 50 GWd/MTU, photons/sec/MTU									
Lower	Upper	3 years	4 years	5 years	6 years	8 years	10 years	12 years	15 years	20 years	30 years
0.0	0.1	7.95E+15	5.29E+15	4.00E+15	3.35E+15	2.79E+15	2.54E+15	2.37E+15	2.18E+15	1.93E+15	1.52E+15
0.1	0.2	1.84E+15	1.14E+15	8.08E+14	6.48E+14	5.14E+14	4.58E+14	4.22E+14	3.80E+14	3.25E+14	2.44E+14
0.2	0.3	5.03E+14	3.19E+14	2.30E+14	1.86E+14	1.50E+14	1.35E+14	1.25E+14	1.14E+14	9.93E+13	7.58E+13
0.3	0.4	3.74E+14	2.28E+14	1.59E+14	1.25E+14	9.81E+13	8.81E+13	8.23E+13	7.57E+13	6.66E+13	5.19E+13
0.4	0.5	3.13E+14	2.08E+14	1.49E+14	1.14E+14	7.64E+13	5.78E+13	4.73E+13	3.82E+13	3.05E+13	2.27E+13
0.5	0.6	1.61E+15	1.02E+15	6.65E+14	4.49E+14	2.24E+14	1.24E+14	7.58E+13	4.34E+13	2.53E+13	1.56E+13
0.6	0.7	8.47E+15	7.22E+15	6.35E+15	5.73E+15	4.91E+15	4.41E+15	4.07E+15	3.71E+15	3.26E+15	2.58E+15
0.7	0.8	3.44E+15	2.47E+15	1.77E+15	1.28E+15	6.77E+14	3.67E+14	2.06E+14	9.53E+13	3.74E+13	1.48E+13
0.8	0.9	2.46E+14	1.73E+14	1.28E+14	9.80E+13	6.30E+13	4.44E+13	3.37E+13	2.44E+13	1.63E+13	8.80E+12
0.9	1.0	6.68E+13	5.00E+13	4.11E+13	3.57E+13	2.93E+13	2.51E+13	2.17E+13	1.76E+13	1.26E+13	6.75E+12
1.0	1.1	1.53E+14	1.07E+14	8.07E+13	6.43E+13	4.60E+13	3.61E+13	2.96E+13	2.29E+13	1.55E+13	7.63E+12
1.1	1.2	1.15E+14	8.07E+13	5.87E+13	4.40E+13	2.67E+13	1.76E+13	1.23E+13	7.91E+12	4.47E+12	2.02E+12
1.2	1.3	1.25E+14	1.11E+14	1.01E+14	9.24E+13	7.82E+13	6.65E+13	5.67E+13	4.47E+13	3.01E+13	1.37E+13
1.3	1.4	1.38E+14	9.90E+13	7.27E+13	5.41E+13	3.12E+13	1.89E+13	1.20E+13	6.70E+12	3.10E+12	1.07E+12
1.4	1.5	1.84E+13	9.46E+12	5.48E+12	3.66E+12	2.31E+12	1.84E+12	1.58E+12	1.30E+12	9.68E+11	5.65E+11
1.5	1.6	1.61E+13	1.03E+13	7.36E+12	5.79E+12	4.27E+12	3.50E+12	2.97E+12	2.36E+12	1.63E+12	8.06E+11
1.6	1.7	3.12E+12	1.60E+12	8.76E+11	5.24E+11	2.65E+11	1.95E+11	1.72E+11	1.55E+11	1.36E+11	1.05E+11
1.7	1.8	3.84E+12	1.94E+12	1.01E+12	5.51E+11	2.09E+11	1.20E+11	9.48E+10	8.21E+10	7.16E+10	5.57E+10
1.8	1.9	1.50E+12	7.48E+11	3.89E+11	2.15E+11	8.84E+10	5.59E+10	4.61E+10	4.06E+10	3.52E+10	2.72E+10
1.9	2.0	2.85E+12	1.42E+12	7.14E+11	3.68E+11	1.12E+11	4.70E+10	2.99E+10	2.35E+10	2.02E+10	1.58E+10
2.0	2.1	1.19E+12	5.86E+11	2.93E+11	1.51E+11	4.63E+10	2.04E+10	1.35E+10	1.09E+10	9.38E+09	7.33E+09
2.1	2.2	2.48E+13	1.03E+13	4.32E+12	1.81E+12	3.22E+11	5.85E+10	1.10E+10	9.85E+08	4.30E+07	6.36E+06
2.2	2.3	1.09E+11	5.50E+10	2.79E+10	1.42E+10	3.74E+09	1.06E+09	3.65E+08	1.46E+08	9.68E+07	6.62E+07
2.3	2.4	1.97E+12	9.87E+11	4.94E+11	2.48E+11	6.28E+10	1.60E+10	4.08E+09	5.44E+08	3.54E+07	1.42E+07
2.4	2.5	1.23E+12	6.10E+11	3.04E+11	1.52E+11	3.82E+10	9.66E+09	2.47E+09	3.34E+08	2.78E+07	1.36E+07
2.5	3.0	7.10E+11	3.57E+11	1.80E+11	9.11E+10	2.36E+10	6.39E+09	2.02E+09	7.21E+08	5.20E+08	4.62E+08
3.0	3.5	9.68E+10	4.90E+10	2.48E+10	1.26E+10	3.26E+09	8.68E+08	2.54E+08	6.61E+07	3.31E+07	2.22E+07
3.5	4.0	7.82E+07	5.57E+07	4.37E+07	3.71E+07	3.07E+07	2.75E+07	2.53E+07	2.25E+07	1.87E+07	1.29E+07
4.0	5.0	3.21E+07	3.08E+07	2.96E+07	2.85E+07	2.64E+07	2.45E+07	2.27E+07	2.03E+07	1.68E+07	1.16E+07
5.0	6.0	1.08E+07	1.04E+07	9.98E+06	9.61E+06	8.91E+06	8.26E+06	7.66E+06	6.84E+06	5.68E+06	3.92E+06
6.0	8.0	4.70E+06	4.51E+06	4.33E+06	4.17E+06	3.87E+06	3.59E+06	3.33E+06	2.97E+06	2.46E+06	1.70E+06
8.0	10.0	5.37E+05	5.15E+05	4.95E+05	4.76E+05	4.42E+05	4.09E+05	3.80E+05	3.39E+05	2.81E+05	1.94E+05
Total		2.54E+16	1.85E+16	1.46E+16	1.23E+16	9.72E+15	8.39E+15	7.58E+15	6.77E+15	5.86E+15	4.57E+15
E, MeV/sec		1.11E+16	8.53E+15	6.89E+15	5.78E+15	4.46E+15	3.73E+15	3.30E+15	2.89E+15	2.46E+15	1.90E+15

Table B.1. Photon Source Terms

Energy, MeV		Photon Source with Enrichment = 4.2%, Burnup = 45 GWd/MTU, photons/sec/MTU									
Lower	Upper	3 years	4 years	5 years	6 years	8 years	10 years	12 years	15 years	20 years	30 years
0.0	0.1	7.48E+15	4.92E+15	3.71E+15	3.10E+15	2.57E+15	2.34E+15	2.19E+15	2.02E+15	1.78E+15	1.41E+15
0.1	0.2	1.74E+15	1.06E+15	7.49E+14	5.96E+14	4.71E+14	4.20E+14	3.88E+14	3.50E+14	3.00E+14	2.26E+14
0.2	0.3	4.73E+14	2.97E+14	2.13E+14	1.72E+14	1.38E+14	1.25E+14	1.16E+14	1.06E+14	9.20E+13	7.03E+13
0.3	0.4	3.53E+14	2.14E+14	1.49E+14	1.17E+14	9.13E+13	8.20E+13	7.67E+13	7.06E+13	6.21E+13	4.84E+13
0.4	0.5	2.87E+14	1.90E+14	1.36E+14	1.04E+14	6.97E+13	5.30E+13	4.35E+13	3.54E+13	2.84E+13	2.12E+13
0.5	0.6	1.41E+15	8.83E+14	5.74E+14	3.87E+14	1.92E+14	1.07E+14	6.60E+13	3.85E+13	2.30E+13	1.44E+13
0.6	0.7	7.48E+15	6.40E+15	5.65E+15	5.11E+15	4.41E+15	3.97E+15	3.68E+15	3.35E+15	2.95E+15	2.34E+15
0.7	0.8	2.91E+15	2.08E+15	1.50E+15	1.08E+15	5.72E+14	3.10E+14	1.74E+14	8.13E+13	3.24E+13	1.31E+13
0.8	0.9	2.12E+14	1.49E+14	1.09E+14	8.38E+13	5.40E+13	3.83E+13	2.91E+13	2.12E+13	1.43E+13	7.82E+12
0.9	1.0	5.92E+13	4.38E+13	3.57E+13	3.10E+13	2.54E+13	2.17E+13	1.88E+13	1.53E+13	1.10E+13	5.97E+12
1.0	1.1	1.34E+14	9.33E+13	6.97E+13	5.53E+13	3.95E+13	3.10E+13	2.54E+13	1.97E+13	1.34E+13	6.64E+12
1.1	1.2	1.01E+14	7.03E+13	5.11E+13	3.84E+13	2.34E+13	1.55E+13	1.09E+13	7.09E+12	4.04E+12	1.85E+12
1.2	1.3	1.07E+14	9.54E+13	8.63E+13	7.89E+13	6.67E+13	5.68E+13	4.84E+13	3.81E+13	2.57E+13	1.18E+13
1.3	1.4	1.18E+14	8.48E+13	6.23E+13	4.66E+13	2.70E+13	1.65E+13	1.06E+13	5.96E+12	2.80E+12	9.83E+11
1.4	1.5	1.77E+13	8.93E+12	5.07E+12	3.31E+12	2.04E+12	1.62E+12	1.39E+12	1.15E+12	8.59E+11	5.08E+11
1.5	1.6	1.42E+13	9.02E+12	6.41E+12	5.02E+12	3.68E+12	3.01E+12	2.55E+12	2.03E+12	1.41E+12	7.02E+11
1.6	1.7	2.91E+12	1.49E+12	8.11E+11	4.85E+11	2.45E+11	1.82E+11	1.60E+11	1.44E+11	1.26E+11	9.80E+10
1.7	1.8	3.53E+12	1.78E+12	9.26E+11	5.05E+11	1.92E+11	1.11E+11	8.81E+10	7.65E+10	6.68E+10	5.20E+10
1.8	1.9	1.40E+12	6.94E+11	3.60E+11	1.99E+11	8.16E+10	5.18E+10	4.28E+10	3.77E+10	3.28E+10	2.53E+10
1.9	2.0	2.62E+12	1.30E+12	6.54E+11	3.37E+11	1.02E+11	4.33E+10	2.78E+10	2.19E+10	1.89E+10	1.47E+10
2.0	2.1	1.10E+12	5.41E+11	2.70E+11	1.39E+11	4.25E+10	1.88E+10	1.26E+10	1.01E+10	8.76E+09	6.84E+09
2.1	2.2	2.50E+13	1.04E+13	4.34E+12	1.81E+12	3.21E+11	5.80E+10	1.08E+10	9.50E+08	3.96E+07	5.76E+06
2.2	2.3	9.80E+10	4.96E+10	2.52E+10	1.28E+10	3.34E+09	9.18E+08	2.93E+08	9.97E+07	6.08E+07	4.14E+07
2.3	2.4	1.80E+12	8.97E+11	4.49E+11	2.25E+11	5.69E+10	1.44E+10	3.69E+09	4.92E+08	3.25E+07	1.32E+07
2.4	2.5	1.12E+12	5.56E+11	2.77E+11	1.38E+11	3.46E+10	8.75E+09	2.23E+09	3.03E+08	2.56E+07	1.27E+07
2.5	3.0	6.43E+11	3.24E+11	1.63E+11	8.24E+10	2.12E+10	5.69E+09	1.74E+09	5.66E+08	3.88E+08	3.45E+08
3.0	3.5	8.74E+10	4.43E+10	2.24E+10	1.14E+10	2.93E+09	7.71E+08	2.17E+08	4.88E+07	2.09E+07	1.39E+07
3.5	4.0	6.07E+07	4.08E+07	3.03E+07	2.47E+07	1.95E+07	1.73E+07	1.58E+07	1.41E+07	1.17E+07	8.07E+06
4.0	5.0	2.00E+07	1.92E+07	1.85E+07	1.78E+07	1.65E+07	1.53E+07	1.42E+07	1.27E+07	1.05E+07	7.28E+06
5.0	6.0	6.75E+06	6.47E+06	6.22E+06	5.99E+06	5.56E+06	5.15E+06	4.78E+06	4.27E+06	3.55E+06	2.45E+06
6.0	8.0	2.93E+06	2.81E+06	2.70E+06	2.60E+06	2.41E+06	2.24E+06	2.08E+06	1.86E+06	1.54E+06	1.06E+06
8.0	10.0	3.35E+05	3.21E+05	3.09E+05	2.97E+05	2.75E+05	2.56E+05	2.37E+05	2.12E+05	1.76E+05	1.21E+05
Total		2.29E+16	1.66E+16	1.31E+16	1.10E+16	8.75E+15	7.60E+15	6.88E+15	6.17E+15	5.35E+15	4.17E+15
E, MeV/sec		9.74E+15	7.49E+15	6.06E+15	5.10E+15	3.97E+15	3.34E+15	2.96E+15	2.61E+15	2.23E+15	1.72E+15

Table B.1. Photon Source Terms

Energy, MeV		Photon Source with Enrichment = 3.6%, Burnup = 50 GWd/MTU, photons/sec/MTU									
Lower	Upper	3 years	4 years	5 years	6 years	8 years	10 years	12 years	15 years	20 years	30 years
0.0	0.1	8.02E+15	5.28E+15	3.95E+15	3.28E+15	2.69E+15	2.44E+15	2.28E+15	2.10E+15	1.85E+15	1.46E+15
0.1	0.2	1.85E+15	1.14E+15	8.02E+14	6.36E+14	4.98E+14	4.41E+14	4.05E+14	3.64E+14	3.10E+14	2.32E+14
0.2	0.3	5.12E+14	3.20E+14	2.28E+14	1.82E+14	1.44E+14	1.29E+14	1.20E+14	1.09E+14	9.44E+13	7.19E+13
0.3	0.4	3.81E+14	2.30E+14	1.57E+14	1.22E+14	9.34E+13	8.32E+13	7.76E+13	7.13E+13	6.27E+13	4.88E+13
0.4	0.5	3.25E+14	2.15E+14	1.53E+14	1.16E+14	7.64E+13	5.69E+13	4.59E+13	3.66E+13	2.89E+13	2.14E+13
0.5	0.6	1.73E+15	1.08E+15	7.06E+14	4.75E+14	2.34E+14	1.28E+14	7.76E+13	4.36E+13	2.47E+13	1.50E+13
0.6	0.7	8.68E+15	7.36E+15	6.45E+15	5.79E+15	4.94E+15	4.43E+15	4.08E+15	3.71E+15	3.26E+15	2.58E+15
0.7	0.8	3.63E+15	2.60E+15	1.87E+15	1.35E+15	7.13E+14	3.86E+14	2.16E+14	9.95E+13	3.85E+13	1.49E+13
0.8	0.9	2.61E+14	1.83E+14	1.34E+14	1.03E+14	6.57E+13	4.61E+13	3.48E+13	2.50E+13	1.66E+13	8.81E+12
0.9	1.0	7.04E+13	5.24E+13	4.29E+13	3.72E+13	3.04E+13	2.59E+13	2.24E+13	1.81E+13	1.29E+13	6.81E+12
1.0	1.1	1.63E+14	1.14E+14	8.53E+13	6.77E+13	4.83E+13	3.78E+13	3.09E+13	2.38E+13	1.61E+13	7.84E+12
1.1	1.2	1.22E+14	8.58E+13	6.23E+13	4.67E+13	2.83E+13	1.86E+13	1.30E+13	8.27E+12	4.61E+12	2.01E+12
1.2	1.3	1.32E+14	1.17E+14	1.06E+14	9.73E+13	8.23E+13	7.00E+13	5.97E+13	4.70E+13	3.16E+13	1.44E+13
1.3	1.4	1.46E+14	1.05E+14	7.71E+13	5.74E+13	3.31E+13	2.01E+13	1.28E+13	7.11E+12	3.27E+12	1.09E+12
1.4	1.5	1.87E+13	9.66E+12	5.62E+12	3.76E+12	2.36E+12	1.88E+12	1.61E+12	1.32E+12	9.73E+11	5.59E+11
1.5	1.6	1.74E+13	1.10E+13	7.83E+12	6.12E+12	4.48E+12	3.66E+12	3.10E+12	2.46E+12	1.69E+12	8.29E+11
1.6	1.7	3.30E+12	1.69E+12	9.15E+11	5.39E+11	2.61E+11	1.87E+11	1.63E+11	1.46E+11	1.28E+11	9.87E+10
1.7	1.8	4.14E+12	2.09E+12	1.08E+12	5.86E+11	2.14E+11	1.18E+11	9.04E+10	7.75E+10	6.74E+10	5.24E+10
1.8	1.9	1.59E+12	7.95E+11	4.12E+11	2.26E+11	8.92E+10	5.42E+10	4.39E+10	3.83E+10	3.32E+10	2.56E+10
1.9	2.0	3.08E+12	1.53E+12	7.73E+11	3.98E+11	1.18E+11	4.75E+10	2.89E+10	2.22E+10	1.90E+10	1.48E+10
2.0	2.1	1.28E+12	6.30E+11	3.16E+11	1.62E+11	4.86E+10	2.04E+10	1.30E+10	1.02E+10	8.81E+09	6.88E+09
2.1	2.2	2.43E+13	1.01E+13	4.25E+12	1.78E+12	3.19E+11	5.84E+10	1.11E+10	1.01E+09	4.62E+07	6.91E+06
2.2	2.3	1.20E+11	6.07E+10	3.08E+10	1.57E+10	4.18E+09	1.22E+09	4.48E+08	2.02E+08	1.41E+08	9.62E+07
2.3	2.4	2.16E+12	1.08E+12	5.42E+11	2.72E+11	6.90E+10	1.76E+10	4.49E+09	5.95E+08	3.61E+07	1.33E+07
2.4	2.5	1.34E+12	6.66E+11	3.32E+11	1.66E+11	4.19E+10	1.06E+10	2.71E+09	3.65E+08	2.78E+07	1.28E+07
2.5	3.0	7.80E+11	3.93E+11	1.98E+11	1.00E+11	2.59E+10	7.05E+09	2.24E+09	8.01E+08	5.76E+08	5.06E+08
3.0	3.5	1.07E+11	5.40E+10	2.74E+10	1.39E+10	3.61E+09	9.73E+08	2.95E+08	8.65E+07	4.79E+07	3.23E+07
3.5	4.0	9.89E+07	7.35E+07	5.99E+07	5.21E+07	4.42E+07	4.00E+07	3.68E+07	3.28E+07	2.72E+07	1.87E+07
4.0	5.0	4.68E+07	4.49E+07	4.32E+07	4.16E+07	3.85E+07	3.57E+07	3.31E+07	2.96E+07	2.45E+07	1.69E+07
5.0	6.0	1.58E+07	1.51E+07	1.46E+07	1.40E+07	1.30E+07	1.20E+07	1.12E+07	9.96E+06	8.26E+06	5.70E+06
6.0	8.0	6.85E+06	6.57E+06	6.32E+06	6.08E+06	5.64E+06	5.22E+06	4.84E+06	4.33E+06	3.59E+06	2.47E+06
8.0	10.0	7.83E+05	7.51E+05	7.22E+05	6.95E+05	6.44E+05	5.97E+05	5.53E+05	4.94E+05	4.10E+05	2.83E+05
Total		2.61E+16	1.89E+16	1.48E+16	1.24E+16	9.69E+15	8.31E+15	7.48E+15	6.66E+15	5.76E+15	4.49E+15
E, MeV/sec		1.15E+16	8.81E+15	7.07E+15	5.91E+15	4.51E+15	3.76E+15	3.31E+15	2.89E+15	2.46E+15	1.89E+15

Table B.1. Photon Source Terms

Energy, MeV		Photon Source with Enrichment = 3.6%, Burnup = 45 GWd/MTU, photons/sec/MTU									
Lower	Upper	3 years	4 years	5 years	6 years	8 years	10 years	12 years	15 years	20 years	30 years
0.0	0.1	7.56E+15	4.93E+15	3.67E+15	3.03E+15	2.49E+15	2.26E+15	2.11E+15	1.94E+15	1.71E+15	1.35E+15
0.1	0.2	1.76E+15	1.07E+15	7.45E+14	5.87E+14	4.58E+14	4.06E+14	3.73E+14	3.36E+14	2.87E+14	2.15E+14
0.2	0.3	4.82E+14	2.99E+14	2.12E+14	1.69E+14	1.33E+14	1.19E+14	1.11E+14	1.01E+14	8.76E+13	6.68E+13
0.3	0.4	3.61E+14	2.16E+14	1.47E+14	1.14E+14	8.71E+13	7.77E+13	7.25E+13	6.66E+13	5.86E+13	4.56E+13
0.4	0.5	2.99E+14	1.97E+14	1.40E+14	1.06E+14	6.99E+13	5.23E+13	4.24E+13	3.40E+13	2.70E+13	2.00E+13
0.5	0.6	1.52E+15	9.50E+14	6.15E+14	4.12E+14	2.03E+14	1.12E+14	6.80E+13	3.88E+13	2.25E+13	1.38E+13
0.6	0.7	7.68E+15	6.54E+15	5.74E+15	5.17E+15	4.44E+15	3.99E+15	3.68E+15	3.35E+15	2.95E+15	2.33E+15
0.7	0.8	3.09E+15	2.21E+15	1.59E+15	1.15E+15	6.07E+14	3.29E+14	1.85E+14	8.56E+13	3.36E+13	1.33E+13
0.8	0.9	2.26E+14	1.58E+14	1.16E+14	8.86E+13	5.68E+13	4.00E+13	3.03E+13	2.19E+13	1.47E+13	7.87E+12
0.9	1.0	6.28E+13	4.63E+13	3.76E+13	3.25E+13	2.66E+13	2.27E+13	1.96E+13	1.59E+13	1.13E+13	6.05E+12
1.0	1.1	1.45E+14	1.00E+14	7.45E+13	5.89E+13	4.19E+13	3.27E+13	2.68E+13	2.07E+13	1.40E+13	6.88E+12
1.1	1.2	1.08E+14	7.53E+13	5.47E+13	4.11E+13	2.50E+13	1.65E+13	1.16E+13	7.46E+12	4.19E+12	1.85E+12
1.2	1.3	1.14E+14	1.02E+14	9.19E+13	8.40E+13	7.10E+13	6.04E+13	5.15E+13	4.06E+13	2.73E+13	1.25E+13
1.3	1.4	1.26E+14	9.07E+13	6.67E+13	4.98E+13	2.89E+13	1.77E+13	1.13E+13	6.37E+12	2.97E+12	1.01E+12
1.4	1.5	1.80E+13	9.13E+12	5.21E+12	3.42E+12	2.10E+12	1.67E+12	1.43E+12	1.17E+12	8.68E+11	5.04E+11
1.5	1.6	1.55E+13	9.77E+12	6.89E+12	5.36E+12	3.90E+12	3.18E+12	2.69E+12	2.14E+12	1.48E+12	7.27E+11
1.6	1.7	3.09E+12	1.58E+12	8.52E+11	5.01E+11	2.43E+11	1.74E+11	1.52E+11	1.36E+11	1.19E+11	9.23E+10
1.7	1.8	3.83E+12	1.93E+12	1.00E+12	5.41E+11	1.97E+11	1.09E+11	8.42E+10	7.23E+10	6.30E+10	4.90E+10
1.8	1.9	1.49E+12	7.42E+11	3.83E+11	2.10E+11	8.27E+10	5.04E+10	4.09E+10	3.57E+10	3.10E+10	2.39E+10
1.9	2.0	2.85E+12	1.42E+12	7.13E+11	3.66E+11	1.09E+11	4.40E+10	2.70E+10	2.07E+10	1.77E+10	1.38E+10
2.0	2.1	1.19E+12	5.85E+11	2.92E+11	1.50E+11	4.49E+10	1.89E+10	1.21E+10	9.58E+09	8.24E+09	6.44E+09
2.1	2.2	2.45E+13	1.02E+13	4.26E+12	1.79E+12	3.18E+11	5.78E+10	1.09E+10	9.78E+08	4.28E+07	6.29E+06
2.2	2.3	1.09E+11	5.53E+10	2.80E+10	1.43E+10	3.75E+09	1.06E+09	3.58E+08	1.39E+08	9.12E+07	6.22E+07
2.3	2.4	1.98E+12	9.91E+11	4.97E+11	2.49E+11	6.31E+10	1.60E+10	4.10E+09	5.44E+08	3.33E+07	1.25E+07
2.4	2.5	1.23E+12	6.12E+11	3.05E+11	1.53E+11	3.83E+10	9.71E+09	2.48E+09	3.34E+08	2.57E+07	1.20E+07
2.5	3.0	7.13E+11	3.59E+11	1.81E+11	9.15E+10	2.36E+10	6.34E+09	1.95E+09	6.36E+08	4.36E+08	3.84E+08
3.0	3.5	9.74E+10	4.93E+10	2.50E+10	1.27E+10	3.27E+09	8.70E+08	2.52E+08	6.39E+07	3.12E+07	2.09E+07
3.5	4.0	7.64E+07	5.38E+07	4.18E+07	3.53E+07	2.90E+07	2.59E+07	2.38E+07	2.12E+07	1.76E+07	1.21E+07
4.0	5.0	3.02E+07	2.90E+07	2.79E+07	2.68E+07	2.49E+07	2.30E+07	2.14E+07	1.91E+07	1.58E+07	1.09E+07
5.0	6.0	1.02E+07	9.76E+06	9.39E+06	9.04E+06	8.38E+06	7.77E+06	7.20E+06	6.44E+06	5.34E+06	3.68E+06
6.0	8.0	4.42E+06	4.24E+06	4.08E+06	3.92E+06	3.64E+06	3.37E+06	3.13E+06	2.79E+06	2.32E+06	1.60E+06
8.0	10.0	5.05E+05	4.84E+05	4.66E+05	4.48E+05	4.15E+05	3.85E+05	3.57E+05	3.19E+05	2.65E+05	1.83E+05
Total		2.36E+16	1.70E+16	1.33E+16	1.11E+16	8.74E+15	7.54E+15	6.80E+15	6.07E+15	5.26E+15	4.10E+15
E, MeV/sec		1.01E+16	7.76E+15	6.24E+15	5.23E+15	4.02E+15	3.37E+15	2.98E+15	2.61E+15	2.22E+15	1.72E+15

Table B.1. Photon Source Terms

Energy, MeV		Photon Source with Enrichment = 3.6%, Burnup = 40 GWd/MTU, photons/sec/MTU									
Lower	Upper	3 years	4 years	5 years	6 years	8 years	10 years	12 years	15 years	20 years	30 years
0.0	0.1	7.06E+15	4.55E+15	3.36E+15	2.77E+15	2.27E+15	2.06E+15	1.93E+15	1.77E+15	1.57E+15	1.24E+15
0.1	0.2	1.66E+15	9.91E+14	6.84E+14	5.35E+14	4.16E+14	3.69E+14	3.40E+14	3.06E+14	2.62E+14	1.97E+14
0.2	0.3	4.50E+14	2.77E+14	1.95E+14	1.54E+14	1.22E+14	1.09E+14	1.01E+14	9.24E+13	8.02E+13	6.13E+13
0.3	0.4	3.38E+14	2.01E+14	1.36E+14	1.05E+14	8.03E+13	7.17E+13	6.69E+13	6.15E+13	5.41E+13	4.21E+13
0.4	0.5	2.72E+14	1.77E+14	1.25E+14	9.49E+13	6.30E+13	4.74E+13	3.86E+13	3.12E+13	2.48E+13	1.84E+13
0.5	0.6	1.31E+15	8.14E+14	5.24E+14	3.50E+14	1.72E+14	9.48E+13	5.82E+13	3.38E+13	2.01E+13	1.26E+13
0.6	0.7	6.68E+15	5.71E+15	5.04E+15	4.56E+15	3.93E+15	3.55E+15	3.28E+15	3.00E+15	2.64E+15	2.09E+15
0.7	0.8	2.56E+15	1.83E+15	1.31E+15	9.49E+14	5.02E+14	2.72E+14	1.53E+14	7.16E+13	2.85E+13	1.15E+13
0.8	0.9	1.92E+14	1.33E+14	9.75E+13	7.44E+13	4.78E+13	3.38E+13	2.57E+13	1.87E+13	1.26E+13	6.88E+12
0.9	1.0	5.48E+13	3.99E+13	3.22E+13	2.77E+13	2.25E+13	1.92E+13	1.67E+13	1.35E+13	9.71E+12	5.26E+12
1.0	1.1	1.25E+14	8.58E+13	6.33E+13	4.98E+13	3.52E+13	2.75E+13	2.26E+13	1.74E+13	1.19E+13	5.88E+12
1.1	1.2	9.30E+13	6.48E+13	4.70E+13	3.53E+13	2.16E+13	1.44E+13	1.02E+13	6.61E+12	3.75E+12	1.67E+12
1.2	1.3	9.62E+13	8.52E+13	7.69E+13	7.02E+13	5.93E+13	5.04E+13	4.30E+13	3.39E+13	2.28E+13	1.05E+13
1.3	1.4	1.06E+14	7.65E+13	5.63E+13	4.22E+13	2.47E+13	1.52E+13	9.86E+12	5.61E+12	2.66E+12	9.13E+11
1.4	1.5	1.72E+13	8.56E+12	4.78E+12	3.06E+12	1.83E+12	1.44E+12	1.23E+12	1.02E+12	7.57E+11	4.46E+11
1.5	1.6	1.36E+13	8.47E+12	5.92E+12	4.56E+12	3.29E+12	2.68E+12	2.27E+12	1.80E+12	1.25E+12	6.21E+11
1.6	1.7	2.87E+12	1.46E+12	7.84E+11	4.60E+11	2.23E+11	1.60E+11	1.40E+11	1.26E+11	1.10E+11	8.53E+10
1.7	1.8	3.50E+12	1.76E+12	9.11E+11	4.92E+11	1.80E+11	1.00E+11	7.75E+10	6.67E+10	5.81E+10	4.52E+10
1.8	1.9	1.38E+12	6.84E+11	3.52E+11	1.92E+11	7.56E+10	4.62E+10	3.76E+10	3.29E+10	2.86E+10	2.20E+10
1.9	2.0	2.60E+12	1.29E+12	6.48E+11	3.32E+11	9.87E+10	4.02E+10	2.48E+10	1.92E+10	1.64E+10	1.28E+10
2.0	2.1	1.10E+12	5.37E+11	2.67E+11	1.36E+11	4.09E+10	1.73E+10	1.12E+10	8.86E+09	7.62E+09	5.95E+09
2.1	2.2	2.45E+13	1.02E+13	4.25E+12	1.78E+12	3.15E+11	5.70E+10	1.06E+10	9.37E+08	3.91E+07	5.65E+06
2.2	2.3	9.79E+10	4.96E+10	2.51E+10	1.28E+10	3.33E+09	9.09E+08	2.86E+08	9.28E+07	5.51E+07	3.75E+07
2.3	2.4	1.79E+12	8.95E+11	4.48E+11	2.25E+11	5.68E+10	1.44E+10	3.68E+09	4.89E+08	3.03E+07	1.15E+07
2.4	2.5	1.12E+12	5.55E+11	2.76E+11	1.38E+11	3.46E+10	8.74E+09	2.23E+09	3.00E+08	2.35E+07	1.11E+07
2.5	3.0	6.42E+11	3.23E+11	1.63E+11	8.22E+10	2.11E+10	5.62E+09	1.67E+09	4.93E+08	3.17E+08	2.80E+08
3.0	3.5	8.74E+10	4.42E+10	2.24E+10	1.13E+10	2.92E+09	7.68E+08	2.14E+08	4.65E+07	1.90E+07	1.26E+07
3.5	4.0	5.86E+07	3.87E+07	2.84E+07	2.28E+07	1.78E+07	1.57E+07	1.43E+07	1.27E+07	1.06E+07	7.30E+06
4.0	5.0	1.81E+07	1.74E+07	1.67E+07	1.61E+07	1.49E+07	1.38E+07	1.28E+07	1.15E+07	9.52E+06	6.58E+06
5.0	6.0	6.11E+06	5.85E+06	5.63E+06	5.42E+06	5.03E+06	4.66E+06	4.33E+06	3.87E+06	3.21E+06	2.22E+06
6.0	8.0	2.65E+06	2.54E+06	2.44E+06	2.35E+06	2.18E+06	2.02E+06	1.88E+06	1.68E+06	1.39E+06	9.63E+05
8.0	10.0	3.03E+05	2.90E+05	2.79E+05	2.69E+05	2.49E+05	2.31E+05	2.14E+05	1.92E+05	1.59E+05	1.10E+05
Total		2.11E+16	1.51E+16	1.18E+16	9.82E+15	7.77E+15	6.73E+15	6.10E+15	5.46E+15	4.74E+15	3.70E+15
E, MeV/sec		8.78E+15	6.71E+15	5.41E+15	4.55E+15	3.53E+15	2.98E+15	2.64E+15	2.32E+15	1.99E+15	1.54E+15

Table B.1. Photon Source Terms

Energy, MeV		Photon Source with Enrichment = 3.6%, Burnup = 35 GWd/MTU, photons/sec/MTU									
Lower	Upper	3 years	4 years	5 years	6 years	8 years	10 years	12 years	15 years	20 years	30 years
0.0	0.1	6.51E+15	4.15E+15	3.04E+15	2.49E+15	2.04E+15	1.85E+15	1.73E+15	1.60E+15	1.41E+15	1.12E+15
0.1	0.2	1.54E+15	9.08E+14	6.18E+14	4.80E+14	3.71E+14	3.29E+14	3.03E+14	2.74E+14	2.36E+14	1.78E+14
0.2	0.3	4.14E+14	2.52E+14	1.76E+14	1.39E+14	1.09E+14	9.78E+13	9.11E+13	8.32E+13	7.24E+13	5.55E+13
0.3	0.4	3.13E+14	1.84E+14	1.24E+14	9.54E+13	7.29E+13	6.51E+13	6.08E+13	5.59E+13	4.92E+13	3.83E+13
0.4	0.5	2.43E+14	1.57E+14	1.11E+14	8.38E+13	5.58E+13	4.23E+13	3.46E+13	2.81E+13	2.25E+13	1.67E+13
0.5	0.6	1.11E+15	6.80E+14	4.35E+14	2.89E+14	1.41E+14	7.83E+13	4.87E+13	2.89E+13	1.76E+13	1.12E+13
0.6	0.7	5.69E+15	4.89E+15	4.33E+15	3.94E+15	3.42E+15	3.10E+15	2.88E+15	2.63E+15	2.32E+15	1.84E+15
0.7	0.8	2.05E+15	1.46E+15	1.05E+15	7.59E+14	4.02E+14	2.18E+14	1.23E+14	5.80E+13	2.35E+13	9.79E+12
0.8	0.9	1.58E+14	1.09E+14	7.95E+13	6.05E+13	3.89E+13	2.76E+13	2.11E+13	1.55E+13	1.06E+13	5.87E+12
0.9	1.0	4.68E+13	3.35E+13	2.67E+13	2.28E+13	1.85E+13	1.58E+13	1.37E+13	1.12E+13	8.08E+12	4.45E+12
1.0	1.1	1.06E+14	7.15E+13	5.22E+13	4.07E+13	2.86E+13	2.23E+13	1.83E+13	1.42E+13	9.70E+12	4.86E+12
1.1	1.2	7.85E+13	5.44E+13	3.95E+13	2.97E+13	1.83E+13	1.23E+13	8.78E+12	5.75E+12	3.30E+12	1.48E+12
1.2	1.3	7.81E+13	6.87E+13	6.18E+13	5.64E+13	4.76E+13	4.05E+13	3.45E+13	2.72E+13	1.83E+13	8.43E+12
1.3	1.4	8.69E+13	6.28E+13	4.63E+13	3.48E+13	2.06E+13	1.28E+13	8.39E+12	4.85E+12	2.34E+12	8.16E+11
1.4	1.5	1.62E+13	7.94E+12	4.32E+12	2.70E+12	1.55E+12	1.21E+12	1.03E+12	8.57E+11	6.44E+11	3.86E+11
1.5	1.6	1.16E+13	7.15E+12	4.93E+12	3.76E+12	2.68E+12	2.17E+12	1.84E+12	1.47E+12	1.02E+12	5.13E+11
1.6	1.7	2.62E+12	1.32E+12	7.10E+11	4.16E+11	2.01E+11	1.45E+11	1.27E+11	1.14E+11	9.99E+10	7.75E+10
1.7	1.8	3.15E+12	1.58E+12	8.15E+11	4.40E+11	1.61E+11	9.04E+10	7.03E+10	6.06E+10	5.28E+10	4.11E+10
1.8	1.9	1.26E+12	6.22E+11	3.18E+11	1.73E+11	6.81E+10	4.17E+10	3.40E+10	2.98E+10	2.59E+10	2.00E+10
1.9	2.0	2.34E+12	1.16E+12	5.79E+11	2.97E+11	8.81E+10	3.61E+10	2.25E+10	1.74E+10	1.49E+10	1.17E+10
2.0	2.1	9.95E+11	4.85E+11	2.41E+11	1.22E+11	3.67E+10	1.56E+10	1.01E+10	8.06E+09	6.94E+09	5.42E+09
2.1	2.2	2.44E+13	1.01E+13	4.21E+12	1.76E+12	3.10E+11	5.57E+10	1.03E+10	8.90E+08	3.52E+07	4.99E+06
2.2	2.3	8.61E+10	4.36E+10	2.21E+10	1.12E+10	2.90E+09	7.73E+08	2.27E+08	5.99E+07	3.05E+07	2.06E+07
2.3	2.4	1.59E+12	7.94E+11	3.97E+11	1.99E+11	5.02E+10	1.27E+10	3.25E+09	4.31E+08	2.71E+07	1.05E+07
2.4	2.5	9.99E+11	4.94E+11	2.45E+11	1.22E+11	3.06E+10	7.72E+09	1.97E+09	2.65E+08	2.11E+07	1.01E+07
2.5	3.0	5.68E+11	2.85E+11	1.44E+11	7.25E+10	1.86E+10	4.89E+09	1.41E+09	3.72E+08	2.19E+08	1.94E+08
3.0	3.5	7.69E+10	3.89E+10	1.97E+10	9.97E+09	2.56E+09	6.67E+08	1.80E+08	3.36E+07	1.07E+07	6.92E+06
3.5	4.0	4.48E+07	2.76E+07	1.88E+07	1.41E+07	1.01E+07	8.65E+06	7.83E+06	6.95E+06	5.77E+06	4.01E+06
4.0	5.0	9.89E+06	9.46E+06	9.09E+06	8.76E+06	8.13E+06	7.54E+06	7.00E+06	6.26E+06	5.21E+06	3.61E+06
5.0	6.0	3.33E+06	3.19E+06	3.07E+06	2.95E+06	2.74E+06	2.54E+06	2.36E+06	2.11E+06	1.75E+06	1.22E+06
6.0	8.0	1.45E+06	1.38E+06	1.33E+06	1.28E+06	1.19E+06	1.10E+06	1.02E+06	9.16E+05	7.62E+05	5.28E+05
8.0	10.0	1.65E+05	1.58E+05	1.52E+05	1.46E+05	1.36E+05	1.26E+05	1.17E+05	1.05E+05	8.69E+04	6.03E+04
Total		1.85E+16	1.31E+16	1.02E+16	8.53E+15	6.79E+15	5.92E+15	5.38E+15	4.84E+15	4.21E+15	3.29E+15
E, MeV/sec		7.44E+15	5.68E+15	4.59E+15	3.88E+15	3.04E+15	2.58E+15	2.30E+15	2.03E+15	1.75E+15	1.35E+15

Table B.1. Photon Source Terms

Energy, MeV		Photon Source with Enrichment = 3.0%, Burnup = 40 GWd/MTU, photons/sec/MTU									
Lower	Upper	3 years	4 years	5 years	6 years	8 years	10 years	12 years	15 years	20 years	30 years
0.0	0.1	7.15E+15	4.56E+15	3.32E+15	2.71E+15	2.19E+15	1.97E+15	1.84E+15	1.69E+15	1.50E+15	1.19E+15
0.1	0.2	1.68E+15	9.97E+14	6.80E+14	5.27E+14	4.02E+14	3.54E+14	3.25E+14	2.92E+14	2.49E+14	1.87E+14
0.2	0.3	4.60E+14	2.79E+14	1.93E+14	1.51E+14	1.17E+14	1.04E+14	9.61E+13	8.75E+13	7.58E+13	5.78E+13
0.3	0.4	3.46E+14	2.03E+14	1.35E+14	1.02E+14	7.62E+13	6.73E+13	6.26E+13	5.75E+13	5.05E+13	3.93E+13
0.4	0.5	2.84E+14	1.85E+14	1.30E+14	9.72E+13	6.31E+13	4.67E+13	3.75E+13	2.97E+13	2.34E+13	1.72E+13
0.5	0.6	1.43E+15	8.80E+14	5.64E+14	3.74E+14	1.82E+14	9.90E+13	5.99E+13	3.40E+13	1.96E+13	1.20E+13
0.6	0.7	6.87E+15	5.83E+15	5.12E+15	4.61E+15	3.96E+15	3.56E+15	3.29E+15	3.00E+15	2.64E+15	2.08E+15
0.7	0.8	2.72E+15	1.95E+15	1.40E+15	1.01E+15	5.34E+14	2.90E+14	1.63E+14	7.55E+13	2.97E+13	1.17E+13
0.8	0.9	2.06E+14	1.42E+14	1.04E+14	7.90E+13	5.04E+13	3.55E+13	2.69E+13	1.95E+13	1.30E+13	6.94E+12
0.9	1.0	5.85E+13	4.25E+13	3.41E+13	2.93E+13	2.37E+13	2.02E+13	1.74E+13	1.41E+13	1.01E+13	5.35E+12
1.0	1.1	1.36E+14	9.26E+13	6.81E+13	5.34E+13	3.76E+13	2.93E+13	2.40E+13	1.85E+13	1.25E+13	6.12E+12
1.1	1.2	1.00E+14	6.97E+13	5.05E+13	3.79E+13	2.32E+13	1.54E+13	1.09E+13	6.99E+12	3.90E+12	1.67E+12
1.2	1.3	1.03E+14	9.15E+13	8.26E+13	7.54E+13	6.37E+13	5.42E+13	4.62E+13	3.64E+13	2.45E+13	1.12E+13
1.3	1.4	1.14E+14	8.21E+13	6.04E+13	4.53E+13	2.65E+13	1.64E+13	1.06E+13	6.02E+12	2.82E+12	9.36E+11
1.4	1.5	1.75E+13	8.77E+12	4.93E+12	3.17E+12	1.90E+12	1.48E+12	1.27E+12	1.04E+12	7.67E+11	4.43E+11
1.5	1.6	1.50E+13	9.25E+12	6.41E+12	4.91E+12	3.52E+12	2.85E+12	2.41E+12	1.91E+12	1.32E+12	6.47E+11
1.6	1.7	3.06E+12	1.55E+12	8.27E+11	4.78E+11	2.20E+11	1.53E+11	1.31E+11	1.18E+11	1.03E+11	7.95E+10
1.7	1.8	3.82E+12	1.92E+12	9.90E+11	5.29E+11	1.86E+11	9.82E+10	7.36E+10	6.25E+10	5.43E+10	4.22E+10
1.8	1.9	1.48E+12	7.34E+11	3.77E+11	2.03E+11	7.69E+10	4.49E+10	3.56E+10	3.09E+10	2.67E+10	2.06E+10
1.9	2.0	2.85E+12	1.41E+12	7.11E+11	3.64E+11	1.06E+11	4.09E+10	2.40E+10	1.79E+10	1.53E+10	1.19E+10
2.0	2.1	1.19E+12	5.84E+11	2.91E+11	1.48E+11	4.35E+10	1.75E+10	1.08E+10	8.29E+09	7.10E+09	5.55E+09
2.1	2.2	2.39E+13	9.97E+12	4.17E+12	1.75E+12	3.12E+11	5.68E+10	1.07E+10	9.66E+08	4.24E+07	6.20E+06
2.2	2.3	1.10E+11	5.55E+10	2.82E+10	1.43E+10	3.76E+09	1.05E+09	3.51E+08	1.31E+08	8.45E+07	5.76E+07
2.3	2.4	1.99E+12	9.95E+11	4.99E+11	2.50E+11	6.34E+10	1.61E+10	4.12E+09	5.44E+08	3.12E+07	1.07E+07
2.4	2.5	1.24E+12	6.14E+11	3.06E+11	1.53E+11	3.85E+10	9.75E+09	2.49E+09	3.33E+08	2.37E+07	1.03E+07
2.5	3.0	7.16E+11	3.61E+11	1.82E+11	9.19E+10	2.37E+10	6.30E+09	1.88E+09	5.57E+08	3.56E+08	3.12E+08
3.0	3.5	9.78E+10	4.95E+10	2.51E+10	1.27E+10	3.29E+09	8.71E+08	2.50E+08	6.14E+07	2.90E+07	1.94E+07
3.5	4.0	7.41E+07	5.15E+07	3.96E+07	3.31E+07	2.69E+07	2.40E+07	2.20E+07	1.96E+07	1.63E+07	1.12E+07
4.0	5.0	2.80E+07	2.68E+07	2.58E+07	2.48E+07	2.30E+07	2.14E+07	1.98E+07	1.77E+07	1.47E+07	1.01E+07
5.0	6.0	9.43E+06	9.04E+06	8.70E+06	8.37E+06	7.76E+06	7.20E+06	6.68E+06	5.96E+06	4.95E+06	3.41E+06
6.0	8.0	4.09E+06	3.93E+06	3.78E+06	3.64E+06	3.37E+06	3.13E+06	2.90E+06	2.59E+06	2.15E+06	1.48E+06
8.0	10.0	4.68E+05	4.48E+05	4.31E+05	4.15E+05	3.85E+05	3.57E+05	3.31E+05	2.96E+05	2.45E+05	1.69E+05
Total		2.17E+16	1.54E+16	1.20E+16	9.91E+15	7.75E+15	6.67E+15	6.01E+15	5.37E+15	4.65E+15	3.63E+15
E, MeV/sec		9.17E+15	6.97E+15	5.58E+15	4.66E+15	3.58E+15	3.00E+15	2.65E+15	2.32E+15	1.98E+15	1.53E+15

Table B.1. Photon Source Terms

Energy, MeV		Photon Source with Enrichment = 3.0%, Burnup = 35 GWd/MTU, photons/sec/MTU									
Lower	Upper	3 years	4 years	5 years	6 years	8 years	10 years	12 years	15 years	20 years	30 years
0.0	0.1	6.61E+15	4.17E+15	3.01E+15	2.44E+15	1.97E+15	1.78E+15	1.66E+15	1.53E+15	1.35E+15	1.07E+15
0.1	0.2	1.56E+15	9.16E+14	6.17E+14	4.73E+14	3.60E+14	3.16E+14	2.91E+14	2.62E+14	2.24E+14	1.69E+14
0.2	0.3	4.25E+14	2.55E+14	1.75E+14	1.36E+14	1.05E+14	9.33E+13	8.66E+13	7.89E+13	6.85E+13	5.23E+13
0.3	0.4	3.22E+14	1.87E+14	1.24E+14	9.30E+13	6.93E+13	6.13E+13	5.70E+13	5.24E+13	4.61E+13	3.59E+13
0.4	0.5	2.55E+14	1.64E+14	1.15E+14	8.60E+13	5.61E+13	4.17E+13	3.37E+13	2.69E+13	2.12E+13	1.57E+13
0.5	0.6	1.21E+15	7.43E+14	4.72E+14	3.12E+14	1.51E+14	8.23E+13	5.03E+13	2.91E+13	1.72E+13	1.07E+13
0.6	0.7	5.87E+15	5.01E+15	4.41E+15	3.99E+15	3.45E+15	3.11E+15	2.88E+15	2.63E+15	2.32E+15	1.83E+15
0.7	0.8	2.20E+15	1.57E+15	1.13E+15	8.16E+14	4.31E+14	2.34E+14	1.32E+14	6.17E+13	2.46E+13	9.97E+12
0.8	0.9	1.71E+14	1.18E+14	8.54E+13	6.48E+13	4.14E+13	2.93E+13	2.23E+13	1.62E+13	1.09E+13	5.94E+12
0.9	1.0	5.03E+13	3.59E+13	2.86E+13	2.44E+13	1.97E+13	1.67E+13	1.45E+13	1.18E+13	8.42E+12	4.54E+12
1.0	1.1	1.16E+14	7.81E+13	5.68E+13	4.42E+13	3.09E+13	2.40E+13	1.97E+13	1.52E+13	1.03E+13	5.10E+12
1.1	1.2	8.53E+13	5.91E+13	4.28E+13	3.22E+13	1.98E+13	1.33E+13	9.42E+12	6.12E+12	3.44E+12	1.49E+12
1.2	1.3	8.50E+13	7.48E+13	6.74E+13	6.14E+13	5.18E+13	4.41E+13	3.75E+13	2.96E+13	1.99E+13	9.12E+12
1.3	1.4	9.42E+13	6.79E+13	5.02E+13	3.77E+13	2.23E+13	1.39E+13	9.09E+12	5.24E+12	2.50E+12	8.40E+11
1.4	1.5	1.65E+13	8.14E+12	4.46E+12	2.80E+12	1.62E+12	1.25E+12	1.07E+12	8.80E+11	6.55E+11	3.84E+11
1.5	1.6	1.29E+13	7.89E+12	5.41E+12	4.10E+12	2.90E+12	2.34E+12	1.98E+12	1.57E+12	1.09E+12	5.39E+11
1.6	1.7	2.81E+12	1.42E+12	7.54E+11	4.34E+11	2.00E+11	1.39E+11	1.20E+11	1.07E+11	9.36E+10	7.25E+10
1.7	1.8	3.46E+12	1.74E+12	8.93E+11	4.77E+11	1.68E+11	8.89E+10	6.69E+10	5.69E+10	4.94E+10	3.85E+10
1.8	1.9	1.36E+12	6.71E+11	3.43E+11	1.85E+11	6.95E+10	4.06E+10	3.23E+10	2.80E+10	2.43E+10	1.88E+10
1.9	2.0	2.58E+12	1.28E+12	6.41E+11	3.27E+11	9.51E+10	3.70E+10	2.18E+10	1.64E+10	1.40E+10	1.09E+10
2.0	2.1	1.08E+12	5.31E+11	2.64E+11	1.34E+11	3.92E+10	1.59E+10	9.78E+09	7.57E+09	6.49E+09	5.06E+09
2.1	2.2	2.38E+13	9.90E+12	4.13E+12	1.73E+12	3.07E+11	5.55E+10	1.04E+10	9.18E+08	3.84E+07	5.52E+06
2.2	2.3	9.76E+10	4.94E+10	2.50E+10	1.27E+10	3.31E+09	8.96E+08	2.76E+08	8.47E+07	4.85E+07	3.29E+07
2.3	2.4	1.78E+12	8.91E+11	4.46E+11	2.24E+11	5.66E+10	1.44E+10	3.67E+09	4.85E+08	2.81E+07	9.81E+06
2.4	2.5	1.11E+12	5.52E+11	2.75E+11	1.37E+11	3.44E+10	8.70E+09	2.22E+09	2.97E+08	2.14E+07	9.41E+06
2.5	3.0	6.40E+11	3.22E+11	1.62E+11	8.19E+10	2.10E+10	5.54E+09	1.60E+09	4.25E+08	2.50E+08	2.20E+08
3.0	3.5	8.71E+10	4.41E+10	2.23E+10	1.13E+10	2.91E+09	7.62E+08	2.11E+08	4.37E+07	1.68E+07	1.11E+07
3.5	4.0	5.60E+07	3.63E+07	2.61E+07	2.06E+07	1.58E+07	1.38E+07	1.26E+07	1.12E+07	9.26E+06	6.40E+06
4.0	5.0	1.59E+07	1.52E+07	1.47E+07	1.41E+07	1.31E+07	1.21E+07	1.13E+07	1.01E+07	8.35E+06	5.78E+06
5.0	6.0	5.36E+06	5.13E+06	4.94E+06	4.75E+06	4.41E+06	4.09E+06	3.79E+06	3.39E+06	2.82E+06	1.95E+06
6.0	8.0	2.33E+06	2.23E+06	2.14E+06	2.06E+06	1.91E+06	1.78E+06	1.65E+06	1.47E+06	1.22E+06	8.45E+05
8.0	10.0	2.66E+05	2.55E+05	2.45E+05	2.36E+05	2.19E+05	2.03E+05	1.88E+05	1.68E+05	1.40E+05	9.64E+04
Total		1.91E+16	1.35E+16	1.04E+16	8.63E+15	6.78E+15	5.86E+15	5.31E+15	4.76E+15	4.13E+15	3.23E+15
E, MeV/sec		7.80E+15	5.92E+15	4.75E+15	3.98E+15	3.09E+15	2.61E+15	2.31E+15	2.04E+15	1.74E+15	1.35E+15

Table B.1. Photon Source Terms

Energy, MeV		Photon Source with Enrichment = 3.0%, Burnup = 30 GWd/MTU, photons/sec/MTU									
Lower	Upper	3 years	4 years	5 years	6 years	8 years	10 years	12 years	15 years	20 years	30 years
0.0	0.1	6.01E+15	3.74E+15	2.68E+15	2.16E+15	1.74E+15	1.57E+15	1.47E+15	1.35E+15	1.20E+15	9.52E+14
0.1	0.2	1.43E+15	8.26E+14	5.48E+14	4.16E+14	3.14E+14	2.77E+14	2.55E+14	2.30E+14	1.98E+14	1.49E+14
0.2	0.3	3.86E+14	2.29E+14	1.56E+14	1.20E+14	9.23E+13	8.22E+13	7.63E+13	6.97E+13	6.06E+13	4.65E+13
0.3	0.4	2.93E+14	1.69E+14	1.11E+14	8.32E+13	6.19E+13	5.47E+13	5.09E+13	4.68E+13	4.12E+13	3.21E+13
0.4	0.5	2.25E+14	1.43E+14	9.96E+13	7.44E+13	4.87E+13	3.64E+13	2.96E+13	2.38E+13	1.89E+13	1.40E+13
0.5	0.6	1.00E+15	6.08E+14	3.83E+14	2.51E+14	1.21E+14	6.62E+13	4.09E+13	2.42E+13	1.48E+13	9.41E+12
0.6	0.7	4.89E+15	4.19E+15	3.71E+15	3.38E+15	2.94E+15	2.67E+15	2.48E+15	2.27E+15	2.00E+15	1.58E+15
0.7	0.8	1.71E+15	1.22E+15	8.74E+14	6.31E+14	3.34E+14	1.82E+14	1.03E+14	4.83E+13	1.96E+13	8.18E+12
0.8	0.9	1.37E+14	9.35E+13	6.74E+13	5.10E+13	3.26E+13	2.31E+13	1.76E+13	1.29E+13	8.81E+12	4.90E+12
0.9	1.0	4.18E+13	2.92E+13	2.29E+13	1.93E+13	1.55E+13	1.32E+13	1.14E+13	9.33E+12	6.75E+12	3.71E+12
1.0	1.1	9.56E+13	6.33E+13	4.53E+13	3.49E+13	2.41E+13	1.87E+13	1.53E+13	1.18E+13	8.10E+12	4.06E+12
1.1	1.2	7.05E+13	4.87E+13	3.52E+13	2.65E+13	1.64E+13	1.11E+13	7.96E+12	5.23E+12	2.97E+12	1.30E+12
1.2	1.3	6.63E+13	5.78E+13	5.19E+13	4.72E+13	3.97E+13	3.38E+13	2.88E+13	2.27E+13	1.53E+13	7.04E+12
1.3	1.4	7.53E+13	5.44E+13	4.03E+13	3.04E+13	1.82E+13	1.15E+13	7.60E+12	4.46E+12	2.16E+12	7.39E+11
1.4	1.5	1.54E+13	7.43E+12	3.96E+12	2.41E+12	1.33E+12	1.02E+12	8.67E+11	7.17E+11	5.39E+11	3.23E+11
1.5	1.6	1.08E+13	6.49E+12	4.37E+12	3.27E+12	2.27E+12	1.82E+12	1.54E+12	1.22E+12	8.52E+11	4.28E+11
1.6	1.7	2.53E+12	1.27E+12	6.72E+11	3.86E+11	1.77E+11	1.24E+11	1.07E+11	9.55E+10	8.36E+10	6.49E+10
1.7	1.8	3.07E+12	1.53E+12	7.86E+11	4.19E+11	1.48E+11	7.89E+10	5.96E+10	5.08E+10	4.42E+10	3.44E+10
1.8	1.9	1.22E+12	6.00E+11	3.05E+11	1.64E+11	6.15E+10	3.60E+10	2.87E+10	2.50E+10	2.17E+10	1.68E+10
1.9	2.0	2.28E+12	1.13E+12	5.63E+11	2.87E+11	8.34E+10	3.26E+10	1.94E+10	1.47E+10	1.25E+10	9.76E+09
2.0	2.1	9.69E+11	4.72E+11	2.33E+11	1.18E+11	3.46E+10	1.40E+10	8.72E+09	6.77E+09	5.81E+09	4.54E+09
2.1	2.2	2.33E+13	9.70E+12	4.04E+12	1.69E+12	2.98E+11	5.35E+10	9.89E+09	8.60E+08	3.41E+07	4.81E+06
2.2	2.3	8.44E+10	4.27E+10	2.16E+10	1.10E+10	2.84E+09	7.51E+08	2.16E+08	5.26E+07	2.48E+07	1.67E+07
2.3	2.4	1.56E+12	7.78E+11	3.89E+11	1.95E+11	4.92E+10	1.25E+10	3.18E+09	4.21E+08	2.47E+07	8.79E+06
2.4	2.5	9.77E+11	4.84E+11	2.40E+11	1.20E+11	3.00E+10	7.56E+09	1.93E+09	2.58E+08	1.89E+07	8.43E+06
2.5	3.0	5.56E+11	2.80E+11	1.41E+11	7.10E+10	1.82E+10	4.75E+09	1.33E+09	3.14E+08	1.65E+08	1.45E+08
3.0	3.5	7.54E+10	3.81E+10	1.93E+10	9.77E+09	2.51E+09	6.51E+08	1.75E+08	3.09E+07	8.75E+06	5.60E+06
3.5	4.0	4.21E+07	2.53E+07	1.66E+07	1.21E+07	8.37E+06	7.03E+06	6.34E+06	5.62E+06	4.66E+06	3.24E+06
4.0	5.0	7.99E+06	7.63E+06	7.34E+06	7.07E+06	6.56E+06	6.09E+06	5.65E+06	5.06E+06	4.21E+06	2.92E+06
5.0	6.0	2.69E+06	2.57E+06	2.47E+06	2.38E+06	2.21E+06	2.05E+06	1.90E+06	1.70E+06	1.42E+06	9.85E+05
6.0	8.0	1.17E+06	1.12E+06	1.07E+06	1.03E+06	9.60E+05	8.91E+05	8.27E+05	7.40E+05	6.15E+05	4.27E+05
8.0	10.0	1.33E+05	1.28E+05	1.23E+05	1.18E+05	1.10E+05	1.02E+05	9.44E+04	8.45E+04	7.02E+04	4.88E+04
Total		1.65E+16	1.15E+16	8.85E+15	7.33E+15	5.80E+15	5.05E+15	4.59E+15	4.13E+15	3.59E+15	2.81E+15
E, MeV/sec		6.46E+15	4.89E+15	3.93E+15	3.31E+15	2.60E+15	2.21E+15	1.97E+15	1.74E+15	1.50E+15	1.16E+15

Table B.1. Photon Source Terms

Energy, MeV		Photon Source with Enrichment = 3.0%, Burnup = 25 GWd/MTU, photons/sec/MTU									
Lower	Upper	3 years	4 years	5 years	6 years	8 years	10 years	12 years	15 years	20 years	30 years
0.0	0.1	5.34E+15	3.28E+15	2.32E+15	1.86E+15	1.49E+15	1.35E+15	1.26E+15	1.16E+15	1.03E+15	8.21E+14
0.1	0.2	1.29E+15	7.28E+14	4.75E+14	3.57E+14	2.67E+14	2.35E+14	2.17E+14	1.97E+14	1.70E+14	1.29E+14
0.2	0.3	3.41E+14	2.00E+14	1.35E+14	1.03E+14	7.90E+13	7.04E+13	6.55E+13	6.00E+13	5.23E+13	4.02E+13
0.3	0.4	2.61E+14	1.49E+14	9.71E+13	7.24E+13	5.38E+13	4.76E+13	4.43E+13	4.08E+13	3.59E+13	2.80E+13
0.4	0.5	1.92E+14	1.21E+14	8.37E+13	6.24E+13	4.10E+13	3.09E+13	2.53E+13	2.05E+13	1.64E+13	1.22E+13
0.5	0.6	7.95E+14	4.76E+14	2.97E+14	1.93E+14	9.22E+13	5.08E+13	3.19E+13	1.94E+13	1.23E+13	8.02E+12
0.6	0.7	3.93E+15	3.39E+15	3.03E+15	2.77E+15	2.43E+15	2.22E+15	2.06E+15	1.89E+15	1.67E+15	1.32E+15
0.7	0.8	1.25E+15	8.91E+14	6.39E+14	4.61E+14	2.44E+14	1.33E+14	7.54E+13	3.58E+13	1.48E+13	6.44E+12
0.8	0.9	1.06E+14	7.08E+13	5.06E+13	3.81E+13	2.42E+13	1.72E+13	1.33E+13	9.82E+12	6.80E+12	3.89E+12
0.9	1.0	3.35E+13	2.28E+13	1.75E+13	1.46E+13	1.16E+13	9.86E+12	8.58E+12	7.04E+12	5.15E+12	2.91E+12
1.0	1.1	7.55E+13	4.89E+13	3.44E+13	2.61E+13	1.77E+13	1.37E+13	1.12E+13	8.71E+12	6.00E+12	3.07E+12
1.1	1.2	5.62E+13	3.86E+13	2.79E+13	2.10E+13	1.32E+13	9.00E+12	6.52E+12	4.33E+12	2.49E+12	1.10E+12
1.2	1.3	4.87E+13	4.20E+13	3.74E+13	3.39E+13	2.85E+13	2.42E+13	2.07E+13	1.63E+13	1.10E+13	5.09E+12
1.3	1.4	5.76E+13	4.17E+13	3.10E+13	2.35E+13	1.43E+13	9.14E+12	6.16E+12	3.68E+12	1.82E+12	6.32E+11
1.4	1.5	1.41E+13	6.65E+12	3.44E+12	2.01E+12	1.05E+12	7.89E+11	6.72E+11	5.59E+11	4.26E+11	2.62E+11
1.5	1.6	8.65E+12	5.12E+12	3.37E+12	2.47E+12	1.68E+12	1.34E+12	1.13E+12	8.99E+11	6.31E+11	3.24E+11
1.6	1.7	2.21E+12	1.10E+12	5.81E+11	3.32E+11	1.53E+11	1.07E+11	9.24E+10	8.30E+10	7.27E+10	5.65E+10
1.7	1.8	2.62E+12	1.31E+12	6.68E+11	3.56E+11	1.26E+11	6.79E+10	5.17E+10	4.42E+10	3.85E+10	3.00E+10
1.8	1.9	1.07E+12	5.21E+11	2.63E+11	1.41E+11	5.27E+10	3.10E+10	2.48E+10	2.16E+10	1.88E+10	1.46E+10
1.9	2.0	1.95E+12	9.59E+11	4.78E+11	2.43E+11	7.06E+10	2.79E+10	1.68E+10	1.28E+10	1.09E+10	8.52E+09
2.0	2.1	8.38E+11	4.06E+11	2.00E+11	1.01E+11	2.94E+10	1.20E+10	7.55E+09	5.90E+09	5.07E+09	3.96E+09
2.1	2.2	2.25E+13	9.35E+12	3.89E+12	1.62E+12	2.84E+11	5.07E+10	9.28E+09	7.88E+08	2.95E+07	4.07E+06
2.2	2.3	7.01E+10	3.55E+10	1.80E+10	9.09E+09	2.34E+09	6.10E+08	1.66E+08	3.23E+07	1.11E+07	7.39E+06
2.3	2.4	1.31E+12	6.53E+11	3.26E+11	1.63E+11	4.10E+10	1.04E+10	2.65E+09	3.50E+08	2.10E+07	7.67E+06
2.4	2.5	8.28E+11	4.08E+11	2.02E+11	1.01E+11	2.51E+10	6.31E+09	1.61E+09	2.15E+08	1.61E+07	7.36E+06
2.5	3.0	4.65E+11	2.33E+11	1.17E+11	5.91E+10	1.51E+10	3.91E+09	1.07E+09	2.25E+08	1.02E+08	8.89E+07
3.0	3.5	6.26E+10	3.17E+10	1.60E+10	8.11E+09	2.08E+09	5.36E+08	1.41E+08	2.18E+07	4.10E+06	2.48E+06
3.5	4.0	3.14E+07	1.76E+07	1.06E+07	6.96E+06	4.06E+06	3.16E+06	2.78E+06	2.45E+06	2.04E+06	1.44E+06
4.0	5.0	3.46E+06	3.30E+06	3.17E+06	3.05E+06	2.84E+06	2.64E+06	2.45E+06	2.20E+06	1.84E+06	1.29E+06
5.0	6.0	1.16E+06	1.11E+06	1.07E+06	1.03E+06	9.56E+05	8.88E+05	8.26E+05	7.41E+05	6.19E+05	4.35E+05
6.0	8.0	5.06E+05	4.82E+05	4.64E+05	4.47E+05	4.15E+05	3.86E+05	3.58E+05	3.22E+05	2.69E+05	1.89E+05
8.0	10.0	5.77E+04	5.50E+04	5.29E+04	5.10E+04	4.74E+04	4.40E+04	4.09E+04	3.67E+04	3.06E+04	2.15E+04
Total		1.38E+16	9.52E+15	7.29E+15	6.04E+15	4.81E+15	4.22E+15	3.85E+15	3.48E+15	3.04E+15	2.39E+15
E, MeV/sec		5.16E+15	3.90E+15	3.14E+15	2.66E+15	2.11E+15	1.81E+15	1.63E+15	1.45E+15	1.25E+15	9.74E+14

Table B.1. Photon Source Terms

Energy, MeV		Photon Source with Enrichment = 2.4%, Burnup = 30 GWd/MTU, photons/sec/MTU									
Lower	Upper	3 years	4 years	5 years	6 years	8 years	10 years	12 years	15 years	20 years	30 years
0.0	0.1	6.12E+15	3.76E+15	2.65E+15	2.11E+15	1.66E+15	1.49E+15	1.39E+15	1.28E+15	1.14E+15	9.07E+14
0.1	0.2	1.46E+15	8.35E+14	5.47E+14	4.10E+14	3.03E+14	2.64E+14	2.42E+14	2.18E+14	1.86E+14	1.40E+14
0.2	0.3	3.97E+14	2.33E+14	1.55E+14	1.18E+14	8.81E+13	7.76E+13	7.18E+13	6.54E+13	5.67E+13	4.33E+13
0.3	0.4	3.03E+14	1.72E+14	1.11E+14	8.09E+13	5.83E+13	5.09E+13	4.72E+13	4.33E+13	3.80E+13	2.96E+13
0.4	0.5	2.37E+14	1.51E+14	1.04E+14	7.67E+13	4.90E+13	3.59E+13	2.86E+13	2.26E+13	1.76E+13	1.30E+13
0.5	0.6	1.11E+15	6.69E+14	4.19E+14	2.73E+14	1.29E+14	6.96E+13	4.23E+13	2.43E+13	1.43E+13	8.90E+12
0.6	0.7	5.05E+15	4.30E+15	3.78E+15	3.42E+15	2.96E+15	2.68E+15	2.48E+15	2.26E+15	2.00E+15	1.58E+15
0.7	0.8	1.84E+15	1.31E+15	9.43E+14	6.80E+14	3.60E+14	1.95E+14	1.10E+14	5.16E+13	2.06E+13	8.33E+12
0.8	0.9	1.49E+14	1.01E+14	7.28E+13	5.49E+13	3.49E+13	2.46E+13	1.87E+13	1.36E+13	9.15E+12	4.96E+12
0.9	1.0	4.53E+13	3.16E+13	2.47E+13	2.08E+13	1.66E+13	1.41E+13	1.22E+13	9.88E+12	7.07E+12	3.80E+12
1.0	1.1	1.06E+14	6.98E+13	4.98E+13	3.82E+13	2.62E+13	2.03E+13	1.66E+13	1.28E+13	8.70E+12	4.29E+12
1.1	1.2	7.71E+13	5.31E+13	3.84E+13	2.89E+13	1.79E+13	1.20E+13	8.59E+12	5.60E+12	3.12E+12	1.31E+12
1.2	1.3	7.28E+13	6.37E+13	5.71E+13	5.20E+13	4.38E+13	3.72E+13	3.17E+13	2.50E+13	1.68E+13	7.69E+12
1.3	1.4	8.19E+13	5.92E+13	4.38E+13	3.31E+13	1.98E+13	1.25E+13	8.29E+12	4.85E+12	2.33E+12	7.64E+11
1.4	1.5	1.57E+13	7.64E+12	4.10E+12	2.51E+12	1.39E+12	1.06E+12	8.99E+11	7.38E+11	5.48E+11	3.21E+11
1.5	1.6	1.21E+13	7.25E+12	4.85E+12	3.60E+12	2.48E+12	1.98E+12	1.67E+12	1.32E+12	9.15E+11	4.53E+11
1.6	1.7	2.73E+12	1.37E+12	7.19E+11	4.06E+11	1.77E+11	1.18E+11	9.94E+10	8.84E+10	7.72E+10	5.98E+10
1.7	1.8	3.40E+12	1.70E+12	8.69E+11	4.59E+11	1.55E+11	7.75E+10	5.62E+10	4.71E+10	4.08E+10	3.17E+10
1.8	1.9	1.33E+12	6.53E+11	3.31E+11	1.76E+11	6.32E+10	3.50E+10	2.70E+10	2.32E+10	2.01E+10	1.55E+10
1.9	2.0	2.54E+12	1.26E+12	6.29E+11	3.20E+11	9.09E+10	3.36E+10	1.88E+10	1.36E+10	1.15E+10	8.98E+09
2.0	2.1	1.06E+12	5.20E+11	2.58E+11	1.31E+11	3.73E+10	1.43E+10	8.38E+09	6.28E+09	5.35E+09	4.18E+09
2.1	2.2	2.27E+13	9.46E+12	3.95E+12	1.65E+12	2.94E+11	5.33E+10	9.98E+09	8.89E+08	3.74E+07	5.35E+06
2.2	2.3	9.66E+10	4.89E+10	2.48E+10	1.26E+10	3.26E+09	8.78E+08	2.64E+08	7.52E+07	4.08E+07	2.76E+07
2.3	2.4	1.76E+12	8.81E+11	4.41E+11	2.21E+11	5.60E+10	1.42E+10	3.63E+09	4.78E+08	2.57E+07	8.09E+06
2.4	2.5	1.10E+12	5.45E+11	2.71E+11	1.36E+11	3.40E+10	8.61E+09	2.19E+09	2.92E+08	1.92E+07	7.76E+06
2.5	3.0	6.33E+11	3.19E+11	1.61E+11	8.10E+10	2.08E+10	5.43E+09	1.53E+09	3.62E+08	1.89E+08	1.64E+08
3.0	3.5	8.63E+10	4.37E+10	2.21E+10	1.12E+10	2.88E+09	7.52E+08	2.05E+08	4.04E+07	1.42E+07	9.27E+06
3.5	4.0	5.28E+07	3.34E+07	2.33E+07	1.80E+07	1.34E+07	1.16E+07	1.05E+07	9.37E+06	7.77E+06	5.37E+06
4.0	5.0	1.33E+07	1.28E+07	1.23E+07	1.18E+07	1.10E+07	1.02E+07	9.44E+06	8.44E+06	7.01E+06	4.85E+06
5.0	6.0	4.50E+06	4.30E+06	4.14E+06	3.99E+06	3.70E+06	3.43E+06	3.18E+06	2.84E+06	2.36E+06	1.63E+06
6.0	8.0	1.95E+06	1.87E+06	1.80E+06	1.73E+06	1.61E+06	1.49E+06	1.38E+06	1.23E+06	1.03E+06	7.09E+05
8.0	10.0	2.23E+05	2.13E+05	2.05E+05	1.98E+05	1.83E+05	1.70E+05	1.58E+05	1.41E+05	1.17E+05	8.09E+04
Total		1.71E+16	1.18E+16	9.02E+15	7.41E+15	5.77E+15	4.99E+15	4.51E+15	4.05E+15	3.51E+15	2.75E+15
E, MeV/sec		6.80E+15	5.11E+15	4.08E+15	3.41E+15	2.64E+15	2.23E+15	1.98E+15	1.74E+15	1.49E+15	1.16E+15

Table B.1. Photon Source Terms

Energy, MeV		Photon Source with Enrichment = 2.4%, Burnup = 25 GWd/MTU, photons/sec/MTU									
Lower	Upper	3 years	4 years	5 years	6 years	8 years	10 years	12 years	15 years	20 years	30 years
0.0	0.1	5.44E+15	3.30E+15	2.30E+15	1.82E+15	1.43E+15	1.29E+15	1.20E+15	1.11E+15	9.83E+14	7.86E+14
0.1	0.2	1.31E+15	7.36E+14	4.75E+14	3.52E+14	2.57E+14	2.25E+14	2.06E+14	1.86E+14	1.60E+14	1.21E+14
0.2	0.3	3.52E+14	2.04E+14	1.35E+14	1.01E+14	7.55E+13	6.66E+13	6.17E+13	5.63E+13	4.90E+13	3.75E+13
0.3	0.4	2.70E+14	1.52E+14	9.70E+13	7.07E+13	5.08E+13	4.44E+13	4.12E+13	3.78E+13	3.33E+13	2.59E+13
0.4	0.5	2.03E+14	1.28E+14	8.76E+13	6.46E+13	4.14E+13	3.05E+13	2.45E+13	1.95E+13	1.53E+13	1.13E+13
0.5	0.6	8.92E+14	5.31E+14	3.29E+14	2.12E+14	9.96E+13	5.39E+13	3.31E+13	1.95E+13	1.19E+13	7.59E+12
0.6	0.7	4.07E+15	3.48E+15	3.09E+15	2.81E+15	2.45E+15	2.22E+15	2.07E+15	1.89E+15	1.67E+15	1.32E+15
0.7	0.8	1.36E+15	9.72E+14	6.97E+14	5.03E+14	2.66E+14	1.45E+14	8.18E+13	3.86E+13	1.57E+13	6.58E+12
0.8	0.9	1.16E+14	7.76E+13	5.53E+13	4.15E+13	2.62E+13	1.85E+13	1.42E+13	1.04E+13	7.09E+12	3.95E+12
0.9	1.0	3.65E+13	2.48E+13	1.90E+13	1.58E+13	1.25E+13	1.06E+13	9.20E+12	7.51E+12	5.43E+12	2.99E+12
1.0	1.1	8.47E+13	5.47E+13	3.83E+13	2.90E+13	1.96E+13	1.51E+13	1.23E+13	9.52E+12	6.51E+12	3.26E+12
1.1	1.2	6.21E+13	4.26E+13	3.08E+13	2.32E+13	1.45E+13	9.85E+12	7.10E+12	4.68E+12	2.64E+12	1.11E+12
1.2	1.3	5.43E+13	4.70E+13	4.19E+13	3.80E+13	3.19E+13	2.71E+13	2.31E+13	1.82E+13	1.23E+13	5.65E+12
1.3	1.4	6.34E+13	4.59E+13	3.41E+13	2.59E+13	1.57E+13	1.01E+13	6.78E+12	4.04E+12	1.98E+12	6.59E+11
1.4	1.5	1.43E+13	6.82E+12	3.56E+12	2.10E+12	1.11E+12	8.26E+11	6.99E+11	5.77E+11	4.34E+11	2.60E+11
1.5	1.6	9.81E+12	5.78E+12	3.79E+12	2.76E+12	1.86E+12	1.47E+12	1.24E+12	9.84E+11	6.85E+11	3.44E+11
1.6	1.7	2.40E+12	1.20E+12	6.25E+11	3.51E+11	1.53E+11	1.02E+11	8.65E+10	7.71E+10	6.74E+10	5.23E+10
1.7	1.8	2.93E+12	1.46E+12	7.45E+11	3.94E+11	1.33E+11	6.70E+10	4.89E+10	4.11E+10	3.56E+10	2.78E+10
1.8	1.9	1.16E+12	5.70E+11	2.87E+11	1.52E+11	5.45E+10	3.02E+10	2.34E+10	2.02E+10	1.75E+10	1.35E+10
1.9	2.0	2.19E+12	1.08E+12	5.39E+11	2.74E+11	7.77E+10	2.89E+10	1.63E+10	1.19E+10	1.01E+10	7.87E+09
2.0	2.1	9.26E+11	4.51E+11	2.23E+11	1.12E+11	3.20E+10	1.23E+10	7.29E+09	5.50E+09	4.69E+09	3.66E+09
2.1	2.2	2.19E+13	9.12E+12	3.80E+12	1.59E+12	2.80E+11	5.05E+10	9.34E+09	8.15E+08	3.25E+07	4.58E+06
2.2	2.3	8.14E+10	4.12E+10	2.09E+10	1.06E+10	2.73E+09	7.17E+08	2.01E+08	4.50E+07	1.91E+07	1.28E+07
2.3	2.4	1.50E+12	7.49E+11	3.74E+11	1.88E+11	4.74E+10	1.20E+10	3.07E+09	4.04E+08	2.20E+07	7.09E+06
2.4	2.5	9.39E+11	4.65E+11	2.31E+11	1.15E+11	2.89E+10	7.28E+09	1.85E+09	2.46E+08	1.65E+07	6.80E+06
2.5	3.0	5.36E+11	2.69E+11	1.36E+11	6.84E+10	1.75E+10	4.54E+09	1.25E+09	2.63E+08	1.19E+08	1.03E+08
3.0	3.5	7.27E+10	3.68E+10	1.86E+10	9.42E+09	2.42E+09	6.26E+08	1.66E+08	2.79E+07	6.85E+06	4.30E+06
3.5	4.0	3.88E+07	2.27E+07	1.44E+07	1.01E+07	6.62E+06	5.44E+06	4.86E+06	4.30E+06	3.57E+06	2.49E+06
4.0	5.0	6.11E+06	5.84E+06	5.61E+06	5.40E+06	5.02E+06	4.66E+06	4.33E+06	3.87E+06	3.22E+06	2.25E+06
5.0	6.0	2.06E+06	1.97E+06	1.89E+06	1.82E+06	1.69E+06	1.57E+06	1.46E+06	1.30E+06	1.09E+06	7.56E+05
6.0	8.0	8.94E+05	8.54E+05	8.21E+05	7.91E+05	7.34E+05	6.81E+05	6.33E+05	5.66E+05	4.71E+05	3.28E+05
8.0	10.0	1.02E+05	9.75E+04	9.38E+04	9.03E+04	8.38E+04	7.78E+04	7.22E+04	6.47E+04	5.38E+04	3.74E+04
Total		1.44E+16	9.83E+15	7.44E+15	6.11E+15	4.79E+15	4.17E+15	3.79E+15	3.42E+15	2.98E+15	2.34E+15
E, MeV/sec		5.46E+15	4.09E+15	3.27E+15	2.75E+15	2.15E+15	1.83E+15	1.64E+15	1.45E+15	1.25E+15	9.69E+14

Table B.1. Photon Source Terms

Energy, MeV		Photon Source with Enrichment = 2.4%, Burnup = 20 GWd/MTU, photons/sec/MTU									
Lower	Upper	3 years	4 years	5 years	6 years	8 years	10 years	12 years	15 years	20 years	30 years
0.0	0.1	4.68E+15	2.80E+15	1.93E+15	1.51E+15	1.19E+15	1.07E+15	9.96E+14	9.20E+14	8.16E+14	6.52E+14
0.1	0.2	1.14E+15	6.27E+14	3.98E+14	2.91E+14	2.11E+14	1.84E+14	1.69E+14	1.54E+14	1.32E+14	1.01E+14
0.2	0.3	3.01E+14	1.72E+14	1.12E+14	8.41E+13	6.24E+13	5.51E+13	5.12E+13	4.68E+13	4.08E+13	3.14E+13
0.3	0.4	2.32E+14	1.29E+14	8.19E+13	5.95E+13	4.27E+13	3.74E+13	3.47E+13	3.19E+13	2.80E+13	2.19E+13
0.4	0.5	1.68E+14	1.04E+14	7.08E+13	5.21E+13	3.35E+13	2.50E+13	2.02E+13	1.62E+13	1.28E+13	9.53E+12
0.5	0.6	6.76E+14	3.97E+14	2.43E+14	1.55E+14	7.21E+13	3.92E+13	2.45E+13	1.49E+13	9.50E+12	6.24E+12
0.6	0.7	3.13E+15	2.69E+15	2.41E+15	2.20E+15	1.94E+15	1.77E+15	1.66E+15	1.52E+15	1.34E+15	1.06E+15
0.7	0.8	9.36E+14	6.65E+14	4.77E+14	3.44E+14	1.82E+14	9.92E+13	5.63E+13	2.68E+13	1.12E+13	4.93E+12
0.8	0.9	8.46E+13	5.57E+13	3.92E+13	2.92E+13	1.84E+13	1.30E+13	1.00E+13	7.45E+12	5.18E+12	2.98E+12
0.9	1.0	2.80E+13	1.85E+13	1.38E+13	1.13E+13	8.81E+12	7.48E+12	6.50E+12	5.34E+12	3.91E+12	2.23E+12
1.0	1.1	6.40E+13	4.03E+13	2.76E+13	2.05E+13	1.35E+13	1.03E+13	8.45E+12	6.56E+12	4.53E+12	2.33E+12
1.1	1.2	4.75E+13	3.24E+13	2.34E+13	1.77E+13	1.12E+13	7.72E+12	5.63E+12	3.76E+12	2.14E+12	9.12E+11
1.2	1.3	3.76E+13	3.19E+13	2.82E+13	2.55E+13	2.14E+13	1.82E+13	1.55E+13	1.22E+13	8.26E+12	3.82E+12
1.3	1.4	4.62E+13	3.35E+13	2.51E+13	1.92E+13	1.18E+13	7.75E+12	5.31E+12	3.23E+12	1.62E+12	5.47E+11
1.4	1.5	1.27E+13	5.92E+12	2.99E+12	1.70E+12	8.33E+11	6.07E+11	5.13E+11	4.27E+11	3.26E+11	2.02E+11
1.5	1.6	7.55E+12	4.36E+12	2.78E+12	1.98E+12	1.29E+12	1.01E+12	8.50E+11	6.78E+11	4.76E+11	2.45E+11
1.6	1.7	2.02E+12	1.00E+12	5.20E+11	2.91E+11	1.27E+11	8.54E+10	7.26E+10	6.49E+10	5.68E+10	4.41E+10
1.7	1.8	2.41E+12	1.20E+12	6.08E+11	3.21E+11	1.09E+11	5.57E+10	4.10E+10	3.46E+10	3.01E+10	2.34E+10
1.8	1.9	9.79E+11	4.75E+11	2.38E+11	1.26E+11	4.49E+10	2.51E+10	1.96E+10	1.69E+10	1.47E+10	1.14E+10
1.9	2.0	1.80E+12	8.83E+11	4.39E+11	2.22E+11	6.32E+10	2.38E+10	1.36E+10	1.00E+10	8.53E+09	6.66E+09
2.0	2.1	7.71E+11	3.73E+11	1.83E+11	9.21E+10	2.62E+10	1.02E+10	6.10E+09	4.64E+09	3.96E+09	3.09E+09
2.1	2.2	2.06E+13	8.54E+12	3.55E+12	1.48E+12	2.60E+11	4.64E+10	8.49E+09	7.23E+08	2.72E+07	3.78E+06
2.2	2.3	6.48E+10	3.28E+10	1.66E+10	8.40E+09	2.16E+09	5.60E+08	1.50E+08	2.67E+07	7.68E+06	5.03E+06
2.3	2.4	1.21E+12	6.03E+11	3.01E+11	1.51E+11	3.79E+10	9.60E+09	2.45E+09	3.22E+08	1.80E+07	5.99E+06
2.4	2.5	7.64E+11	3.77E+11	1.87E+11	9.28E+10	2.32E+10	5.83E+09	1.48E+09	1.97E+08	1.36E+07	5.75E+06
2.5	3.0	4.29E+11	2.16E+11	1.08E+11	5.46E+10	1.39E+10	3.59E+09	9.65E+08	1.82E+08	6.88E+07	5.92E+07
3.0	3.5	5.79E+10	2.93E+10	1.48E+10	7.50E+09	1.92E+09	4.95E+08	1.29E+08	1.91E+07	2.91E+06	1.69E+06
3.5	4.0	2.81E+07	1.53E+07	8.88E+06	5.57E+06	2.95E+06	2.18E+06	1.88E+06	1.65E+06	1.37E+06	9.75E+05
4.0	5.0	2.31E+06	2.20E+06	2.12E+06	2.04E+06	1.90E+06	1.77E+06	1.64E+06	1.48E+06	1.24E+06	8.79E+05
5.0	6.0	7.79E+05	7.42E+05	7.14E+05	6.88E+05	6.40E+05	5.95E+05	5.54E+05	4.98E+05	4.17E+05	2.96E+05
6.0	8.0	3.38E+05	3.22E+05	3.10E+05	2.99E+05	2.78E+05	2.58E+05	2.40E+05	2.16E+05	1.81E+05	1.28E+05
8.0	10.0	3.86E+04	3.68E+04	3.54E+04	3.41E+04	3.17E+04	2.95E+04	2.74E+04	2.46E+04	2.06E+04	1.46E+04
Total		1.16E+16	7.82E+15	5.88E+15	4.83E+15	3.82E+15	3.35E+15	3.06E+15	2.77E+15	2.42E+15	1.90E+15
E, MeV/sec		4.17E+15	3.11E+15	2.49E+15	2.11E+15	1.67E+15	1.44E+15	1.30E+15	1.16E+15	1.00E+15	7.80E+14

Table B.1. Photon Source Terms

Energy, MeV		Photon Source with Enrichment = 2.4%, Burnup = 15 GWd/MTU, photons/sec/MTU									
Lower	Upper	3 years	4 years	5 years	6 years	8 years	10 years	12 years	15 years	20 years	30 years
0.0	0.1	3.79E+15	2.23E+15	1.52E+15	1.18E+15	9.23E+14	8.30E+14	7.77E+14	7.17E+14	6.36E+14	5.07E+14
0.1	0.2	9.34E+14	5.05E+14	3.14E+14	2.26E+14	1.62E+14	1.42E+14	1.31E+14	1.19E+14	1.03E+14	7.91E+13
0.2	0.3	2.43E+14	1.37E+14	8.83E+13	6.55E+13	4.86E+13	4.30E+13	4.00E+13	3.67E+13	3.21E+13	2.48E+13
0.3	0.4	1.88E+14	1.03E+14	6.50E+13	4.71E+13	3.38E+13	2.96E+13	2.76E+13	2.53E+13	2.23E+13	1.74E+13
0.4	0.5	1.30E+14	7.93E+13	5.34E+13	3.92E+13	2.54E+13	1.91E+13	1.57E+13	1.27E+13	1.01E+13	7.57E+12
0.5	0.6	4.68E+14	2.70E+14	1.63E+14	1.03E+14	4.73E+13	2.60E+13	1.66E+13	1.06E+13	7.11E+12	4.83E+12
0.6	0.7	2.23E+15	1.94E+15	1.75E+15	1.61E+15	1.44E+15	1.33E+15	1.24E+15	1.14E+15	1.01E+15	8.02E+14
0.7	0.8	5.69E+14	4.02E+14	2.88E+14	2.07E+14	1.10E+14	6.01E+13	3.43E+13	1.66E+13	7.27E+12	3.41E+12
0.8	0.9	5.64E+13	3.62E+13	2.50E+13	1.84E+13	1.15E+13	8.23E+12	6.41E+12	4.85E+12	3.46E+12	2.09E+12
0.9	1.0	2.00E+13	1.26E+13	9.07E+12	7.25E+12	5.57E+12	4.72E+12	4.13E+12	3.43E+12	2.57E+12	1.53E+12
1.0	1.1	4.42E+13	2.70E+13	1.79E+13	1.29E+13	8.30E+12	6.29E+12	5.14E+12	4.02E+12	2.82E+12	1.50E+12
1.1	1.2	3.36E+13	2.28E+13	1.65E+13	1.25E+13	8.04E+12	5.65E+12	4.18E+12	2.83E+12	1.63E+12	7.04E+11
1.2	1.3	2.31E+13	1.91E+13	1.67E+13	1.49E+13	1.25E+13	1.06E+13	9.02E+12	7.14E+12	4.85E+12	2.27E+12
1.3	1.4	3.08E+13	2.24E+13	1.69E+13	1.31E+13	8.27E+12	5.54E+12	3.88E+12	2.42E+12	1.24E+12	4.28E+11
1.4	1.5	1.07E+13	4.87E+12	2.37E+12	1.29E+12	5.80E+11	4.09E+11	3.45E+11	2.90E+11	2.26E+11	1.46E+11
1.5	1.6	5.35E+12	3.01E+12	1.86E+12	1.28E+12	7.98E+11	6.17E+11	5.17E+11	4.15E+11	2.96E+11	1.58E+11
1.6	1.7	1.59E+12	7.81E+11	4.03E+11	2.25E+11	9.87E+10	6.71E+10	5.74E+10	5.15E+10	4.51E+10	3.51E+10
1.7	1.8	1.84E+12	9.07E+11	4.59E+11	2.42E+11	8.30E+10	4.32E+10	3.23E+10	2.75E+10	2.39E+10	1.87E+10
1.8	1.9	7.68E+11	3.70E+11	1.84E+11	9.66E+10	3.46E+10	1.96E+10	1.54E+10	1.34E+10	1.17E+10	9.06E+09
1.9	2.0	1.37E+12	6.68E+11	3.30E+11	1.67E+11	4.75E+10	1.82E+10	1.06E+10	7.98E+09	6.80E+09	5.31E+09
2.0	2.1	5.97E+11	2.87E+11	1.40E+11	6.99E+10	1.99E+10	7.84E+09	4.78E+09	3.69E+09	3.16E+09	2.47E+09
2.1	2.2	1.83E+13	7.60E+12	3.15E+12	1.31E+12	2.29E+11	4.05E+10	7.31E+09	6.06E+08	2.14E+07	2.93E+06
2.2	2.3	4.71E+10	2.39E+10	1.21E+10	6.11E+09	1.57E+09	4.03E+08	1.05E+08	1.57E+07	2.55E+06	1.58E+06
2.3	2.4	9.00E+11	4.46E+11	2.22E+11	1.11E+11	2.78E+10	7.02E+09	1.79E+09	2.36E+08	1.36E+07	4.78E+06
2.4	2.5	5.73E+11	2.81E+11	1.39E+11	6.88E+10	1.71E+10	4.28E+09	1.08E+09	1.44E+08	1.04E+07	4.58E+06
2.5	3.0	3.15E+11	1.58E+11	7.94E+10	3.99E+10	1.02E+10	2.61E+09	6.88E+08	1.17E+08	3.44E+07	2.90E+07
3.0	3.5	4.21E+10	2.13E+10	1.08E+10	5.45E+09	1.40E+09	3.58E+08	9.24E+07	1.27E+07	1.10E+06	5.26E+05
3.5	4.0	1.93E+07	1.01E+07	5.41E+06	3.04E+06	1.21E+06	7.17E+05	5.65E+05	4.81E+05	4.08E+05	3.04E+05
4.0	5.0	6.51E+05	6.18E+05	5.96E+05	5.75E+05	5.38E+05	5.04E+05	4.72E+05	4.29E+05	3.67E+05	2.73E+05
5.0	6.0	2.19E+05	2.08E+05	2.01E+05	1.94E+05	1.81E+05	1.70E+05	1.59E+05	1.44E+05	1.23E+05	9.17E+04
6.0	8.0	9.52E+04	9.03E+04	8.70E+04	8.40E+04	7.86E+04	7.36E+04	6.89E+04	6.25E+04	5.34E+04	3.97E+04
8.0	10.0	1.09E+04	1.03E+04	9.93E+03	9.59E+03	8.96E+03	8.39E+03	7.85E+03	7.13E+03	6.08E+03	4.51E+03
Total		8.80E+15	5.83E+15	4.35E+15	3.57E+15	2.84E+15	2.52E+15	2.32E+15	2.11E+15	1.85E+15	1.45E+15
E, MeV/sec		2.95E+15	2.19E+15	1.76E+15	1.50E+15	1.21E+15	1.06E+15	9.65E+14	8.68E+14	7.54E+14	5.89E+14

Table B.2. Neutron Source Terms

Neutron Source, neutrons/sec/MTU

E, %	Burnup, GWd/MTU	Cooling time, years 3	4	5	6	8	10	12	15	20	30
2.4	15	1.95E+07	1.86E+07	1.80E+07	1.75E+07	1.65E+07	1.57E+07	1.48E+07	1.37E+07	1.21E+07	9.67E+06
2.4	20	6.79E+07	6.48E+07	6.24E+07	6.03E+07	5.64E+07	5.27E+07	4.94E+07	4.47E+07	3.81E+07	2.81E+07
2.4	25	1.78E+08	1.70E+08	1.64E+08	1.58E+08	1.47E+08	1.37E+08	1.28E+08	1.15E+08	9.63E+07	6.85E+07
2.4	30	3.88E+08	3.71E+08	3.57E+08	3.44E+08	3.20E+08	2.97E+08	2.76E+08	2.47E+08	2.06E+08	1.44E+08
3.0	25	1.01E+08	9.67E+07	9.31E+07	8.99E+07	8.38E+07	7.82E+07	7.31E+07	6.60E+07	5.59E+07	4.05E+07
3.0	30	2.33E+08	2.23E+08	2.14E+08	2.06E+08	1.92E+08	1.79E+08	1.66E+08	1.49E+08	1.25E+08	8.83E+07
3.0	35	4.62E+08	4.43E+08	4.26E+08	4.10E+08	3.81E+08	3.54E+08	3.29E+08	2.94E+08	2.45E+08	1.71E+08
3.0	40	8.12E+08	7.78E+08	7.49E+08	7.21E+08	6.69E+08	6.21E+08	5.76E+08	5.16E+08	4.29E+08	2.98E+08
3.6	35	2.88E+08	2.76E+08	2.65E+08	2.56E+08	2.38E+08	2.21E+08	2.05E+08	1.84E+08	1.54E+08	1.09E+08
3.6	40	5.27E+08	5.05E+08	4.86E+08	4.68E+08	4.34E+08	4.03E+08	3.75E+08	3.36E+08	2.80E+08	1.95E+08
3.6	45	8.77E+08	8.41E+08	8.09E+08	7.79E+08	7.23E+08	6.71E+08	6.22E+08	5.57E+08	4.63E+08	3.22E+08
3.6	50	1.36E+09	1.30E+09	1.25E+09	1.21E+09	1.12E+09	1.04E+09	9.62E+08	8.60E+08	7.15E+08	4.96E+08
4.2	45	5.83E+08	5.58E+08	5.37E+08	5.17E+08	4.80E+08	4.46E+08	4.14E+08	3.71E+08	3.09E+08	2.16E+08
4.2	50	9.33E+08	8.94E+08	8.60E+08	8.28E+08	7.68E+08	7.13E+08	6.62E+08	5.92E+08	4.93E+08	3.42E+08
4.2	55	1.41E+09	1.35E+09	1.30E+09	1.25E+09	1.16E+09	1.08E+09	9.97E+08	8.92E+08	7.41E+08	5.14E+08
4.2	60	2.03E+09	1.94E+09	1.87E+09	1.79E+09	1.66E+09	1.54E+09	1.43E+09	1.27E+09	1.06E+09	7.33E+08
4.8	55	9.83E+08	9.42E+08	9.06E+08	8.73E+08	8.09E+08	7.51E+08	6.97E+08	6.24E+08	5.19E+08	3.61E+08
4.8	60	1.45E+09	1.39E+09	1.34E+09	1.29E+09	1.19E+09	1.11E+09	1.03E+09	9.17E+08	7.62E+08	5.29E+08
4.8	65	2.06E+09	1.97E+09	1.89E+09	1.82E+09	1.68E+09	1.56E+09	1.45E+09	1.29E+09	1.07E+09	7.44E+08
4.8	70	2.84E+09	2.71E+09	2.60E+09	2.49E+09	2.30E+09	2.12E+09	1.97E+09	1.76E+09	1.46E+09	1.01E+09

Table B.2. Neutron Source Terms

PWR Neutron Source, neutrons/sec/assembly

425.9 kgU/assembly (17 x 17 OFA)

	Burnup,	Cooling time, years									
E, %	GWd/MTU	3	4	5	6	8	10	12	15	20	30
2.4	15	8.29E+06	7.90E+06	7.65E+06	7.43E+06	7.04E+06	6.67E+06	6.32E+06	5.85E+06	5.17E+06	4.12E+06
2.4	20	2.89E+07	2.76E+07	2.66E+07	2.57E+07	2.40E+07	2.25E+07	2.10E+07	1.91E+07	1.62E+07	1.20E+07
2.4	25	7.59E+07	7.25E+07	6.98E+07	6.73E+07	6.26E+07	5.83E+07	5.43E+07	4.88E+07	4.10E+07	2.92E+07
2.4	30	1.65E+08	1.58E+08	1.52E+08	1.47E+08	1.36E+08	1.26E+08	1.17E+08	1.05E+08	8.78E+07	6.14E+07
3.0	25	4.31E+07	4.12E+07	3.96E+07	3.83E+07	3.57E+07	3.33E+07	3.11E+07	2.81E+07	2.38E+07	1.72E+07
3.0	30	9.91E+07	9.48E+07	9.12E+07	8.79E+07	8.17E+07	7.60E+07	7.07E+07	6.35E+07	5.32E+07	3.76E+07
3.0	35	1.97E+08	1.89E+08	1.81E+08	1.75E+08	1.62E+08	1.51E+08	1.40E+08	1.25E+08	1.05E+08	7.30E+07
3.0	40	3.46E+08	3.32E+08	3.19E+08	3.07E+08	2.85E+08	2.64E+08	2.45E+08	2.20E+08	1.83E+08	1.27E+08
3.6	35	1.23E+08	1.17E+08	1.13E+08	1.09E+08	1.01E+08	9.41E+07	8.75E+07	7.85E+07	6.56E+07	4.62E+07
3.6	40	2.24E+08	2.15E+08	2.07E+08	1.99E+08	1.85E+08	1.72E+08	1.60E+08	1.43E+08	1.19E+08	8.31E+07
3.6	45	3.73E+08	3.58E+08	3.44E+08	3.32E+08	3.08E+08	2.86E+08	2.65E+08	2.37E+08	1.97E+08	1.37E+08
3.6	50	5.79E+08	5.55E+08	5.34E+08	5.14E+08	4.76E+08	4.42E+08	4.10E+08	3.66E+08	3.04E+08	2.11E+08
4.2	45	2.48E+08	2.38E+08	2.29E+08	2.20E+08	2.05E+08	1.90E+08	1.76E+08	1.58E+08	1.32E+08	9.19E+07
4.2	50	3.97E+08	3.81E+08	3.66E+08	3.53E+08	3.27E+08	3.04E+08	2.82E+08	2.52E+08	2.10E+08	1.46E+08
4.2	55	6.01E+08	5.76E+08	5.54E+08	5.33E+08	4.94E+08	4.58E+08	4.25E+08	3.80E+08	3.16E+08	2.19E+08
4.2	60	8.64E+08	8.28E+08	7.95E+08	7.64E+08	7.07E+08	6.55E+08	6.07E+08	5.43E+08	4.51E+08	3.12E+08
4.8	55	4.19E+08	4.01E+08	3.86E+08	3.72E+08	3.45E+08	3.20E+08	2.97E+08	2.66E+08	2.21E+08	1.54E+08
4.8	60	6.18E+08	5.92E+08	5.69E+08	5.48E+08	5.08E+08	4.71E+08	4.37E+08	3.91E+08	3.25E+08	2.25E+08
4.8	65	8.77E+08	8.40E+08	8.07E+08	7.75E+08	7.17E+08	6.64E+08	6.15E+08	5.50E+08	4.57E+08	3.17E+08
4.8	70	1.21E+09	1.15E+09	1.11E+09	1.06E+09	9.78E+08	9.04E+08	8.37E+08	7.47E+08	6.21E+08	4.30E+08

Table B.3. Pressurized Water Reactor Decay Heat

Decay Heat, watts/assembly[(a)]											
	Burnup,	Cooling time, years									
E, %	GWd/MTU	3	4	5	6	8	10	12	15	20	30
2.4	15	669	443	335	279	231	211	199	186	170	145
2.4	20	874	592	452	379	313	285	269	251	229	196
2.4	25	1,080	746	576	485	401	364	342	319	291	248
2.4	30	1,294	905	709	603	497	449	420	390	355	300
3.0	25	1,036	719	558	474	394	359	337	314	286	242
3.0	30	1,236	871	683	582	485	439	411	383	347	293
3.0	35	1,440	1,029	819	700	585	527	492	456	412	345
3.0	40	1,658	1,202	965	827	693	623	582	537	484	403
3.6	35	1,380	992	791	677	567	515	482	447	403	337
3.6	40	1,582	1,154	926	798	670	605	566	523	471	392
3.6	45	1,797	1,323	1,073	931	779	704	655	604	544	451
3.6	50	2,018	1,506	1,228	1,067	899	812	756	693	622	512
4.2	45	1,719	1,273	1,033	896	754	685	637	589	530	440
4.2	50	1,931	1,444	1,180	1,025	864	784	730	675	603	498
4.2	55	2,153	1,628	1,337	1,167	985	890	828	765	684	561
4.2	60	2,383	1,821	1,506	1,321	1,118	1,006	937	860	768	627
4.8	55	2,065	1,560	1,288	1,123	954	860	801	741	661	546
4.8	60	2,283	1,745	1,445	1,266	1,071	971	901	833	743	610
4.8	65	2,513	1,937	1,613	1,420	1,204	1,087	1,009	927	826	677
4.8	70	2,753	2,139	1,793	1,579	1,344	1,214	1,128	1,035	917	746
(a) 425.9 kg U/assembly (17 x 17 OFA).											

References

Barner JO. 1985. *Characterization of LWR Spent Fuel MCC-Approved Testing Material—ATM-101*. PNL-5109 Rev. 1, Pacific Northwest Laboratory; Richland, Washington.

Guenther RJ, DE Blahnik, TK Campbell, UP Jenquin, JE Mendel, LE Thomas, and CK Thornhill. 1988. Characterization of Spent Fuel Approved Testing Material—ATM-103, PNL-5109-103, Pacific Northwest Laboratory, Richland, Washington.

Luksic A. 1989. *Spent Fuel Assembly Hardware: Characterization and 10 CFR 61 Classification for Waste Disposal*. PNL-6906 Vol. 1, Pacific Northwest Laboratory; Richland, Washington.

Appendix C

MCNP Calculated Cask Dose Rates

Appendix C:
MCNP Calculated Cask Dose Rates

Calculated dose rates on the surface of the cask with the load-pattern fuel are given in Tables C.1 through C.3. Calculated dose rates for the TN-24P cask are compared with measured dose rates in Table C.4. Calculational uncertainties range from 1 to 10 mrem/hr.

Table C.1. Dose Rates on the Top of the Cask with the Load-Pattern Fuel

Rad., cm	Source-1/1			Source-2/2			Source-3/4		
	Neutrons	Photons	Total	Neutrons	Photons	Total	Neutrons	Photons	Total
5	13.5	5.3	18.8	67.7	4.1	71.9	31.1	7.4	38.5
15	13.6	5.6	19.2	67.9	4.1	72.0	30.4	7.2	37.6
25	13.3	5.5	18.8	66.5	4.0	70.5	29.9	6.4	36.3
35	12.6	5.4	18.0	63.2	3.7	66.9	28.2	5.6	33.7
45	11.7	4.7	16.5	58.6	3.4	62.0	25.9	4.5	30.4
55	10.4	4.3	14.7	52.2	3.2	55.4	22.8	3.5	26.3
65	9.4	4.4	13.8	47.1	3.4	50.5	20.5	2.8	23.3
75	8.3	6.3	14.6	41.7	5.0	46.7	17.8	3.5	21.3
85	7.3	12.4	19.8	36.6	11.0	47.6	15.6	6.6	22.2
95	5.0	8.4	13.4	25.2	6.7	31.9	10.7	4.1	14.9
110	4.6	18.1	22.7	23.0	14.5	37.5	9.8	10.2	20.0
135	3.7	27.6	31.4	18.7	23.1	41.8	7.9	17.4	25.3
175	2.4	15.9	18.4	12.2	12.8	25.0	5.2	9.8	14.9
225	1.5	9.9	11.3	7.3	7.2	14.5	3.0	6.1	9.1
275	0.9	8.3	9.2	4.7	5.3	10.0	2.0	4.4	6.4

Rad, cm	Source-7/4			Source-4/7			Source-6/5		
	Neutrons	Photons	Total	Neutrons	Photons	Total	Neutrons	Photons	Total
5	45.0	7.7	52.7	38.9	2.9	41.7	42.7	4.5	47.2
15	44.0	7.4	51.4	40.1	3.2	43.3	43.8	4.6	48.4
25	43.2	6.6	49.8	39.2	3.8	43.0	42.8	4.6	47.4
35	40.7	5.6	46.4	37.5	3.9	41.5	40.9	4.6	45.5
45	37.4	4.4	41.8	35.2	4.6	39.8	38.3	4.5	42.8
55	32.9	3.5	36.4	31.7	4.7	36.4	34.4	4.5	38.9
65	29.6	2.8	32.4	28.7	6.3	35.0	31.1	4.9	36.0
75	25.7	3.5	29.2	26.0	9.7	35.7	28.0	7.9	35.9
85	22.5	6.3	28.8	22.8	18.4	41.2	24.6	15.2	39.8
95	15.5	3.9	19.4	15.7	12.3	28.0	16.9	9.7	26.6
110	14.2	10.2	24.4	14.3	26.7	41.0	15.4	22.5	37.9
135	11.4	17.1	28.5	11.8	40.3	52.1	12.7	34.9	47.6
175	7.4	10.0	17.4	7.7	22.9	30.7	8.3	19.5	27.9
225	4.3	6.1	10.3	4.7	13.0	17.7	5.1	11.2	16.2
275	2.9	4.4	7.3	3.0	9.8	12.8	3.2	8.1	11.3

Table C.2. Dose Rates on the Side of the Cask with the Load-Pattern Fuel

	Source-1/1			Source-2/2			Source-3/4		
Ht., cm	Neutrons	Photons	Total	Neutrons	Photons	Total	Neutrons	Photons	Total
1.65	10.9	2.1	13.0	54.5	1.2	55.7	20.3	0.5	20.8
4.95	15.1	3.1	18.2	75.6	1.8	77.4	28.8	0.8	29.5
8.25	18.9	6.4	25.3	94.4	3.7	98.1	37.1	1.6	38.7
11.55	23.9	10.6	34.5	119.6	6.3	125.9	45.9	3.1	49.0
14.85	29.2	29.4	58.6	146.2	12.8	159.0	55.7	6.9	62.6
18.15	34.8	62.8	97.6	173.9	25.7	199.6	66.7	14.3	80.9
21.45	41.6	68.4	110.0	208.0	42.2	250.1	78.6	22.0	100.6
24.75	48.4	89.2	137.6	241.9	67.9	309.7	91.5	39.0	130.5
28.05	56.6	134.8	191.4	282.9	92.9	375.7	108.1	54.5	162.6
31.35	68.9	162.4	231.3	344.5	107.5	452.0	129.6	69.9	199.4
34.65	5.3	18.6	23.9	26.3	13.5	39.8	10.1	7.5	17.6
43.15	0.7	32.4	33.1	3.7	14.0	17.6	1.3	9.7	11.0
75	1.2	46.9	48.1	6.2	15.6	21.8	1.9	10.6	12.5
125	2.1	59.6	61.7	10.6	18.2	28.8	3.2	11.0	14.2
175	2.3	62.7	65.0	11.7	18.2	29.8	3.5	11.0	14.6
225	2.3	60.2	62.5	11.4	18.0	29.4	3.5	10.9	14.4
275	2.2	58.2	60.4	10.9	17.9	28.8	3.4	14.4	17.8
325	1.8	57.7	59.5	8.8	17.4	26.2	2.7	12.0	14.6
375	0.8	39.5	40.3	3.8	13.4	17.2	1.2	12.7	13.9
410.1	0.4	29.3	29.6	1.8	17.8	19.6	0.7	16.3	17.0
421.85	3.4	23.4	26.8	17.1	18.2	35.3	6.9	17.3	24.2
425.15	36.0	146.0	182.1	180.1	119.3	299.4	72.7	105.5	178.2
428.45	30.7	131.9	162.6	153.7	111.6	265.3	63.9	94.1	158.0
431.75	26.8	118.9	145.7	133.9	99.1	233.1	53.9	83.8	137.7
435.05	23.9	109.8	133.7	119.7	92.3	212.0	49.6	79.8	129.3
438.35	21.8	102.1	124.0	109.1	86.9	196.0	44.7	81.1	125.9
441.65	19.8	94.8	114.5	98.8	81.8	180.7	40.3	81.5	121.8
444.95	17.1	81.3	98.5	85.7	72.2	157.9	35.2	73.8	109.1
448.25	14.6	60.4	75.0	73.1	53.5	126.5	29.7	53.5	83.2
451.55	11.8	41.1	53.0	59.2	35.6	94.8	24.2	34.2	58.4
454.85	9.6	24.9	34.5	47.9	20.4	68.3	20.2	17.7	37.9

Table C.2. (contd)

	Source-7/4			Source-4/7			Source-6/5		
Ht., cm	Neutrons	Photons	Total	Neutrons	Photons	Total	Neutrons	Photons	Total
1.65	29.1	0.5	29.6	38.3	6.1	44.5	40.3	4.6	44.8
4.95	41.4	0.8	42.1	52.3	6.2	58.5	55.1	3.0	58.2
8.25	53.3	1.7	55.1	63.6	12.5	76.0	67.4	8.9	76.3
11.55	65.9	3.3	69.2	82.2	26.2	108.4	86.8	15.3	102.1
14.85	80.0	6.1	86.1	101.1	31.2	132.3	106.6	23.5	130.1
18.15	95.8	13.9	109.7	119.6	57.1	176.7	126.3	41.6	167.9
21.45	112.9	22.6	135.5	144.7	84.9	229.6	152.4	65.0	217.4
24.75	131.4	38.5	170.0	168.2	130.2	298.4	177.1	98.7	275.9
28.05	155.3	55.7	211.0	195.1	177.5	372.6	205.8	135.6	341.4
31.35	186.1	67.4	253.4	240.6	220.1	460.7	253.2	163.5	416.7
34.65	14.5	7.6	22.1	18.0	28.5	46.5	19.0	21.5	40.5
43.15	1.9	8.5	10.4	2.7	37.7	40.4	2.8	26.9	29.7
75	2.7	10.5	13.3	4.9	53.5	58.4	5.0	31.9	36.9
125	4.6	9.9	14.5	8.6	62.2	70.7	8.8	36.2	45.0
175	5.0	10.5	15.5	9.4	66.1	75.5	9.6	37.4	47.0
225	5.0	12.0	17.0	9.2	64.6	73.7	9.4	38.0	47.4
275	4.8	13.8	18.6	8.8	62.8	71.6	9.0	37.2	46.2
325	3.8	10.3	14.1	7.2	65.1	72.2	7.3	37.3	44.7
375	1.8	11.7	13.4	3.0	52.0	54.9	3.1	31.1	34.2
410.1	1.0	16.9	17.8	1.2	31.2	32.4	1.3	27.0	28.3
421.85	9.9	17.4	27.3	11.3	29.9	41.2	12.0	26.7	38.7
425.15	104.7	109.5	214.2	118.3	194.1	312.4	126.1	178.3	304.4
428.45	92.1	97.1	189.2	98.3	179.2	277.4	105.4	163.2	268.5
431.75	77.6	85.7	163.3	88.3	163.1	251.4	94.0	147.2	241.2
435.05	71.4	85.4	156.9	76.9	144.7	221.5	82.3	134.4	216.7
438.35	64.5	82.0	146.4	70.7	130.0	200.7	75.6	123.0	198.5
441.65	58.1	85.0	143.2	64.3	115.4	179.7	68.6	113.5	182.2
444.95	50.8	77.3	128.0	55.4	96.3	151.6	59.2	96.6	155.8
448.25	42.8	56.0	98.8	47.7	73.3	121.0	50.9	72.2	123.1
451.55	34.8	36.2	71.0	38.6	51.5	90.1	41.2	50.5	91.7
454.85	29.1	17.9	47.0	30.2	32.2	62.4	32.4	29.4	61.9

Table C.3. Dose Rates on the Bottom of the Cask with the Load-Pattern Fuel

	Source-1/1			Source-2/2			Source-3/4		
Rad., cm	Neutrons	Photons	Total	Neutrons	Photons	Total	Neutrons	Photons	Total
5	68.9	88.5	157.5	344.7	63.7	408.5	180.7	140.2	320.9
15	67.3	82.9	150.2	336.6	63.1	399.7	176.2	132.4	308.6
25	64.8	90.0	154.7	324.0	61.9	385.8	165.1	137.6	302.7
35	61.2	84.2	145.4	306.3	60.6	366.9	146.2	112.1	258.3
45	58.4	78.2	136.6	292.0	57.7	349.8	132.2	73.5	205.6
55	54.3	62.9	117.2	271.6	45.0	316.6	114.4	35.7	150.2
65	47.7	45.7	93.4	238.7	29.5	268.2	95.9	14.7	110.6
75	38.5	21.4	59.9	192.7	14.6	207.2	74.8	3.5	78.3
85	26.7	15.7	42.4	133.5	12.7	146.3	51.2	4.4	55.6
95	14.4	2.0	16.4	72.2	1.6	73.8	27.8	0.4	28.2
110	11.6	9.3	20.9	58.0	4.3	62.3	21.7	2.3	24.0
135	8.5	17.1	25.6	42.4	8.8	51.1	16.2	5.3	21.5
175	3.9	13.6	17.6	19.5	7.3	26.9	7.4	4.5	11.9
225	2.0	11.7	13.7	9.9	5.5	15.4	3.8	3.4	7.2
275	1.2	8.7	9.9	6.2	4.2	10.4	2.3	2.4	4.7

	Source-7/4			Source-4/7			Source-6/5		
Rad., cm	Neutrons	Photons	Total	Neutrons	Photons	Total	Neutrons	Photons	Total
5	262.8	134.9	397.7	164.2	24.0	188.2	189.2	61.0	250.2
15	256.2	135.3	391.5	160.7	24.4	185.0	185.0	60.8	245.8
25	239.8	130.1	369.9	161.5	30.3	191.8	183.8	64.0	247.8
35	211.9	111.0	323.0	167.4	47.4	214.8	186.1	69.8	256.0
45	191.2	73.3	264.5	170.6	73.9	244.5	186.6	74.9	261.6
55	165.1	36.2	201.3	171.3	81.0	252.3	184.2	68.9	253.1
65	138.1	14.2	152.4	157.5	61.9	219.4	167.7	47.8	215.5
75	107.5	3.5	111.0	131.1	69.6	200.7	138.7	15.9	154.6
85	73.6	4.4	78.0	91.8	12.7	104.5	96.9	11.4	108.3
95	39.9	0.4	40.3	49.5	2.0	51.5	52.3	1.7	54.0
110	31.2	2.2	33.4	40.6	10.9	51.5	42.7	7.9	50.6
135	23.3	4.9	28.2	29.2	20.5	49.7	30.8	14.3	45.1
175	10.6	4.3	14.9	13.5	17.5	31.0	14.3	12.1	26.4
225	5.4	3.3	8.7	6.9	13.0	19.9	7.2	8.9	16.2
275	3.3	2.4	5.7	4.3	9.8	14.1	4.5	7.1	11.6

Table C.4. Comparison of Measured and Calculated Dose Rates on the Top and Bottom of the TN-24P Cask.

Dose Rates on Top of the TN-24P Cask

	Photons @ 45°			Photons @ 90°			Neutrons @ 45°			Neutrons @ 90°		
Rad., cm	Measured	MCNP	Ratio	Measured	MCNP	Ratio	Measured	MCNP	Ratio	Measured	MCNP	Ratio
0.0	50.6	93.4	1.8	45.5	93.4	2.1	31.1	23.6	0.8	27.5	23.6	0.9
11.5				42.9	94.8	2.2				30.5	24.8	0.8
14.0	57.7	85.5	1.5				33.2	24.3	0.7			
23.0	46.8	87.3	1.9	36.9	91.9	2.5		26.2		27.3	27.3	1.0
34.5	35.7	81.5	2.3	34.9	82.5	2.4	26.7	23.2	0.9	30.2	22.2	0.7
46.0	30.8	67.6	2.2	28.3	74.6	2.6	27.9	22.4	0.8	28.9	22.2	0.8
57.5	20.8	44.2	2.1	24.4	66.7	2.7	30.5	20.0	0.7	19.7	21.8	1.1
69.0				16.8	54.7	3.3				17.1	14.1	0.8
70.5	11.3	19.3	1.7				15.4	14.8	1.0			
89.4				297.2	322.7	1.1				18.7	26.5	1.4

Dose Rates on Bottom of the TN-24P Cask

	Photons @ 45°			Photons @ 90°			Neutrons @ 45°			Neutrons @ 90°		
Rad., cm	Measured	MCNP	Ratio	Measured	MCNP	Ratio	Measured	MCNP	Ratio	Measured	MCNP	Ratio
0.0	126.4	88.2	0.7	143.0	88.2	0.6	63.8	66.7	1.0	62.1	66.7	1.1
11.5	135.0	82.4	0.6	136.6	87.2	0.6	63.8	67.5	1.1	63.4	78.9	1.2
14.0												
23.0	128.0	84.6	0.7	124.9	88.3	0.7	57.7	69.2	1.2	61.3	66.6	1.1
34.5	125.8	113.2	0.9	115.1	97.3	0.8	55.9	58.8	1.1	55.8	64.3	1.2
46.0	103.3	69.1	0.7	104.9	76.2	0.7	54.4	69.7	1.3	52.5	58.9	1.1
57.5	69.8	61.4	0.9	91.0	80.4	0.9	59.3	58.6	1.0	44.6	58.1	1.3
69.0				54.1	32.1	0.6				32.7	47.5	1.5
70.5	25.4	16.3	0.6				41.9	41.7	1.0			
74.1				33.8	17.8	0.5				29.7	38.8	1.3
79.2				17.4	3.3	0.2				15.5	33.0	2.1
84.3				8.5	0.0	0.0				20.2	17.0	0.8
89.4				3.6	1.9	0.5				15.4	16.6	1.1
94.5				1.7	3.0	1.7				9.3	11.8	1.3
98.7				1.1	1.1	1.0				7.2	10.9	1.5

Appendix D

Feasibility of Mixed Loadings for Minimizing Cask Derating

Appendix D

Feasibility of Mixed Loadings for Minimizing Cask Derating[a]

D.1 Introduction

A major consideration in the design of casks for transporting spent fuel from the commercial power reactors to the receiving facilities of the federal waste management system (FWMS) is the selection of the design basis of the cask in regard to the burnup and age of the fuel to be accommodated. As the burnup of the spent fuel increases, the shielding on the cask must increase to ensure meeting the Department of Transportation (DOT) specifications for external radiation dose rates from the cask. Because the cask is usually constrained by the total allowable weight of the loaded cask, adding shielding generally reduces the payload capacity of the cask.

One approach to accommodating spent fuel that exceeds the cask design basis burnup is to provide a family of cask baskets with a range of capacities, permitting some additional shielding around the basket perimeter while maintaining the basic cask body. Alternatively, the cask basket may be under-loaded, i.e., some of the basket locations are left empty, thereby reducing the volume of source material within the cask and reducing the external radiation dose rate outside the cask. A third approach would arrange the loading of the spent fuel within the cask by placing lower-burnup/longer-cooled fuel around the basket periphery and placing higher-burnup/shorter-cooled fuel in the basket interior, taking advantage of the shielding properties of the spent fuel assemblies themselves. The calculations described in this appendix were made for the third alternative: patterned arrangements of fuel of different burnups and cooling times, with a limited examination of the second approach, i.e., leaving some locations empty.

D.2 Summary

Nineteen calculations were made of the radiation dose rate on the exterior surface of a spent fuel cask. These calculations encompassed three cask designs and five burnup/cooling time sets of fuel characteristics. The cask designs had a common basket configuration (24 pressurized water reactor [PWR] assemblies), and the neutron and gamma shields were adjusted to be optimum for three sets of fuel characteristics: 35,000 MWD/MTU - 10 years cooled; 45,000 MWD/MTU - 14 years cooled; and 55,000 MWD/MTU 20 years cooled. The loading patterns within the casks varied from uniform arrays of the same fuel to mixtures of two types of fuel, in various combinations of the five fuel types. The calculations were performed using a two-dimensional transport theory code (TWODANT) with explicit representation of each fuel assembly location in the cask basket.

The results show that the external radiation dose rates on the surface of the casks were determined primarily by the characteristics of the fuel assemblies immediately adjacent to the cask cavity wall. Removing assemblies from the interior locations in the cask had little effect (0.2%) on the exterior radiation

(a) Material prepared by RI Smith and UP Jenquin in 1990. Figures, tables, and text have been edited for inclusion in this document.

dose rate. Inserting higher-burnup/shorter-cooled fuel into the interior locations of the cask produced rather small (+ 2%) increases in the exterior dose rates.

These results, coupled with the expected distributions of fuel burnup and cooling times arising from reactor operations throughout the lifetime of the first repository, suggest that the quantities of high burnup/ short-cooled fuel requiring transport from the reactors could likely be accommodated by inserting that material into the interior locations of casks which were optimized for lower burnup/longer-cooled fuel. A more comprehensive study of these possibilities should be initiated to identify the burnup/cooling-time set that would maximize the cask capacity, within the weight constraint of 100 tons loaded, and still permit transport of the required quantities of the higher-burnup/shorter-cooled fuel.

D.3 Calculational Approach

A common cask basket configuration (24 PWR assemblies) was selected for these calculations because it is within the range of capacities developed during the recent conceptual design efforts under the Request for Proposal for *Development of From-Reactor Casks* (DOE 1986). The cask shielding thickness necessary to satisfy DOT transportation regulations were derived using the CAPSIZE code (Bucholz 1987) for three burnup/cooling-time combinations: 35,000 MWD/MTU, 10 years cooled; 45,000 MWD/MTU, 14 years cooled; and 55,000 MWD/MTU, 20 years cooled. The primary gamma-ray shield material was steel, and the neutron shield material was the borated hydrogenous material specified in the CAPSIZE code. The total weight of the casks was allowed to vary above the nominal 100-ton size to satisfy the DOT requirements on external radiation dose rate while maintaining the 24-assembly cask basket configuration. The basket was assumed to be made of aluminum and had a 1-inch web thickness. The physical dimensions of the three casks are given in Table D.1.

Table D.1. Cask Physical Dimensions

Parameter	35,000/10	45,000/14	55,000/20
Cavity Inside Diameter (in.)	62.45	62.45	62.45
Gamma Shield Thickness (in.)	10.26	10.35	10.37
Neutron Shield Thickness (in.)	3.85	4.13	4.37
Outer Skin Thickness (in.)	0.75	0.75	0.75
Loaded Cask Weight (lb.)	225,871	228,404	229,392

X-Y representations of the design basis casks were created for use in TWODANT, a two-dimensional multi-group transport code (Alcouffe et al. 1984). Figure D.1 shows a two-dimensional representation of the cask similar to that used in the analysis. Each basket location was represented explicitly in the 24-assembly array within the cask, allowing the composition of the material within each basket location to be defined separately. Thus each basket location could contain fuel of a different type or no fuel at all. The X-Y representation leads to the irregular boundaries shown in Figure D.1. To minimize the effect of those irregular boundaries on the calculated dose rate of the cask exterior, the location selected for the dose rate determination was just outside the cask skin, on the centerline between two assemblies forming the outer ring of basket locations. The dose rate determination point is shown in Figure D.1.

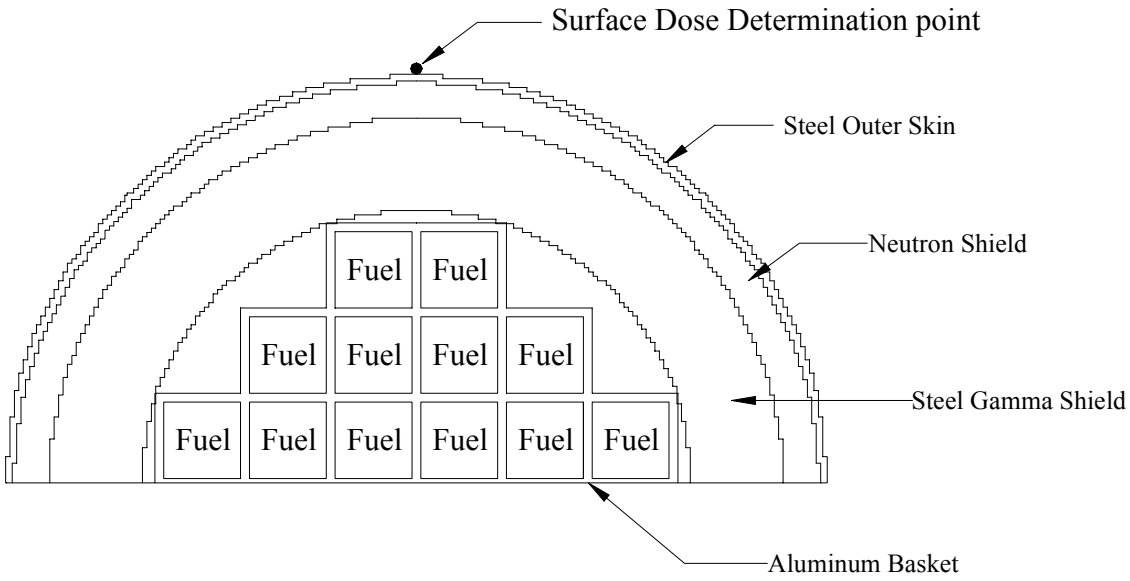

Figure D.1. X-Y Representation of the Spent Fuel Cask

The fuel assembly locations in the cask basket were filled with a homogenized material comprising uranium oxide and zirconium cladding with the appropriate density corresponding to an intact 17 by 17 Westinghouse PWR assembly. The basket webs and outer region were assumed to be of aluminum. The source terms for photons and neutrons were derived from ORIGEN2 (Croff 1980) calculations for UO_2 initially enriched to 3.2 wt% ^{235}U for the 35,000 MWD/MTU 10-year cooled fuel and to 4.0 wt% ^{235}U for the higher burnup fuels using the PUD5O library (Croff and Bjerke 1980), with an assumed power density of 25 MW/MTU during the irradiation period. The photon (gamma ray) and neutron source terms used in the calculations are given in Tables D.2 and D.3.

Table D-2. Photon Source Terms for the Various Fuel Types Studied

TWODANT Group	Energy (MeV)	Fuel Types				
		35/10	**45/14**	**55/20**	**60/5**	**60/14**
31	9-10	7.080+4	1.190+5	2.312+5	5.850+5	4.166+5
32	8-9	7.080+4	1.190+5	2312.5	5.850~5	4.166+5
33	7-8	6.160+5	1.035+6	2.012+6	5.100+6	1.626+6
34	6-7	6.160+5	1.035+6	2.012+6	5.100+6	3.626+6
35	5.5-6	5.350+6	8.990+6	1.746+7	4.416+7	3.144+7
36	4-5.5	5.350+6	8.990+6	1.746+7	4.416+7	3.144+7
37	3-4	3.488+8	7.884+7	8.232+7	2.282+10	1.934+8
38	2-3	6.609+10	3.990+9	1.309+9	4.184+12	5.379+9
39	1-2	1.186+14	1.133+14	9.204+13	4.986+14	1.693+14
40	0.45-1	3.724+15	3.936+15	3.962+15	1.176+16	5.205+15
Total		3.724+15	4.049+15	4.054+15	1.227+16	5.375+15

Table D.3. Neutron Source Terms for the Various Fuel Types Studied[(a)]

Fuel Type	α, η	Spontaneous Fissions	Total
35/10	7.075+6	2.427+8	2.498+8
45/14	1.119+7	4. 082+8	4.194+8
55/20	1.751+7	7.946+8	8.121+8
60/5	2.744+7	2.041+9	2.068+9
60/14	2.371+7	1.433+9	1.457+9
(a) Based on operating reactor fission energy spectrum.			

The calculations were performed for four loading configurations, as shown in Figure D.2. The loading configurations and results of the dose rate calculations are further described in Table D.4 for each of the nineteen cask loading configurations used. The radiation dose rates presented in Table D.4 are for the dose rate determination point illustrated in Figure D.2.

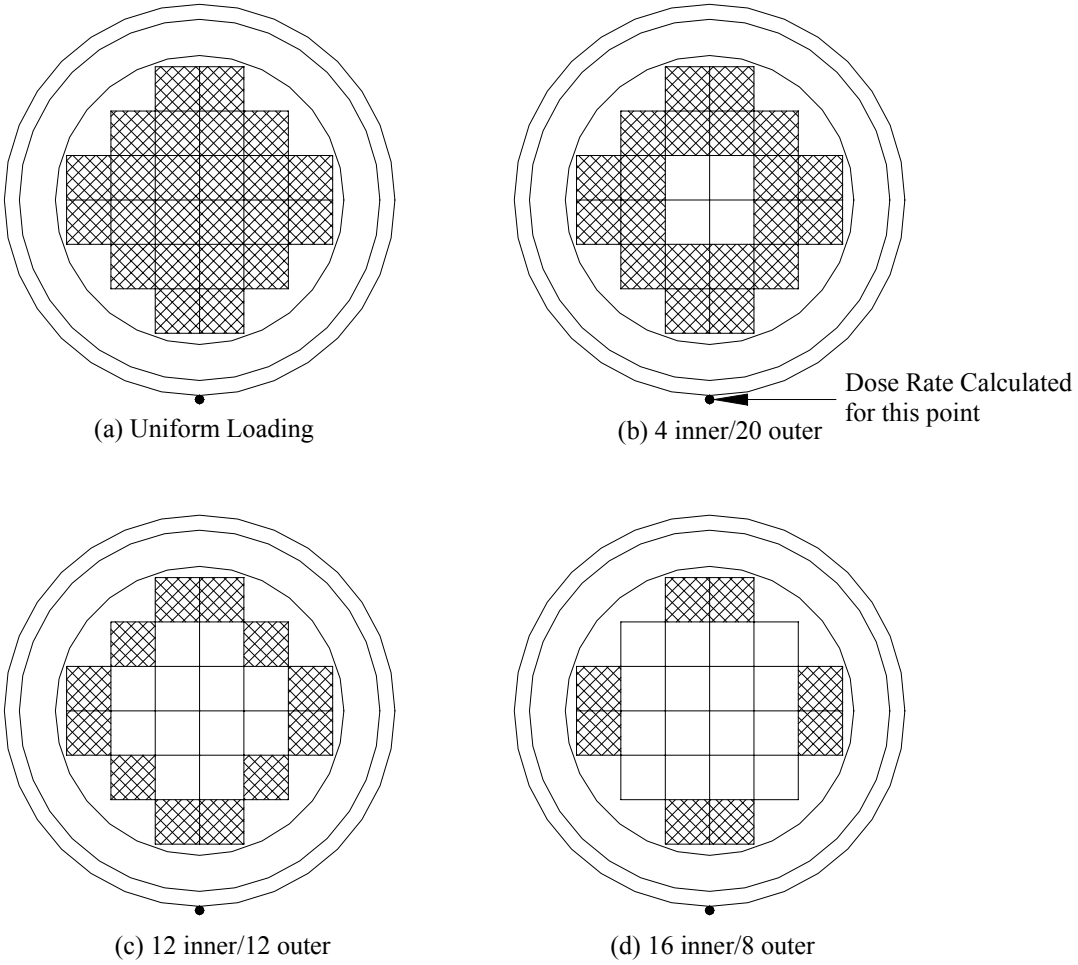

Figure D.2. Cask Loading Patterns

Table D.4. Load Patterns and Associated Calculated Surface Radiation Dose Rates

Case	Load Pattern from Figure D.2	Inner Assemblies			Outer Assemblies			Surface Dose Rates, mR/h				
		Number of Assemblies	Burnup, GWd/MTU	Cooling Time, yr	Number of Assemblies	Burnup, GWd/MTU	Cooling Time, yr	Neutron	Secondary Photons	Primary Photons	Total	% Change[a]
1	a	24	35	10	uniform loading			1.5	0.7	46.7	48.8	base
2	b	4	empty		20	35	10	1.5	0.7	46.6	48.7	-0.2
3	b	4	60	14	20	35	10	1.8	1.0	46.7	49.5	1.4
4	b	4	60	5	20	35	10	2.0	1.1	46.6	49.8	2.0
5	c	12	60	14	12	35	10	3.2	1.8	47.0	52.0	6.6
6	c	12	60	5	12	35	10	4.1	2.4	4.98	56.3	15.4
7	a	24	60	14	uniform loading			8.7	3.1	66.1	77.9	59.6
8	d	16	60	14	8	empty		6.2	3.2	40.0	49.4	1.2
9	a	24	45	14	uniform loading			1.9	1.1	39.8	42.8	base
10	b	4	empty		20	45	14	1.8	1.0	39.8	42.7	-0.2
11	b	4	60	14	20	45	14	2.1	1.3	39.9	43.3	1.2
12	b	4	60	5	20	45	14	2.2	1.5	39.8	43.5	1.2
13	c	12	60	14	12	45	14	3.0	2.0	40.3	45.3	5.8
14	c	12	60	5	12	45	14	3.7	2.6	42.9	49.0	14.5
15	a	24	60	14	uniform loading			6.6	3.7	58.2	68.5	60.0
16	d	16	60	14	8	empty		4.7	3.0	35.5	43.1	0.7
17	a	24	55	20	uniform loading			3.0	2.0	32.2	37.1	base
18	b	4	60	14	20	55	20	3.1	2.1	32.1	37.3	0.5
19	c	12	60	14	12	55	20	3.5	2.5	31.6	37.6	1.3

(a) Total may differ from the sum of individual contributors due to rounding.

D.4 Results and Conclusions

It can be seen from Table D.4 that the influence of the contents of the four central locations in the cask upon the radiation dose rate at the cask surface is very small, whether those locations are filled with hot fuel or are left empty. These results suggest that small quantities of high-burnup and/or short-cooled fuel could be shipped in a cask otherwise filled with fuel whose age and burnup were within the design basis of the cask, with no significant penalty, assuming that the cask heat removal capability was adequate to avoid overheating any of the fuel rods in the assemblies. In addition, the cask surface dose rate is only mildly influenced by loading the inner 12 locations with fuel whose age and burnup are above the cask design basis, as long as the outer 12 locations contained the design basis fuel. A third observation is that the same surface dose rate is achieved if the outer eight locations in the cask are left empty when the inner 16 locations are filled with fuel whose age and burnup exceed the cask design basis (i.e., derating the cask). This latter approach obviously results in a serious penalty in terms of cask carrying capacity and increases in transport costs.

The conclusions to be drawn from this preliminary study are the following:

- The surface dose rate from a cask is very strongly controlled by the makeup of the fuel in the outer locations in the basket, adjacent to the cavity wall.
- The surface dose rate from a cask is very weakly controlled by the makeup of the material in the central locations in the basket.
- Considering the relative fractions of the fuel inventory that are above and below the cask design basis, there would appear to be little or no difficulty in accommodating that portion of the inventory that was above the design basis by placing that material in the interior locations of the cask basket. Thus, providing that a reasonable design basis is chosen for the cask, no derating of the cask should be necessary to transport everything anticipated to be in the spent fuel inventory.
- Some additional calculations should be performed to determine the minimum burnup/age criteria for design basis (providing the maximum cask capacity) that would permit accommodation of the entire anticipated fuel inventory when loaded in the manner explored in this study.

D.5 References

Alcouffe RE, FW Brinkley, DR Marr, and RD O'Dell. 1984. *User's Guide for TWODANT: A Code Package for Two-Dimensional, Diffusion-Accelerated, Neutral-Particle Transport.* LA-10049-M Rev. 1, Los Alamos National Laboratory, Los Alamos, New Mexico.

Bucholz JA. 1987. *CAPSIZE: A Personal Computer Program and Cross-Section Library for Determining the Shielding Requirements, Size, and Capacity of Shipping Casks Subject to Various Proposed Objectives.* ORNL/CSD/TM-248, Oak Ridge National Laboratory, Oak Ridge, Tennessee.

Croff AG and MA Bjerke. 1980. *Alternative Fuel Cycle PWR Models for the ORIGEN Computer Code.* ORNL/TM-7005, Oak Ridge National Laboratory, Oak Ridge, Tennessee.

Croff AG. 1980. *ORIGEN2: A Revised and Updated Version of the Oak Ridge Isotope Generation and Depletion Code.* ORNL-5621, Oak Ridge National Laboratory, Oak Ridge, Tennessee.

DOE. 1986. *Development of from-Reactor Casks.* Request for Proposal, DE-RPO7-861D12625, U.S. Department of Energy, Idaho Operations Office, Idaho Falls, Idaho.